Bioactive Materials 50 (2025) 61–94

Contents lists available at ScienceDirect

Bioactive Materials

journal homepage: www.keaipublishing.com/en/journals/bioactive-materials

Review article

Nanotherapeutic strategies exploiting biological traits of cancer stem cells

Hongyu Wang [a,1], Wenjing Zhang [b,1], Yun Sun [a], Xican Xu [a], Xiaoyang Chen [b], Kexu Zhao [b], Zhao Yang [b,**], Huiyu Liu [a,*]

[a] State Key Laboratory of Organic-Inorganic Composites, Beijing Advanced Innovation Center for Soft Matter Science and Engineering, Beijing Key Laboratory of Bioprocess, Beijing Laboratory of Biomedical Materials, Beijing University of Chemical Technology, 100029, Beijing, China
[b] State Key Laboratory of Green Biomanufacturing, Innovation Center of Molecular Diagnostics, College of Life Science and Technology, Beijing University of Chemical Technology, 100029, Beijing, China

ARTICLE INFO

Keywords:
Nanomaterials
Nanomedicine-based therapeutics
Cancer stem cells
Biological characteristics
Tumor microenvironments

ABSTRACT

Cancer stem cells (CSCs) represent a distinct subpopulation of cancer cells that orchestrate cancer initiation, progression, metastasis, and therapeutic resistance. Despite advances in conventional therapies, the persistence of CSCs remains a major obstacle to achieving cancer eradication. Nanomedicine-based approaches have emerged for precise CSC targeting and elimination, offering unique advantages in overcoming the limitations of traditional treatments. This review systematically analyzes recent developments in nanomedicine for CSC-targeted therapy, emphasizing innovative nanomaterial designs addressing CSC-specific challenges. We first provide a detailed examination of CSC biology, focusing on their surface markers, signaling networks, microenvironmental interactions, and metabolic signatures. On this basis, we critically evaluate cutting-edge nanomaterial engineering designed to exploit these CSC traits, including stimuli-responsive nanodrugs, nanocarriers for drug delivery, and multifunctional nanoplatforms capable of generating localized hyperthermia or reactive oxygen species. These sophisticated nanotherapeutic approaches enhance selectivity and efficacy in CSC elimination, potentially circumventing drug resistance and cancer recurrence. Finally, we present an in-depth analysis of current challenges in translating nanomedicine-based CSC-targeted therapies from bench to bedside, offering critical insights into future research directions and clinical implementation. This review aims to provide a comprehensive framework for understanding the intersection of nanomedicine and CSC biology, contributing to more effective cancer treatment modalities.

1. Introduction

Cancer remains one of the most formidable challenges to global public health, ranking as the second leading cause of mortality worldwide [1]. The latest statistics from the International Agency for Research on Cancer (IARC) reveal approximately 20 million new cancer cases worldwide and 9.7 million cancer-related deaths in 2022 [2]. Despite significant advances in multimodal treatment approaches combining surgery [3], radiotherapy [4], chemotherapy [5], and immunotherapy [6], therapeutic resistance leading to metastasis and recurrence continues to compromise clinical outcomes. This therapeutic failure is largely attributed to the persistence of cancer stem cells (CSCs), which have emerged as a focal point in contemporary cancer research. CSCs represent a distinct subpopulation of cancer cells with self-renewal, differentiation, and high tumor-forming abilities. They resist non-selective treatments such as radiotherapy and chemotherapy and adapt rapidly to treatment stress or nutrient scarcity, leading to therapy failure. Consequently, developing targeted strategies for CSC eradication has become imperative for improving cancer treatment outcomes [7].

The ability of CSCs to initiate tumor formation upon transplantation into immunodeficient mice is its first stemness characteristic [8]. Secondly, CSCs primarily expand through symmetric and asymmetric division, with these two divisions maintaining a certain balance in stabilized tumors. When this balance is disrupted in favor of symmetric division, the self-renewal capacity of CSCs enhances, leading to a higher

Peer review under the responsibility of editorial board of Bioactive Materials.
* Corresponding author.
** Corresponding author.
E-mail addresses: yangzhao@mail.buct.edu.cn (Z. Yang), liuhy@mail.buct.edu.cn (H. Liu).
[1] Hongyu Wang and Wenjing Zhang contributed equally to this work.

https://doi.org/10.1016/j.bioactmat.2025.03.016
Received 30 November 2024; Received in revised form 8 March 2025; Accepted 20 March 2025

malignancy of the cancer [9,10]. Furthermore, the plasticity of CSCs enables them to switch between undifferentiated and differentiated states, is a critical factor in cancer development, metastasis, and drug resistance [11]. Meanwhile, the differentiation potential of CSCs enables them to differentiate into cancer cells of various phenotypes, thereby conferring heterogeneity [12]. Lastly, CSCs highly express ATP-binding cassette (ABC) transporters, including MDR1 (ABCB1), MRP1 (ABCC1), and ABCG2. These transporters are multidrug resistance proteins that protect leukemia and some solid tumor cells from drug-induced damage, thereby inducing drug resistance [13]. Additionally, CSCs can activate DNA repair mechanisms, which leads to resistance against chemotherapy and radiotherapy strategies that induce DNA damage and cell apoptosis [14]. Therefore, developing therapeutic strategies targeting CSCs is advantageous for inhibiting cancer progression by eradicating CSCs, thereby achieving effective cancer treatment.

However, precisely targeting CSCs poses a significant challenge, on account of CSCs prominently located in the core region of tumor tissue [15]. The specificity of developed inhibitors targeting CSCs needs thorough evaluation, as localized administration to reduce systemic toxicity is difficult to achieve [16]. Moreover, the heterogeneity and plasticity of CSCs, as well as their intrinsic mechanisms in metastasis and treatment resistance remain to be elucidated [12,17]. Therefore, a comprehensive understanding of CSC biological characteristics and the mechanisms maintaining their stemness, coupled with the development of innovative strategies targeting specific CSC, holds the potential to bring new hope to cancer patients. Nanomaterials (NMs)-based cancer therapeutic strategies exhibit distinct advantages in specifically targeting CSCs [18,19]. First, stimuli-responsive nanomedicines can achieve therapeutic effects by generating hyperthermia or reactive oxygen species (ROS) through endogenous [20,21] or exogenous [22–24] triggers with precise spatiotemporal control. Second, NMs utilize the enhanced permeability and retention effects and surface modifications to enhance tumor penetration and CSCs targeting through both passive and active targeting while minimizing off-target effects. Furthermore, by loading various therapeutic agents((*e.g.* small molecules [25], peptides/proteins [26], and genetic material [27]), NMs enables multimodal combination therapies targeting CSCs. The annual publications of CSC therapy based on nanomedicine now exceeding 100, reflecting its increasing significance (Fig. 1).

Despite the promising potential of nanotherapeutic strategies for CSC targeting, several critical challenges persist. Limited understanding of CSC biology and regulatory mechanisms hampers the development of precise therapeutic interventions, particularly in designing targeted nanotherapeutics that effectively address CSC-specific features. This review provides a comprehensive analysis of CSC biology and nanotherapeutic approaches. We begin with an examination of CSC roles in cancer progression, followed by a detailed discussion of CSC biological characteristics, including surface markers, signaling pathways, microenvironment interactions, and metabolic features. We then critically evaluate nanotherapeutic strategies designed to target these specific characteristics. Finally, we address current challenges in CSC treatments and corresponding nanotherapeutic solutions, aiming to provide guidance for developing more effective CSC-targeted therapies.

2. Biological traits of cancer stem cells

2.1. Surface markers

CSC surface markers refer to biomolecules specifically and highly expressed on the cell membrane of CSCs, which are usually related to their stemness maintenance and carcinogenic ability and can be used for the isolation, identification, and targeted therapy of CSCs. With the proposal of the CSCs theory and the deepening of the study, a growing number of potential surface markers for CSCs have been identified (Table 1), such as CD133, CD44, CD24, and CD90 [28]. Among them, several typical and widely used surface markers that have been reported for nanotherapeutic targeting were focused on.

2.1.1. CD34

CD34 is a highly glycosylated type I transmembrane glycoprotein expressed on endothelial cells and associated with angiogenesis. In 1994, it was first identified by Dick et al. as a surface marker of CSCs [41]. They reported that isolated $CD34^{+}CD38^{-}$ human leukemia cells initiated acute leukemia after transplantation into immunodeficient mice [67]. Therefore, the isolated $CD34^{+}CD38^{-}$ cells were subsequently named leukemia stem cells (LSCs), with characteristics of self-renewal and high carcinogenicity [41,67]. CD34 were shown to be potential surface markers for a variety of CSCs, including gastric cancer, HCC, and NSCLC (Table 1) [42].

Park et al. conducted a study to assess the proportion of $CD34^{+}$ cell

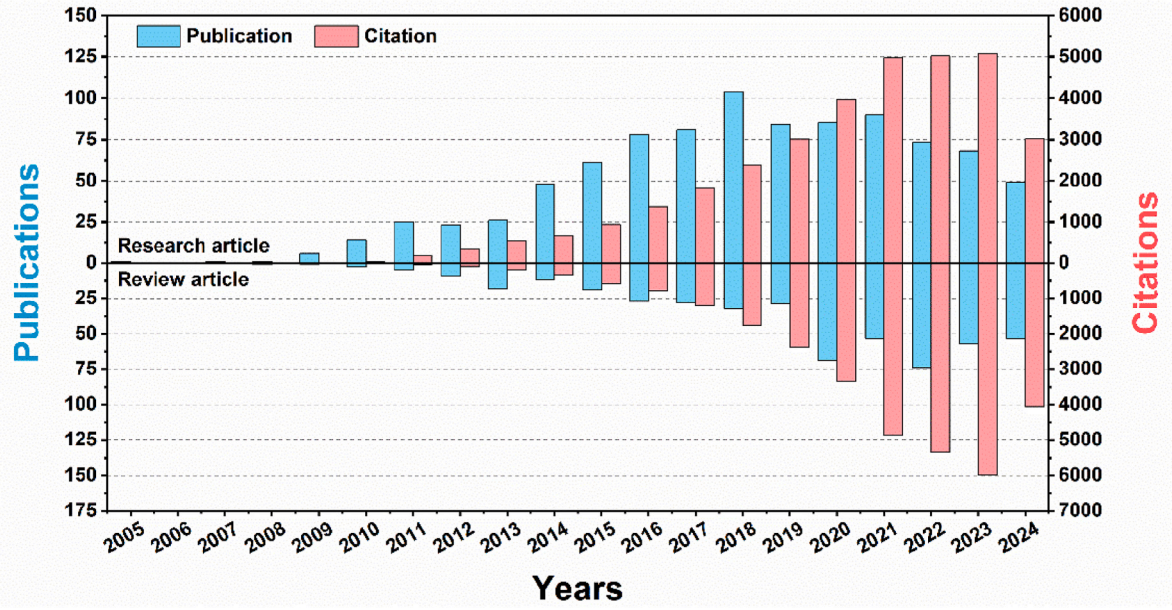

Fig. 1. The publication and citation data were gathered using "nanomedicine" and "cancer stem cell" as keywords through the Web of Science. The statistical data collection is up to October 2024.

Table 1
Common types of surface markers in CSCs.

Surface marker	Cancer types	Ref.
ABCB5	melanoma, oral squamous cell carcinoma (OSCC), ocular surface squamous neoplasia (OSSN)	[29–31]
Aldehyde dehydrogenase 1 (ALDH1)	breast cancer, head and neck cancer (HNC), pancreatic cancer	[32]
CD13	cholangiocarcinoma, hepatocellular carcinoma (HCC)	[33,34]
CD14	colorectal cancer (CRC)	[35]
CD19	acute lymphoblastic leukemia (ALL), chronic lymphocyte leukemia (CLL), multiple myeloma (MM)	[36]
CD20	melanoma, oral cancer	[37,38]
CD24	bladder cancer, breast cancer, colon cancer, HCC, lung cancer, melanoma, MM, ovarian cancer, pancreatic cancer	[39]
CD26	breast cancer, chronic myeloid leukemia (CML), CRC, gastric cancer, glioblastoma multiforme (GBM)	[40]
CD34	acute myeloid leukemia (AML), gastric cancer, HCC, non-small cell lung cancer (NSCLC)	[41,42]
CD38	ALL, AML, CRC, glioma, nasopharyngeal carcinoma, prostatic cancer	[43]
CD44	breast cancer, CRC, HCC, HNC, lung cancer, pancreatic cancer	[44]
CD54	gastric cancer, prostatic cancer	[45,46]
CD55	breast cancer, cervical carcinoma, ovarian cancer	[47]
CD61	breast cancer, HCC, NSCLC	[48–50]
CD66	cervical carcinoma	[51]
CD90	gastric cancer, leukemia, HCC, lung cancer	[52]
CD110	CRC	[53]
CD114	melanoma, neuroblastoma	[54]
CD117	NSCLC, ovarian cancer	[55]
CD133	breast cancer, CRC, gastric cancer, glioma, HCC, melanoma, lung cancer, ovarian cancer, pancreatic cancer, prostate cancer	[56]
CD166	CRC, HNC, lung cancer, melanoma, ovarian cancer, prostate cancer	[57]
CD271	melanoma, head and neck squamous cell carcinomas (HNSCC), OSCC	[37,58,59]
Epithelial cell adhesion molecule (EpCAM)	breast cancer, CRC, HCC, NSCLC, pancreatic cancer	[60,61]
Leucine-rich repeat-containing G-protein-coupled receptor 5 (LGR5)	cervical cancer, colon cancer, nasopharyngeal carcinoma	[62–64]
Side population (SP)	OSCC, pancreatic cancer	[59,65]
Stro-1	bone cancer	[66]

populations in seven HCC cell lines through flow cytometry [68]. They observed that the proportion of $CD34^+$ cells in PLC/PRF/5 hepatoma cells (PLCs) was 3–6 %, higher than the other six cell lines. $CD34^+$ cell populations isolated from PLCs formed xenografts in immunodeficient mice after inoculation with only 100 cells, whereas $CD34^-$ cell populations required inoculation with 100,000 or more cells to form tumors, suggesting that these $CD34^+$ PLCs were more tumorigenic and characterized them as liver CSCs. Additionally, three types of human liver carcinomas were generated from $CD34^+$ PLC: HCC, cholangiocarcinoma, and combined hepatocellular cholangiocarcinoma, indicating that liver CSCs contribute to cancer cell heterogeneity.

2.1.2. CD133

CD133 is a pentosane transmembrane glycoprotein that can interact with vascular endothelial growth factors (VEGF) and participate in signal transduction [56]. In 1997, CD133 was first identified as a surface marker of hematopoietic stem cells by Weigmann et al. [69] It was not until 2003 that Singh and colleagues prospectively isolated a $CD133^+$ cell subpopulation from human brain tumors, which exhibited stem cell properties *in vitro* and could form tumors in NOD-SCID mice with the injection of as few as 100 $CD133^+$ cells. These findings suggested the potential of CD133 as a surface marker for CSCs [70]. In subsequent studies, CD133 was found to be a potential marker for a variety of CSCs, such as breast cancer, CRC, gastric cancer, glioma, HCC, melanoma, lung cancer, ovarian cancer, pancreatic cancer, prostate cancer, *etc*. (Table 1) [56].

The Wilcoxon-Mann-Whitney test was used by Mersakova et al. to compare the percentage of $CD133^+$ cells in all samples of primary and metastatic CRC tumors and found that the percentage of $CD133^+$ cells in metastatic tumors was significantly higher than that in primary tumors and higher levels of $CD133^+$ cells correlated with TNM stage and the invasiveness of CRC into the lymphatic system [71]. The above results indicated that $CD133^+$ cancer cells can differentiate into heterogeneous cancer cells and promote the development of metastases. Attia et al. collected 77 samples of gastric cancer cases and detected CD133 expression in tumor tissues by immunohistochemistry (IHC), which showed CD133 positive cases in 58.4 % of cases and the presence of CD133 positive staining in a few cell populations [72]. It suggested that the expression of CD133 is positively correlated with tumor metastasis and recurrence, and is promising to be a good marker for predicting recurrence and metastasis of gastric cancer.

2.1.3. CD44

CD44, a type I transmembrane glycoprotein, acts as a receptor for hyaluronic acid (HA) and plays a crucial role in cell-cell interactions, adhesion, and migration [44,73]. In 2003, Al-Hajj et al. identified a $CD44^+CD24^{-/low}Lineage^-$ subpopulation in breast cancer patients. Remarkably, as few as 100 cells with this phenotype demonstrated tumorigenic capacity in murine models, marking the first definitive characterization of CD44 as a CSC surface marker [74]. To date, the surface marker CD44 has been reported as a potential marker for CSCs in breast cancer, CRC, HCC, HNC, lung cancer, and pancreatic cancer (Table 1) [44].

Kim et al. sorted and counted 1.6 % of $CD44^-CD133^-$ cells, 75.0 % of $CD44^-CD133^+$ cells, and 23.4 % of $CD44^+CD133^+$ cells from a subset of Caco-2 CRC cells, in which $CD44^+CD133^+$ cells were larger and more mitotically active demonstrated by cell cycle analysis [75]. Notably, non-obese diabetic (NOD)-severe combined immune deficiency (SCID) interleukin (IL)-$2R\gamma^{null}$ (NSG) mice revealed that only the $CD44^+CD133^+$ subset of Caco-2-derived primary tumors had tumorigenic potential and faster secondary xenografts rate. These results indicated that the $CD44^+CD133^+$ subpopulation of Caco-2 cells is highly enriched in tumorigenic cells and has the characteristics of CSCs. Our research team utilized CD44 antibody in combination with CD31 and CD45 antibodies to isolate $CD31^-CD45^-CD44^+$ and $CD31^-CD45^-CD44^-$ cells from three cases of human bladder cancer tissues [76]. Compared to $CD31^-CD45^-CD44^-$ cells, $CD31^-CD45^-CD44^+$ cells displayed the capabilities of self-renewal and sphere formation, and upregulated expression levels of CSC-related genes (*Nanog*, *SOX2*, and *Gli1*, *etc*.). Notably, $CD31^-CD45^-CD44^+$ cells (bladder CSCs) outperformed $CD31^-CD45^-CD44^-$ cells (bladder cancer non-stem cells) in initiating bladder cancer in the limiting dilutions xenograft and serial transplantation assays. The above validation suggested that CD44 can be used as a reliable marker for bladder CSC sorting.

2.1.4. CD24

CD24 is a small glycophosphatidylinositol-anchored cell surface receptor with functions in signal transduction and cell adhesion [39,77]. In 2007, Dou et al. isolated a $CD44^+CD133^+CD24^+$ subpopulation from B16F10 cells with enhanced tumorigenic potential compared to $CD44^-CD133^-CD24^-$ counterparts, which marked the first documented application of CD24 as a discriminative marker for CSCs identification [78]. CD24 has also been confirmed as a potential marker of CSCs, including bladder cancer, breast cancer, colon cancer, HCC, lung cancer, melanoma, MM, ovarian cancer, and pancreatic cancer (Table 1) [39].

Ooki et al. isolated CD24-overexpressing cells from a patient-derived xenograft (PDX) cancer model demonstrated enhanced sphere formation, chemoresistance, elevated expression of CSC-related molecules, and larger tumors in mice [79]. Further analysis revealed that lentivirus-based stable CD24 knockdown cells exhibited increased sensitivity to cisplatin treatment compared to control cells. Quantitative real-time PCR (qPCR) assays indicated that CD24 knockdown led to the down-regulation of numerous CSC-related molecules. Subsequently, CD24 expression in 48 urine samples (24 UCB samples and 24 control samples) was evaluated, which found significantly higher CD24 levels in UCB patient urine compared to controls, with 45.8 % of sensitivity and 95.8 % of specificity of CD24 for cancer detection, respectively. In summary, these findings indicated that CD24 is critical in characterizing the stemness of urothelial CSCs and may serve as a valuable surface marker for urothelial CSC identification. By evaluating IHC staining of 60 paired primary and metastatic human bladder cancer samples, Overdevest et al. detected 75.0 % and 93.3 % of $CD24^+$ cells in primary tumors and lung metastases, respectively [80]. Analysis showed that 61.7 % of metastases had increased CD24 staining intensity and 38.3 % had increased CD24 staining proportion compared with matched primary tumors, which indicated that CD24 expression was higher in metastatic tumors of the same patient than in their parent primary tumors, suggesting that CD24 high-expression cells influenced metastatic tumorigenesis.

2.1.5. CD90

The glycosylphosphatidylinositol-anchored glycoprotein CD90, first identified in mouse T lymphocytes, whose encoded protein is widely used as a marker of hematopoietic stem cells [52,81]. In 2008, Yang et al. first demonstrated the potential of CD90 as a marker for HCC CSCs by characterizing $CD90^+$ cells derived from HCC cell lines, which were capable of generating nodules and forming metastatic foci in immunodeficient mice, whereas $CD90^-$ cells were not. Furthermore, $CD90^+$ populations were identified in 91.6 % of blood samples from tumor specimens of patients with liver cancer [82]. CD90 has been identified as a potential marker for CSCs such as gastric cancer, leukemia, HCC, and lung cancer (Table 1) [52].

Shu et al. assessed the expression of C90 after gastric cancer cells formed spheres by flow cytometry analysis with the percentage of $CD90^+$ increasing to 6.18 % and 8.25 % in SNU-5 and SNU-16 cells, respectively [83]. Subcutaneous injection of $CD90^+$ cells purified into nude mice revealed that it only need 200 $CD44^-CD90^+$ cells to produce tumors in 33.3 % of mice, whereas $CD44^-CD90^-$ cells required at least 2×10^4 cells to form tumors. With CD90 expression correlating positively with the self-renewal capacity and oncogenicity of CSCs. These findings indicated that $CD90^+$ cells possess stemness characteristics, thereby serving as a distinguishing marker for CSCs. Liu et al. conducted a study using 30 Sprague-Dawley male healthy rats, dividing them into a normal control group, a sham operation group undergoing laparotomy, and a liver cancer model group induced by diethylnitrosamine [84]. The CD90 expressions in three groups were 1.18 ± 0.02, 1.19 ± 0.02, and 54.38 ± 24.48, respectively. qPCR results showed that the expression levels of *IL-6*, monocyte chemoattractant protein-1 (*MCP-1*), transforming growth factor (*TGF*)-*β1*, and *CD90* of HCC tissues in liver cancer model group were significantly higher than those in the other two groups. Besides, the inhibition of related inflammatory factors could distinctly suppress the growth, migration, and invasion of HCC cells, while promoting apoptosis. And a significant positive correlation between the changes in the expression of IL-6, MCP-1, and TGF-β and the up-regulation of CD90 was revealed by correlation analysis. These studies demonstrated that CD90 could promote tumor growth by increasing the expression of inflammatory factors.

2.1.6. EpCAM

EpCAM, a type I transmembrane polypeptide, is linked to cell adhesion, proliferation, differentiation, and migration. It is commonly expressed in most normal epithelial cells and gastrointestinal cancers [85]. EpCAM was first discovered in 1979 by Herlyn et al. and was originally described as a dominant surface antigen in human CRC [86]. It has been recognized as a potential marker of CSCs, such as breast cancer, CRC, HCC, NSCLC, and pancreatic cancer (Table 1) [61].

Hwang et al. collected peripheral blood preoperatively and on postoperative days 1 and 7, respectively, from 25 HCC patients with living liver transplantation, and then EpCAM was detected by FACSs [87]. It was demonstrated that the number of $EpCAM^+$ circulating cancer cells was significantly higher in patients with recurrent HCC than in patients without recurrent HCC on preoperative and 1 day postoperative, suggesting that $EpCAM^+$ circulating cancer cells can be used as a key biomarker before surgery and 1 day after living liver transplantation. Mederer et al. collected bone marrow aspirate from 104 non-metastatic NSCLC patients with potentially curative tumor resection, detected and isolated $EpCAM^+$ disseminated cancer cells with anti-EpCAM antibody HEA-125 staining, and performed whole transcriptome amplification and PCR on the sorted them [88]. EpCAM transcripts were found in 84 % of the cells and the $EpCAM^+$ group showed significantly lower progression-free survival and tumor-specific survival. These results suggested that $EpCAM^+$ disseminated cancer cells are specifically related to the development of metastasis and may serve as important therapeutic targets to prevent metastasis.

2.2. Self-renewal and epithelial-mesenchymal transition

Numerous signaling pathways that promote normal stem cell survival, proliferation, self-renewal, and differentiation properties are aberrantly activated or inhibited in tumorigenesis or CSCs. These signaling pathways can also induce the expression of downstream genes of CSCs, such as cytokines, growth factors, apoptosis/anti-apoptosis/value-added/transfer genes, and regulate the growth of CSCs and EMT through an intertwined network of signal mediators [89]. Common signaling pathways include Wnt/β-catenin, Hedgehog (Hh), Notch, TGF-β, Janus kinase (JAK)/signal transducer and activator of transcription (STAT) 3, and nuclear factor kappa-light-chain-enhancer of activated B cells (NF-κB) pathways, *etc*. (Fig. 2).

EMT is a process of phenotypic transformation from epithelial cells to mesenchymal cells that occurs in a specific state. E-cadherin, a key marker of epithelial cell phenotype, is a transmembrane protein responsible for anchoring adjacent cells to each other and forming adhesions, whose cytoplasmic component is connected to the actin cytoskeleton *via* α- and β-linked proteins. Snail, Zeb, and Twist are well-known E-cadherin repressors that act by inducing epigenetic silencing of the E-cadherin promoter in the form of hypermethylation and histone deacetylation. The intermediate filament protein, vimentin, is a marker that distinguishes mesenchymal cells from epithelial cells and affects cell-cell and cell-extracellular matrix (ECM) adhesion. EMT mediates metastasis and invasion of CSCs by regulating the E-cadherin/vimentin axis, and endows stem cell characteristics and self-renewal ability [90].

2.2.1. Wnt/β-catenin signaling pathway

Nusse et al. identified the mouse *Wnt* gene as the proto-oncogene of breast cancer in 1982 [91,92]. The Wnt pathway primarily governs stem cell pluripotency, playing a crucial role in cell self-renewal and differentiation. Activation of the classical Wnt signaling pathway involves Wnt proteins binding to Frizzled receptors, leading to the activation of downstream Dvl (or Dsh) that prevents β-catenin degradation. Stably accumulated β-catenin in the cytoplasm enters the nucleus and binds to the *TCF/LEF* transcription factors to initiate transcription of downstream target genes (*e.g.*, *MYC*, *Cyclin D1*) that are closely associated with the development of many tumors (Fig. 2) [93].

He et al. discovered an elevated expression of human-specific protein kinase, membrane-associated tyrosine/threonine 1 (PKMYT1)-associated lncRNA (*PKMYT1AR*) in NSCLC cell lines (H358, H1975, H1299, H1650, A549, and SPC-A1) compared to the normal human bronchial

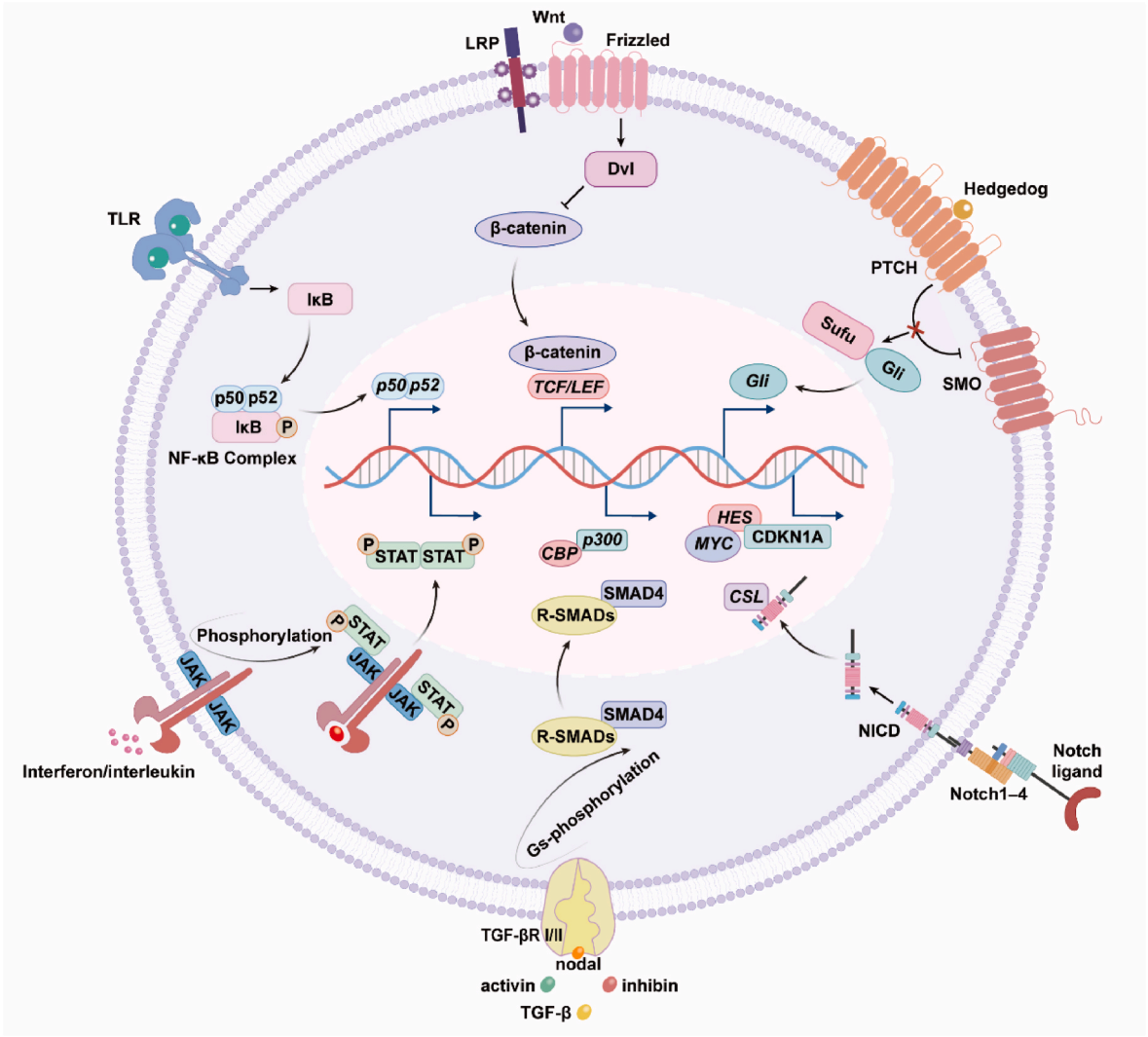

Fig. 2. Common self-renewal related signal pathways of CSCs. LRP: low-density lipoprotein (LDL) receptor-related protein; Dvl: disheveled protein (also called Dsh); *TCF/LEF*: T-cell factor/lymphoid enhancer-binding factor; PTCH: Patched protein; SMO: Smoothened protein; Sufu: suppressor of fused; NICD: Notch intracellular domain; *CSL*: centromere binding factor 1/suppressor of hairless/longevity-assurance gene-1; *HES*: hairy and enhancer of split; CDKN1A: cyclin-dependent kinase (CDK) inhibitor 1A; SMAD: SMA ("small" worm phenotype) and MAD (mothers against decapentaplegic) protein; R-SMADs: receptor-regulated SMAD; *CBP*: cAMP response element-binding (CREB) binding protein; TLR: toll-like receptors; IκB: inhibitor of κB.

epithelial cell line (BEAS-2B) as demonstrated by bioinformatic analysis, real-time RT-PCR, and web available dataset assays [94]. Knockdown of *PKMYT1AR* inhibited the proliferation of A549 and SPC-A1 cells, reduced the colony-forming and migration ability of cells *in vitro* and delayed tumor progression in mice *in vivo*. Conversely, the forced expression of *PKMYT1AR* significantly overcame this phenotype. *PKMYT1AR* functioned as a ceRNA in NSCLC tissues and cell lines to block the inhibitory effect of miR-485-5p on PKMYT1, thereby upregulating PKMYT1 expression. PKMYT1 physically interacted with β-catenin to block E3-ligase$SCF^{\beta\text{-}TrCP}$ recognition, resulting in the stabilization of β-catenin and constitutive activation of Wnt signaling, thereby promoting self-renewal of CSCs, tumorigenesis, and metastasis. Tang et al. identified that LncCCAT1 was highly expressed in breast cancer tissues and breast CSCs sorted from MCF-7 and MDA-MB-231 cells [95]. LncCCAT1 overexpression significantly promoted the proliferation of adherent cells and increased the proportion of breast CSCs among them, and also significantly improved the tumorsphere formation efficiency of breast cancer cells, as well as promoting the migration and invasion in MCF-7 and MDA-MB-231 cells. Mechanistically, LncCCAT1 enhanced *TCF4* levels through competitive binding of miR-204/211 and promoted nuclear translocation of β-catenin by interacting with miR-148a/152 and Annexin A2, leading to activation of Wnt/β-catenin signaling, EMT, and lncCCAT1 transcription, which promoted self-renewal, metastasis, and invasion of breast CSCs.

2.2.2. *Hh signaling pathway*

The *Hh* gene was first discovered by Nüsslein-Volhard et al., in 1980 when screening genes affecting Drosophila embryo development [96]. The classical Hh signaling pathway plays a crucial role in embryonic development, regulation of stem cell renewal, and tissue homeostasis in cancer, and its signaling response is mainly controlled by two transmembrane proteins, the tumor suppressor Patched (Ptc) and the proto-oncogene Smoothened (*Smo*). The downstream molecule of the PTCH protein is the G protein-coupled receptor protein Smo. In the absence of Hh, PTCH indirectly repressed Smo protein by unknown means, while the binding of Hh to PTCH lifts this repression, thus activating Smo and its downstream pathways to induce transcription of target genes and expression of development-related proteins (Fig. 2) [97].

Our research team utilized BCMab1 and anti-CD44 antibodies to identify the $BCMab1^{+}CD44^{+}$ cell subpopulation as bladder CSCs [98]. Transcriptome analysis showed that $BCMab1^{+}CD44^{+}$ cells had > 7-fold

higher levels of N-acetylgalactosaminyltransferase 1 (GALNT1) mRNA than BCMab1^{-}CD44^{-} cells. IHC staining further confirmed the elevated expression of GALNT1 in bladder cancer tissues. Silencing GALNT1 revealed that knockdown of GALNT1 significantly reduced tumorsphere formation and anchorage-independent colony formation. Mechanistic studies were conducted and found that highly expressed GALNT1 in bladder CSCs mediates the O-linked glycosylation of sonic Hh (Shh) to promote the activation of the Hh pathway, thereby promoting the self-renewal of bladder CSCs and the occurrence of bladder tumors. Sun et al. treated UM-UC3 and EJ tumorspheres with cigarette smoke extract (CSE) for 7 days, and the data showed that CSE treatment increased the size and number of tumorspheres, while significantly elevating the expression levels of bladder CSC markers, including CD44, CD133, ALDH1A1, octamer-binding transcription factor 4 (*OCT4*) [99]. And both immunofluorescence (IF) staining and flow cytometry analysis showed that CSE dose-dependently increased the percentage of CD44-positive cells. In addition, CSE treatment significantly increased the invasive ability of bladder CSCs, decreased protein expression of the epithelial cell markers E-cadherin and zonula occludens-1 (Zo-1), and increased protein expression of the mesenchymal cell markers vimentin and N-cadherin. Mechanistic analyses revealed that CSE treatment increased the expression of *Shh*, *Smo*, *Gli1*, and *Gli2* in UM-UC3 and EJ tumor spheroid-forming cells, *i.e.*, CSE promoted stemness and EMT in bladder CSCs by activating the Hh signaling pathway.

2.2.3. Notch signaling pathway

In 1919, Ellisen et al. first discovered the *Notch* gene, which is implicated in human tumors, through their investigation of the chromosome 9-7 translocation in T-cell ALL [100,101]. The Notch signaling pathway comprises the Notch receptor, Notch ligand, and ligand-DNA binding protein regulatory molecules. When activated, Notch signaling binds the transmembrane ligands on one cell to Notch receptor analogs (Notch1, Notch2, Notch3, or Notch4) on adjacent cells, which are subsequently hydrolytically cleaved by progerin-dependent γ-secretase to form soluble NICD and translocated to the nucleus to bind to the transcription factor *CSL*, thereby in turn regulating the function of downstream target genes. Important target genes of the Notch signaling pathway include *HES* family genes (as transcriptional repressors associated with CSC phenotype), proto-oncogene *MYC*, and CDKN1A (Fig. 2) [102].

Yang et al. demonstrated the increased expression of Notch1 and HES1 in GBM tissues and observed that both Notch1 and Cys-X-Cys (CXC) motif chemokine receptor (CXCR) 4 were upregulated in glioma stem cells (GSCs) by IF and showed a strong correlation with stemness markers in GBM cell lines [103]. Tumorsphere formation and limited dilution assays using U87 and U251 cell lines revealed an increase in the number of cells required to produce tumorspheres in the shNotch1 group, and downregulation of Notch1 expression could significantly inhibit the invasion and migration of U87 and U251 GSCs. Mechanistic studies have shown that in GSCs, Notch1 signaling may aggravate the transcription of CXCR4 by straightly targeting the CXCR4 promoter through the transcription factor *RBPJ* to enhance the CXC motif chemokine ligand (CXCL) 12/CXCR4 axis while enhancing the protein kinase B (PKB, also known as Akt)/mammalian target of rapamycin (mTOR) pathway to promote invasion, self-renewal, and growth of GSCs. By verifying the relationship between EMT and CSCs in HCC cells, Jing et al. revealed that overexpressed hypoxia inducible factor (HIF)-1α-induced EMT exhibited a reduction in E-cadherin alongside an enhancement in N-cadherin and Slug expression [104]. Western blotting assay showed that overexpression of HIF-1α induced the expression of CSC-associated surface markers CD44, CD90, and EpCAM, as well as the expression of CSC-associated transcription factors *OCT4*, *Bmi1*, and *Nanog*. When EMT was inactivated by *Slug*-siRNA transfection, the induction of CSC-associated proteins by HIF-1α was attenuated. Moreover, cells overexpressing HIF-1α exhibited a stronger ability to form tumorspheres and colonies, which also facilitated cell migration and invasion. Further investigations demonstrated that HIF-1α activated the Notch1 signaling pathway through direct interaction with the Notch intracellular domain to promote the EMT process and maintenance of stemness characteristics in liver CSCs.

2.2.4. TGF-β signaling pathway

The TGF-β signaling pathway is extensively involved in a variety of cellular processes including cell proliferation, differentiation, and apoptosis. Once activated, ligands of TGF-β, activin, inhibin, Nodal, and bone morphogenic protein could bind transmembrane receptor type I and type II complexes on the cell surface and induce phosphorylation of the GS-domain (rich in glycine and serine residues) in type I receptors *via* constitutively active type II receptor kinases, which can recruit R-SMADs. R-SMADs form complexes with common SMAD4, and the activated SMAD complexes are translocated to the nucleus, which in turn regulate the transcription of target genes, such as *CBP* and *p300* [105]. TGF-β has dual roles in different periods of tumor development. In the early stage, TGF-β secreted by tumor or stromal cells plays an oncostatic role by inducing cell cycle arrest and promoting apoptosis, which can inversely promote cancer cell invasion and metastasis by regulating genomic instability, EMT, and neo-angiogenesis in the late stage (Fig. 2) [106].

Wang et al. identified an HCC progenitor cell-specific gene, *RALY* RNA binding protein-like (*RALYL*), which was expressed at high levels in Huh7, Hep3b, and H2M cells [107]. Functional studies showed that *RALYL* overexpression could upregulate the levels of CSC-related markers including AFP, CD133, *Nanog*, sex-determining region Y (SRY)-box 2 (*SOX2*), and *MYC*, and significantly enhance the frequencies of primary and secondary tumorspheres formation, as well as the metastatic ability of HCC cells and the formation of metastatic nodules in xenograft tumor-bearing mice. *RALYL* could downregulate epithelial markers (*E-cadherin*) expression and upregulate EMT-related transcription factors (*Snail* and *Slug*). After treatment with two commonly used chemotherapeutic agents (cisplatin and 5-fluorouracil), the cell survival rate of *RALYL* overexpressed cells was significantly higher than that of controls. Mechanistic studies demonstrated that *RALYL* promoted TGF-β2 expression in HCC cells by reducing N6-methyladenosine (m^6A) modification to upregulate *TGF-β2* mRNA stability, and TGF-β2 regulated stem cell-associated phosphoinositide 3-kinase (PI3K)/Akt and STAT3 pathways, thereby promoting stemness metastasis, and chemoresistance in HCC. Death-associated protein kinase 1 (DAPK1) is a classical anti-oncogene that is involved in the development of multiple cancers. In CRC, Yuan et al. have revealed that DAPK1 expression is notably reduced in tumor tissues [108]. Experimental findings also demonstrated that downregulation of DAPK1 expression significantly enhanced the sphere-forming and migration abilities of SW480 and DLD1, as well as chemotherapy resistance, while reducing the apoptosis rates of both cell types. Additionally, simultaneous down-regulation of DAPK1 significantly inhibited the expression of epithelial markers E-cadherin and Zo-1, and increased the expression of mesenchymal marker N-cadherin. Mechanistic investigations unveiled that the downregulation of DAPK1 upregulated the expression of both TGF-β1 and TGF-β receptor ACVR2A, which induced the upregulation of Smad2 expression and thus activated the TGF-β signaling pathway. In the meanwhile, the expression of the Wnt receptor was also upregulated, resulting in the activation of the Wnt signaling pathway. The simultaneous activation of TGF-β and Wnt signaling pathways promoted the expression of Zeb1 in cells, which facilitated EMT progression, chemoresistance, and stemness in CRCs.

2.2.5. JAK/STAT3 signaling pathway

The JAK/STAT3 is a cytokine-stimulated signal transduction pathway that includes tyrosine kinase-related receptors, tyrosine kinases JAK (JAK1, JAK2, JAK3, and TYK 2), and effect-producing transcription factors *STAT* (*STAT1*, *STAT2*, *STAT3*, *STAT4*, *STAT5a*, *STAT5b*, and *STAT6*). Interferons (IFNs), ILs, growth factors, or other chemical signals

activate tyrosine kinase-associated receptors, which activate the kinase function of JAK, leading to phosphorylation of the receptor itself. Subsequently, the STAT protein binds to the phosphorylated receptor and is phosphorylated by JAK, which then binds to another phosphorylated STAT (p-STAT) protein and translocates to the nucleus, where it binds to DNA and initiates the transcription of STAT-responsive genes. Each of the seven STAT genes binds and initiates the expression of distinct DNA sequences that drive cancer cell proliferation, survival, invasion, and metastasis, while strongly suppressing the anti-tumor immune response (Fig. 2) [109,110].

Hypoxia is a common pathological feature of high-grade gliomas, with HIF-1α levels being significantly increased in GSCs under hypoxic conditions. Israel et al. observed that the proportion of spherical cells in the typical S100β-v-erbB/p53$^{-/-}$ cell line, TSC1, was significantly reduced when HIF-1α expression was inhibited under hypoxic conditions [111]. Furthermore, the inhibition of STAT3 phosphorylation significantly reduced the subsphere formation potential of S100β-v-erbB/p53$^{-/-}$ GSCs. Mechanically, HIF-1α increased the expression of cytokines such as VEGF in an autocrine/paracrine manner, promoted STAT3 phosphorylation, and activated the JAK/STAT3 signaling pathway, ultimately enhancing the self-renewal of GSCs. Through qPCR analysis, Wang et al. observed that blockade of JAK/-STAT3 by pan-JAK small molecule inhibitor AZD1480 downregulated several key lipid metabolism genes in breast CSCs, including carnitine palmitoyltransferase 1 (CPT1) and the rate-limiting enzyme for fatty acid oxidation (FAO), suggesting that JAK regulates lipid metabolism in breast CSCs [112]. Moreover, breast CSCs exhibited elevated FAO rates, and inhibition of FAO could reduce their tumorsphere-formation potential and the tumorsphere-initiating cell number. Mechanistic investigations revealed that human adipocyte-derived leptin stimulated STAT3 phosphorylation by activating JAK/STAT3, and p-STAT3 entered the nucleus to bind to the *CPT1B* promoter to promote its transcription, and the CPT1B enzyme encoded a key enzyme for FAO, thus facilitating the process of lipid metabolism and the self-renewal of breast CSCs.

2.2.6. NF-κB signaling pathway

NF-κB is a family of transcription factors consisting of five members including *RelA* (*p65*), *RelB*, *c-Rel*, NF-κB1 (*p50*), and NF-κB2 (*p52*), which can form various heterodimers or homodimers and activate a large number of genes by binding to the κB site in the promoter [113]. The NF-κB pathway promotes cell growth by inducing the expression of various regulatory cell proliferation genes such as *cyclin D1*, *D2*, *D3*, *E*, *CDK2*, and *MYC*. It can also activate the transcription of several genes involved in the suppression of exogenous and endogenous apoptosis, such as the inhibitory proteins FLIP [Fas-associated protein with death domain (FADD)-like IL-1β-converting enzyme (FLICE)-like inhibitory protein], B cell lymphoma (BCL)-2, BCL-extra-large (BclxL), and some inhibitors of apoptosis, to inhibit apoptosis to accumulate mutated precancerous and malignant cells, and promote the development of cancer. NF-κB has also been found to play a crucial role in the formation of new blood vessels in tumors (angiogenesis) by regulating the production of cytokines such as tumor necrosis factor (TNF), IL-1, and IL-6 (Fig. 2) [114].

Yamamoto et al. hypothesized that NF-κB could regulate CSC populations, especially in basal-like cells [115]. To confirm this hypothesis, "low NF-κB cells" and "high NF-κB cells" were generated, and it was found that high NF-κB cells exhibited an expanded population of CSCs in basal-like cells compared to low NF-κB cells. Functional assays indicated that the carcinogenicity of breast cancer cells is highly correlated with the NF-κB levels. Mechanistic studies suggested that inflammatory cytokines or epigenetically abnormal NF-κB-interacting kinase (NIK) induced NF-κB activation, and NF-κB-activated cells induce *Jagged1* (*JAG1*) expression in a basal-like subtype-specific manner. And *JAG1* induction occurred in both CSC and non-CSC populations, but the vast majority occurred in non-CSC populations. Upregulation of *JAG1* in non-CSCs stimulated Notch1 signaling in CSCs to promote CSCs self-renewal. Thus, the NIK-NF-κB-JAG1-Notch1 axis could establish an intra-tumor ecological niche that regulated the CSC populations in a subset of basal-like breast tumors *in vivo*.

2.3. Microenvironments

CSCs interact with surrounding non-cancerous cells and the extracellular matrix to form a microenvironment that supports tumor growth. This not only provides a suitable space for the self-renewal and differentiation of CSCs but also shields them from immune system attacks, enhancing their resistance to chemotherapy and radiotherapy [116,117]. Tumor microenvironment (TME) is primarily composed of tumor-associated macrophages (TAMs), cancer-associated fibroblasts (CAFs), and tumor-infiltrating lymphocytes (TILs) (Fig. 3). These cells interact with CSCs by secreting soluble molecules and extracellular vesicles, supporting the maintenance and development of CSCs. Meanwhile, CSCs can not only adapt to changes in the tumor microenvironment, but also alter the tumor microenvironment. The TME, in turn, can not only affect the self-renewal capability of CSCs, but also induce the transformation of normal cells and non-CSCs into CSCs [118]. Therefore, the TME plays an indispensable role in maintaining the stemness of CSCs, tumor growth and metastasis processes [119,120].

2.3.1. Tumor-associated macrophages

TAMs are among the most abundant infiltrating immune cells in the TME stroma, which can be categorized into two main phenotypes, M1 and M2, based on their functions [121]. M1-TAMs exerted pro-inflammatory and anti-tumor effects, while M2-TAMs play a role in anti-inflammation and promoting tumorigenesis, which can promote cancer occurrence, suppress anti-tumor immunity, stimulate angiogenesis, and enhance cancer cell invasion, motility, and infiltration [122]. Additionally, M2-TAMs can hinder immune reactions, aiding cancer cells in evading immune detection and developing resistance to treatments [122]. Notably, these two polarization forms are interconvertible under certain circumstances and in the presence of certain stimuli (Fig. 3) [123].

By detecting several M2 macrophage markers (CD163, IL-10, Arg-1, and CD206^{+}CD11b^{+}), Wu et al. identified that small extracellular vesicles (sEVs) from CD133^{+}CD44^{+} OSCC cells promoted the M2 polarization of macrophages [124]. Functional experiments demonstrated that M2-TAMs enhanced the migration and invasive ability of OSCC cells *in vitro* and the carcinogenicity of OSCC xenograft in nude mice. Mechanistic analysis was performed revealing that OSCC-CSC-sEVs transfer lncRNA *UCA1*, by targeting protein laminin γ2 (LAMC2), promoted the polarization of M2 macrophages and inhibited CD4^{+} T cell proliferation and IFN-γ production *in vitro* and *in vivo*, thereby promoting tumor progression and immunosuppression. Wang et al. co-cultured human-derived HCC line HepG2 cells with two types of M2-TAMs (TAMs^{CM} and M2 Mφs^{Cyto}) and observed a significant increase in the average percentage of CD44^{+}/CD133^{+} cells to 14.1 % and 35.9 %, respectively, compared to 0.6 % in HepG2 monoculture [125]. Concurrently, the gene expression of cancer stemness markers *Nanog*, *SOX2*, and *OCT4* in HepG2 cells also showed a noticeable increase. Further functional studies revealed that the number of HepG2 spheroids increased to 29.8 and 46, respectively, after co-culture with TAMs^{CM} and M2 Mφs^{Cyto}, surpassing the 17.5 spheroids in HepG2 monoculture. In the presence of sorafenib, the apoptotic rates of co-cultured HepG2 cells were 13.75 % and 16.97 %, respectively, which were lower than HepG2 monoculture (21.36 %). Mechanistic studies suggested a significant upregulation of the cytokines CXCL1 and CXCL2 in the media of M2-TAMs monoculture as well as HepG2 cells/M2-TAMs co-culture, compared to HepG2 monoculture medium, which suggested that increased secretion of CXCL1 and CXCL2 in co-culture media is attributed to M2-TAMs, and promoting stemness maintenance and drug resistance in CSCs of HCC.

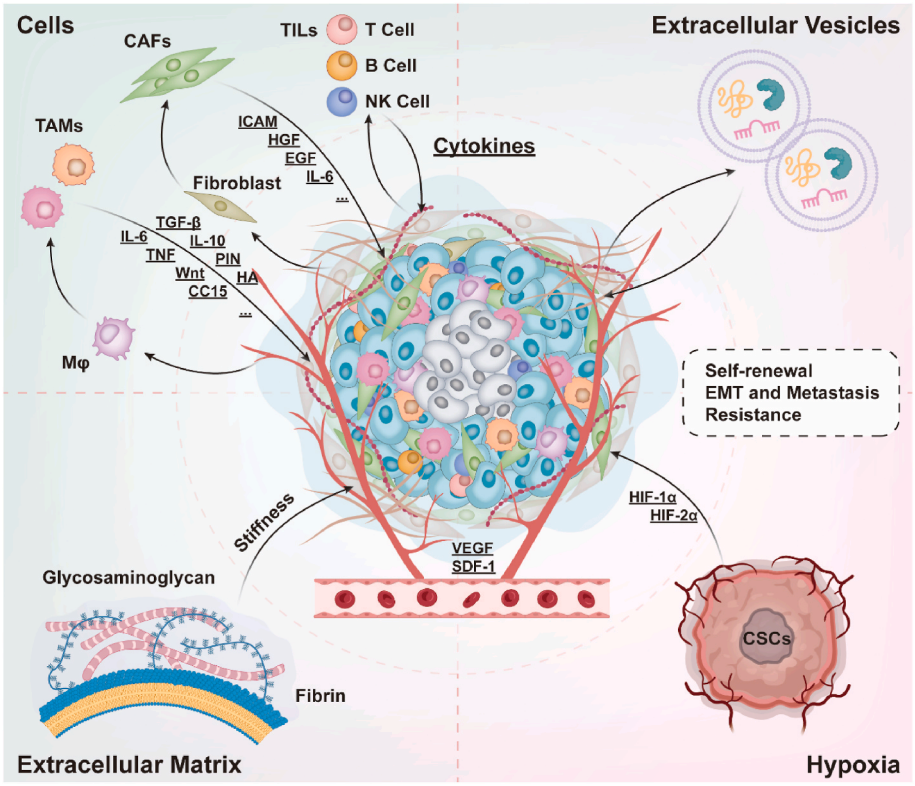

Fig. 3. Common self-renewal related signal pathways of CSCs. Mφ: monocytes/macrophages; PIN: pin-formed protein; CC15: Clara cell protein 15; ICAM: intercellular adhesion molecule; HGF: hepatocyte growth factor; EGF: epidermal growth factor; NK cell: natural killer cell; SDF-1: stromal cell-derived factor-1.

2.3.2. *Cancer-associated fibroblasts*

CAFs are fibroblasts that are present within tumors or surrounding tumor tissues. Among the non-immune cell types of the tumor stroma, CAFs are the most abundant cells in almost all solid tumors. And CAFs exhibit heterogeneity and are composed of different cell subpopulations at various stages of their maturation. As one of the end products of the differentiation of CSCs, CAFs promote cancer cell survival, proliferation, and metastasis through ICAM and cytokines such as HGF, EGF, and IL-6 (Fig. 3) [126].

Zhao et al. isolated CAFs from gastric cancer patients with or without liver metastases within two years post-gastrectomy [127]. Through RNA-sequencing and *in vivo* experiments, the authors identified a CAF subpopulation with high expression of podoplanin (PDPN), a type I transmembrane glycoprotein associated with gastric cancer metastasis. Functional experiments showed that co-culturing HGC27 and AGS cells with PDPN(+) CAFs resulted in higher migration ability than co-culturing with PDPN(−) CAFs or monoculture. Mechanistic studies have shown that PDPN(+) CAFs regulated CSCs through the focal adhesion kinase (FAK)/Akt phosphorylation-mediated secretion of periostin (POSTN). In addition, POSTN activated the FAK/yes-associated protein (YAP) signaling pathway in gastric cancer cells to produce more IL-6, which in turn induced PI3K/Akt phosphorylation in PDPN(+) CAFs, prolonging the activation of PI3K/Akt pathway. This cascade of events sustained POSTN production and its effects on CSC enrichment and gastric cancer cell migration. Pradhan et al. co-cultured oral cancer cell line H-357 cells with CAFs and observed that CSC markers CD133, ALDH1, *OCT4*, and *Nanog* were upregulated by 4.5-, 3.4-, 2.2-, and 1.6-fold, respectively, compared to parental H-357 cells [128]. Notably, the proportion of $CD24^{+}$, $CD133^{+}$, and $ALDH1^{+}$ CSCs in the co-culture group was approximately 1.3 %, 71.5 %, and 69.3 %, respectively, whereas there were no traces of these stemness markers in the parental H-357 cells. These findings suggested that co-cultured cells exhibit characteristics of CSCs. Furthermore, the expression of endogenous CXCL-12 and IL-6 in co-cultured H-357 cells increased by 3.8 and 2.4 times, respectively, compared to the parental cells, indicating that CAFs-derived CXCL-12 and IL-6 are associated with the growth and proliferation of oral cancer CSCs.

2.3.3. *Hypoxia*

One of the most effective ways in which CSCs interact with adjacent TME is through the regulation of hypoxia based on HIFs and their interaction with stemness pathways, transcription factors, and other cancer factors. The effects on CSCs are mainly manifested in promoting their self-renewal, stimulating stem cell-related signaling pathways, facilitating the EMT progression leading to malignancy and distant tumor metastasis, and dysregulated angiogenesis (Fig. 3) [89].

Erices et al. cultured GSCs derived from three different GBM cells (U87MG, GBM38, and GBM27) under hypoxic (0.5 % of oxygen) conditions and observed increased both mRNA and protein levels of A2B adenosine receptor ($A_{2B}AR$) in GSCs [129]. Additionally, GSCs showed enhanced migration and invasive capabilities *in vitro*, as well as increased angiogenesis *in vivo* under hypoxic conditions, suggesting a correlation between hypoxia and $A_{2B}AR$ overexpression, as well as the infiltrative phenotype and angiogenesis of GSCs. According to mechanistic research, $A_{2B}AR$ signaling activation enhanced matrix metalloproteinase (MMP)-9 activity and EMT gene expression under hypoxic conditions, leading to the augmented migration and invasive capacity of GSCs. Ye et al. found that hypoxia significantly increased the concentration of HMGB1 in the culture supernatant of GSCs [130]. Knockdown of HMGB1 resulted in a decrease in cell survival and a significant inhibition of tumorsphere formation of GSCs under hypoxic conditions. And *in vitro* restriction dilution assay showed that silencing HMGB1 led to a reduction in the self-renewal ability of GSCs under hypoxic conditions. EdU staining assay further demonstrated that HMGB1 deletion impaired the proliferation of GSCs under hypoxia. Mechanistic studies suggested that hypoxia-induced HMGB1 bound to the receptor of advanced glycation endproducts (RAGE), activating the RAGE-dependent extracellular regulated protein kinases (ERK) 1/2 signaling pathway, and

maintained the proliferation and self-renewal of GSCs by promoting cell cycle progression.

2.3.4. Extracellular vesicle

EVs are typically categorized into exosomes, microvesicles, and apoptotic bodies, which are membrane-enclosed structures released by any cell type. EVs are highly stable in the extracellular environment and serve as carriers of various molecules, such as proteins, lipids, and different types of RNA [131]. There is mounting proof that EVs from CSCs can promote cancer cell survival, EMT, migration, and endothelial cell angiogenesis (Fig. 3) [132].

Cifola et al. employed omics analysis to study the miRNA and protein profile of sEVs secreted by GBM cell lines and primary GSCs [133]. Among the top 10 upregulated miRNAs in GSC-sEVs, three miRNAs (*miR-5189-3p*, *miR-3621*, and *miR-135b-5p*) have been demonstrated to possess pro-tumor activity, while another three (*miR-1236-5p*, *miR-363-3p*, and *miR-450a-5p*) exhibited tumor-suppressive functions. GSC-sEVs can benefit from the expression of both tumor-suppressive and oncogenic miRNAs, the stemness of CSCs may allow them to evade drug treatment. Moreover, overexpression of proteins associated with GSCs stemness was identified in GSC-sEVs, including ephrin type-A receptor 2 (EPHA2), Copine III (CPNE3), N-cadherin (CDH2), and mitogen-activated protein kinase kinase kinase kinase 4 (MAP4K4). Among these, EPHA2 is known to be overexpressed in GSCs, serving as an indicator of their stemness potential and dissemination ability, which is also related to angiogenesis, migration, adhesion, proliferation, and differentiation; CPNE3 regulates the invasion, migration; and proliferation of GBM cells *via* FAK pathway; CDH2 acts as a marker for GSCs; and MAP4K4 is involved in regulating tumor initiation and proliferation. Chung et al. treated NSCCs of MB49 mouse bladder cancer with sublethal doses of cisplatin or GEM and collected EVs to assess their effect on CSC functionality under chemotherapy conditions [134]. Pretreatment of MB49 CSCs with post-chemotherapy EVs in CSC cultures revealed enhanced resistance of NSCC-EVs to cisplatin and GEM. The data emphasized that chemotherapy eliminated most of the cancer cells, however, EVs released before their death could support CSCs survival under therapeutic conditions, ultimately leading to drug resistance and disease progression. Moreover, NSCC-EVs promoted colony formation in MB49 CSCs and enhanced their migratory and invasive abilities compared with controls. Except for *ALDH1A1*, almost all CSC markers showed greater upregulation after NSCC-EVs treatment compared to PBS. Mechanistic studies unclosed that NSCC-EVs contain ribosomal protein-rich carriers could be employed by CSCs to induce rapid protein synthesis and enable CSCs to adapt to the dynamic TME.

2.3.5. Cytokines

CSCs actively reshape their niche by secreting a range of factors that recruit other cells and alter the characteristics of the ECM. Many of these molecules are secreted in exosomes or extracellular vesicles, while others may be released as freely secreted factors, proteins, cytokines, or RNA (Fig. 3) [135].

The hypoxic niche is mainly induced through HIFs, which belong to the basic helix-loop-helix-Per-ARNT-Sim (bHLH-PAS) family of transcription factors that regulate numerous genes and play a role in oxygen homeostasis, glucose and iron metabolism, and erythropoiesis. Increasing evidence suggests that HIFs are one of the major regulators in maintaining the CSC subpopulation, and play a part in regulating CSC proliferation, self-renewal, and carcinogenicity [136]. Lysyl oxidase (LOX) is an enzyme that cross-links ECM proteins like collagen and facilitates breast cancer metastasis, with its release being modulated by HIF-1α. Ko et al. discovered that radiotherapy-resistant (RT-R)-MDA-MB-231 cells showed an increased production of CSCs, higher expression of HIF-1α, and improved secretion of LOX compared with MDA-MB-231 cells [137]. Mice transplanted with RT-R-MDA-MB-231 cells also exhibited accelerated tumor growth as well as elevated levels of CSC markers (CD44, Notch-4, and *OCT3/4*). Furthermore, these mice exhibited raised expression of HIF-1α in tumor tissues, elevated secretion of LOX in plasma, and a higher degree of induced cross-linked collagen. These findings suggested that RT-R-MDA-MB-231 cells facilitate tumor progression by promoting the formation of a pre-metastatic ecological niche *via* HIF-1α-LOX. TGF-β belongs to a protein family that is influenced by hypoxia, which leads to the secretion of TGF-β by cancer cells and stimulates angiogenesis in various types of tumors. Research by Ghosh et al. demonstrated that in hypoxic conditions, TAMs and regulatory T cells (Tregs) achieved self-renewal of CSCs by significantly increasing TGF-β expression levels and then promoting the induction of glucosylceramide synthase in melanoma CSCs through the PKCα/P38/c-Fos signaling pathway [138]. Overexpression of other cytokines such as fibronectin is similarly associated with aging triggered by external stressors, such as hypoxia. Expression of thrombospondin in the perivascular area keeps CSCs in a dormant state, while tenascin C and fibronectin produced by endothelial cells accelerate the growth of CSCs. The production of these molecules (tenascin C, fibronectin, *etc*.) that allow CSCs to leave their dormant state is associated with hypoxia, suggesting that hypoxia may also promote metastasis and development by allowing CSCs at secondary sites to leave their dormant state [135].

Angiogenesis is an essential component in maintaining the TME and plays a central role in immune evasion, overproliferation, metastasis, and therapeutic resistance. Angiogenesis is initiated by stem cells through VEGF, angiopoietin-2 (Ang-2), ERK-2, TGF-β1, IL-6, and IL-8, and angiogenic mimicry is also regulated by the stemness pathway [139]. Zhao et al. treated cells with VEGF and found that VEGF increased mammosphere formation and ALDH1 activity in triple-negative breast cancer (TNBC) MDA-MB-231, significantly increasing the abundance of tumor-initiating cells (TICs, *i.e.* CSCs) and tumor metastatic potential [140]. Further probing revealed that VEGF activated STAT3 binding to *MYC* and *SOX2* promoters and induced their expression by rapidly stimulating VEGFR-2/JAK2/STAT3 binding. Once upregulated, these three transcription factors promoted the sustained activation of other transcription factors, forming a feed-forward activation loop that drives the self-renewal program. Thus, VEGF not only had an angiogenic role but also promoted self-renewal of CSCs through the VEGFR-2/STAT3 signaling pathway. In addition, IL-6 is an important tumor growth-associated cytokine produced by lymphoid and some non-lymphoid cells, such as T lymphocytes and macrophages, which promotes tumor growth, metastasis, and invasion by activating signaling pathways and inducing angiogenesis [141].

2.3.6. Extracellular matrix

As a core component of TME, ECM also plays a key role in determining proliferative trends during angiogenesis and in regulating the differentiation capacity of CSCs by affecting cell stiffness (Fig. 3) [142,143]. Biondani et al. generated a series of 3D organic culture platforms by using a matrix consisting of different ratios of laminin-rich Matrigel and type I collagen to explore how ECM regulates the dynamics of pancreatic ductal adenocarcinoma (PDAC) CSCs [144]. Using these culture platforms, it was found that when growing on early tumor ECM, CSCs were committed to activating their growth program by secreting high levels of pro-angiogenic/growth factors and assembling them into a VEGF/VEGFR2-mediated vascular mimicry (VM) networks that eventually transdifferentiated into endothelial-like networks. Meanwhile, on Matrigel, the growth rate of the more differentiated parenchymal cancer cell population was reduced, while highly secreted VEGFR-2 by CSCs stimulated tumors to produce high invasive capacity. However, there is no fixed conclusion on the effect of ECM hardness differentiation on CSC, so the authors will not delve into it here.

2.4. Metabolism characteristics

Tumor metabolism refers to the various metabolic pathways by which cancer cells meet increased bioenergetics and biosynthetic

demands. Metabolic remodeling and abnormal alterations, known as metabolic reprogramming, exist between differentiated cancer cells and CSCs [145]. In contrast to normally differentiated cells, even with adequate oxygen supply, cancer cells catabolize excess glucose intake mainly through the glycolytic pathway [rather than the tricarboxylic acid cycle (TCA) and oxidative phosphorylation (OXPHOS) pathway], which is known as the Warburg effect [146]. Nowadays, the Warburg effect is no longer limited to alterations in glycolysis and the TCA but also includes alterations in fatty acid metabolism, amino acid metabolism, and other metabolic pathways (Fig. 4) [147]. The metabolic reprogramming of CSCs can effectively regulate important life activities such as cell proliferation, cell growth, cell migration, and cell invasion.

2.4.1. Glycolysis

The glycolytic pathway is a widely utilized pathway for the breakdown of carbon in various organisms (Fig. 4). Within CSCs, there is an elevated glucose uptake, increased expression of glycolytic enzymes, higher lactate production, and a notable rise in ATP levels compared to differentiated cancer cells. Additionally, CSCs exhibit lower levels of ROS to maintain homeostasis.

The cell adhesion molecule CD44v10 is associated with tumor invasion and malignancy. Guo et al. identified that the expression of CD44v10 in four human TNBC cell lines (MDA-MB-468, MDA-MB-231, Hs578t, and BT-549) was higher than that in human normal breast epithelial cells (MCF 10A) by IHC analysis [148]. Additionally, ectopic expression of CD44v10 was shown to increase glucose consumption and lactate secretion, while decreasing intracellular ROS levels, significantly enhancing tumorspheres formation of TNBC cells. RNA sequencing and functional annotation of CD44v10 transcriptome profiles in BT-549 cells demonstrated that glycolysis-related genes were upregulated in CD44v10 overexpressing cells. Deeper mechanistic studies revealed that CD44v10 upregulated GLUT1 by activating the MAPK/ERK and PI3K/AKT signaling pathways to promote glycolysis, thereby promoting the self-renewal of CSCs in TNBC.

HectH9, a tumor-associated protein, is a new glucose regulator. Lee et al. discovered that HectH9 was increased in prostate cancer cells induced by hypoxia conditions, whereas deletion of HectH9 increases ROS production and decreases the number and size of tumorspheres [149]. Mechanistic investigations indicated an endogenous connection between HectH9 and hexokinase 2 (HK2). As an E3 ligase of HK2, HectH9 interacted to promote the ubiquitination of HK2, regulating the mitochondrial localization of HK2. Subsequently, in conjunction with the ATP cofactor, the mitochondrial HK2 catalyzes the conversion of glucose to glucose-6-phosphate (G6P), initiating glycolysis, which is also the rate-limiting step of glycolysis. HK2, in coordination with downstream enzymes pyruvate kinase (PK) isozyme type M2 (PKM2), maintains high glycolytic efficiency, supporting the energy demands of CSCs. Lactate dehydrogenase (LDHA) catalyzes its end product, pyruvate, into lactate, providing substrate for oxidative phosphorylation and sustaining NAD^+ regeneration for continuous glycolysis [150]. The latest research by Nguyen et al. indicated that lactic acid promoted histone acetylation and epigenetically activates MYC by increasing mitochondrial metabolism and intermediate products of the tricarboxylic acid cycle, thereby raising the level of acetyl coenzyme A and reversing differentiated cancer cells into CSCs. They established organoid models TPO3 and TPO4 to study the role of lactic acid in regulating the stemness and plasticity of CSCs and its epigenetic mechanism. Research data showed that after 5 days of co-culture with lactic acid, the proportion of CSCs in TPO3 and TPO4 increased from 13 % to about 20 % and from 12 % to about 20 % respectively. Under lactic acid conditions, cell differentiation decreased significantly by about 50 %, while the dedifferentiation phenomenon of cancer differentiated cells into CSCs increased significantly by about 27 %. In addition, lactic acid increased the frequency of CSCs asymmetric division to 18.3 %, while in the control group it was only 5 % [151]. In gliomas, HK2 promotes the degradation of IκBα through phosphorylation, thereby activating the pathway, which in turn facilitates PD-L1 expression and tumor immune evasion [152]. In addition, HK2 has atypical functions that directly regulate CSCs. In small cell lung cancer, HK2 localized outside the mitochondria interacts with CD133, enhancing the interaction between the deubiquitinating enzyme USP11 and CD133. This promotes deubiquitination, thereby stabilizing the expression of CD133, which in turn upregulates the expression of OCT4 and Lin28, ultimately promoting the stemness of CSCs [153]. Overexpression of nuclear HK2 can enhance the characteristics of leukemia stem cells and reduce differentiation, while knockdown of nuclear HK2 promotes differentiation and diminishes stem cell functionality. HK2 interacts with nuclear proteins that regulate chromatin openness, increasing chromatin accessibility at DNA repair sites, which can reduce DNA double-strand breaks and confer chemoresistance to leukemia CSCs [154].

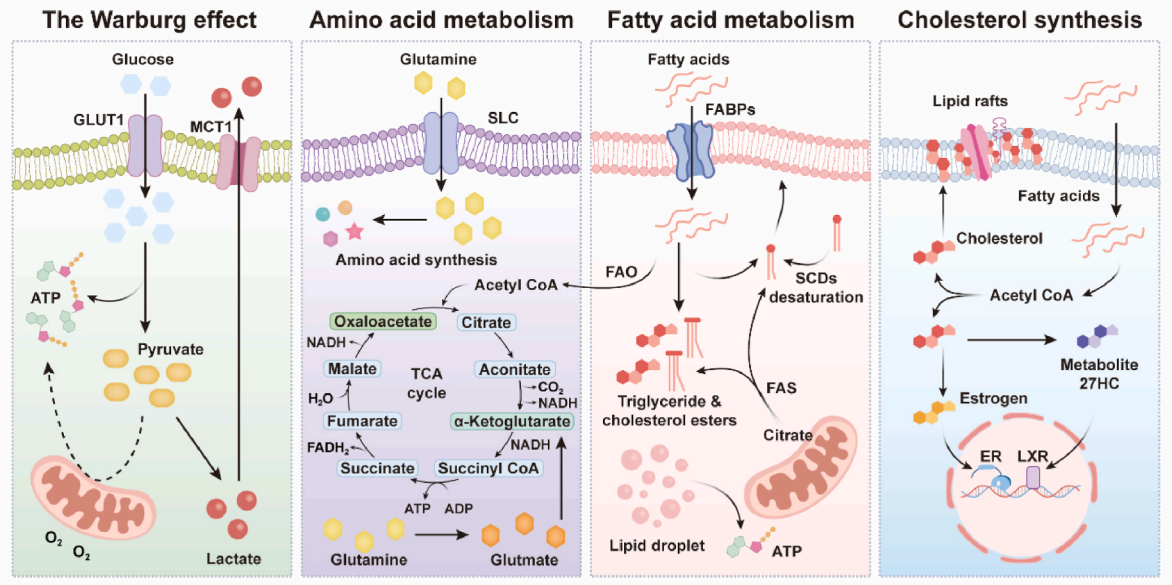

Fig. 4. Main metabolic pathways of CSCs. GLUT1: glucose transporter 1; MCT1: monocarboxylate transporter 1; SLC: solute carrier family; NADH: nicotinamide adenine dinucleotide (reduced form); $FADH_2$: flavin adenine dinucleotide (reduced form); FABPs: fatty acid binding proteins; SCDs: stearoyl-CoA desaturases; FAS: fatty acid synthase; 27HC: 27-hydroxycholesterol; ER: endoplasmic reticulum; LXR: liver X receptor.

Fat mass and obesity-associated protein (FTO) can remove m^6A modification on genes and play a key role in cancer development. Yang et al. found that removal of FTO expression in H322 and H358 lung adenocarcinoma cells with two different shRNAs (*shFTO-1* and *shFTO-2*) significantly enhanced cell proliferation and depletion of FTO accelerated migration and invasion of H322 and H358 cells [155]. Subcutaneous injection of FTO-depleted H358 cells into athymic nude mice significantly promoted tumor growth, while intravenous injection into mice enhanced lung metastasis. Mechanistic studies have shown that the Wnt signaling pathway induced histone methyltransferases EZH2 to bind to β-catenin, and the resulting protein complex binds to the binding element of the FTO promoter region, inhibiting the expression of FTO. Downregulation of FTO enhanced the m^6A level in *c-Myc* mRNA, which recruits YTH domain family protein 1 (YTHDF1) to promote ribosome loading onto m^6A-containing mRNA, thereby enhancing *c-Myc* mRNA translation. This led to high expression of the *MYC* gene and the glycolytic gene *HK2*, and promoted the glycolytic process of CSCs and tumor proliferation, metastasis, and invasion.

2.4.2. Oxidative phosphorylation

OXPHOS is essential for the metabolism of CSCs (Fig. 4). CSCs favoring OXPHOS have lower rates of glucose consumption and lactate production, slower energy production rates, but can produce more ATP and have higher mitochondrial mass.

Lee et al. performed targeted capture next-generation sequencing in 18 TNBC patients treated with neoadjuvant chemotherapy and found that stemness-related genes *MYC* and anti-apoptotic protein *MCL1* were overexpressed in post-chemotherapy TNBC [156]. Knockdown of *MYC* or *MCL1* was found to reduce mammosphere formation in MDAMB-436 and SUM159PT cells, and tumor initiation in mice *in vivo*. It was found that upregulation of Myc and MCL1 protein levels enhanced mammosphere formation in paclitaxel-resistant SUM159PT and MDA-MB-436 cells. Mechanistic analysis revealed that breast CSCs mainly rely on mitochondrial OXPHOS (mtOXPHOS), which is synergistically enhanced by *MYC* and *MCL1* to promote the enrichment of CSCs in TNBC, leading to chemoresistance. At the same time, Myc- and MCL1-induced mtOXPHOS led to increased ROS production, which subsequently induced the expression of HIF-1α to promote stemness maintenance and tumorigenesis of CSCs.

Heterogeneous oxygen supply in solid tumors leads to hypoxic and normoxic regions, in which hypoxic cells secrete increased lactate, forming an acidic TME that positively correlates with tumor metastasis. Liu et al. quantified normoxic CSCs in tumor specimens from patients with different stages of CRC and identified that the formation of more metastases in mice preprocessed with lactate-pretreated cells than with control cells [157]. Moreover, lactate treatment decreased the expression of the epithelial marker E-cadherin and increased the expression of the mesenchymal marker vimentin in normoxic CSCs. Metabolic analysis revealed that the OXPHOS activity of normoxic CSCs was enhanced after lactate treatment, while hypoxic CSCs were barely changed. At the molecular level, peroxisome proliferator-activated receptor-gamma coactivator-1α (PGC-1α), a master regulator of lactate oxidation, was increased in normoxic CSCs. In addition, PGC-1α knockdown significantly reduced the metastatic potential of normoxic CSCs. In summary, in CRC normoxic CSCs, PGC-1α cooperates with lactate oxidation to promote the OXPHOS process and facilitates the migration and invasion of normoxic CSCs.

2.4.3. Metabolic adaptation

CSCs have broad metabolic adaptations, and it is uncertain whether they mainly rely on glycolysis or OXPHOS during their survival. Different subpopulations of CSCs have various metabolic patterns, and changes in metabolism depend on a variety of factors, such as changes in oncogenes, tumor suppressor genes, hypoxic microenvironment, mtRNA mutations, genetic factors, and proliferation rates [158]. Liu et al. identified that breast CSCs exist in different mesenchymal-like and epithelial-like states by IF detection, and mesenchymal-like CSCs were more dependent on glycolysis than epithelial-like CSCs [159]. In the GBM model established by Janiszewska et al., under steady-state conditions, OXPHOS-dependent GSCs could achieve a reversible transition to a glycolytic phenotype, which was affected by environmental factors such as hypoxia [160]. Glycolysis-dependent GSCs may have a higher affinity for hypoxic environments, while OXPHOS-dependent GSCs showed a preference for the perivascular regions, and these two metabolic phenotypes could coexist in GBM. Metabolic adaptation enables CSCs to better cope with environmental changes during growth and to benefit their survival, which may be the reason for the high proliferation, invasion, and drug resistance of CSCs.

2.4.4. Lipid metabolism

In recent years, with the in-depth study on the metabolism of CSCs, it was found that fatty acid metabolism in CSCs is highly active as well (Fig. 4). It is mainly manifested in the abnormal active de novo synthesis of fatty acids, increasing the intracellular synthesis of fatty acid and cholesterol to supply energy. Additionally, the β-oxidation of fatty acids is also enhanced to improve energy utilization.

Li et al. employed IHC staining to detect the expression of sterol regulatory element-binding protein 2 (*SREBP-2*, a transcription factor that primarily controls cholesterol biosynthesis and homeostasis in normal cells) in specimens from prostate cancer patients with different Gleason grades and bone metastases, and found that SREBP-2 protein was significantly upregulated in prostate cancer and bone metastasis tumor tissues compared with normal tissues [161]. Analysis of clinical data indicated a positive correlation between the expression of SREBP-2 and poor prognosis of patients. Therefore, functional verification was performed to prove that overexpression of SREBP-2 increased the number of prostate CSCs, prostate bulb formation capacity, and tumor initiation capacity. Mechanism studies have shown that SREBP-2 is positively associated with *c-Myc* and induced its activation by directly interacting with the SREBP-2-binding element in the 5' region of the *c-Myc* promoter, thereby driving stemness and metastasis. Previous studies by Chen et al. demonstrated that hepatitis C virus (HCV) *Ns5a*-mediated ectopic expression of TLR4 in hepatocytes/hepatoblasts activated the CSC marker *Nanog*, thereby promoting the development of HCC [162,163]. Based on previous studies, *Nanog* was found to be the most consistently upregulated gene of liver specimens from alcohol-, obesity-, or HCV-induced tumor models by Chen et al. Functional studies in several mouse models of liver cancer showed that silencing *Tlr4* in CSCs could suppress the stemness genes expression and tumor growth in immunocompromised mice. Mechanistic research revealed that TLR4 acted as a mediator for the activation of *Nanog*, which controlled the expression of genes involved in the mitochondrial metabolic pathway of CSCs and hence suppressed OXPHOS. Therefore, to meet the cellular energy demand, *Nanog* had to activate fatty acid β-oxidation, an extra catabolic pathway. In conclusion, *Nanog* promotes the FAO process by regulating mitochondrial FAO gene expression, supporting CSCs self-renewal and drug resistance. Li et al. conducted a CRISPR/Cas9 screen targeting 1121 differentially expressed metabolism-related genes *in vivo* and identified 67 metabolism-related genes as candidate oncogenes for HCC. Among these, four metabolic enzymes (ACC1, ALDOA, FABP5, and HK2) were highly associated with CSC characteristics. HK2 was highly expressed in liver CSCs, and both knockdown and overexpression of HK2 could influence the expression of CSC markers CD13 and EpCAM, with consistent trends. Sphere formation assays demonstrated that shRNA-mediated elimination of HK2 inhibited tumor sphere formation, while overexpression had the opposite effect. Additionally, *in vivo* xenograft tumor experiments and *in vitro* functional assays yielded consistent results. Mechanistically, HK2 accumulates acetyl-CoA in HCC cells, induces promoter and enhancer histone acetylation, activates the transcription of the fatty acid activation enzyme ACSL4, thereby regulating fatty acid β-oxidation and modulating the maintenance of CSCs stemness [164].

2.4.5. Amino acid metabolism

Amino acids can not only serve as building blocks for proteins but also intermediate metabolites fueling multiple biosynthetic pathways (Fig. 4). Amino acid metabolism is another metabolic pathway in CSCs. CSCs exhibit a requirement for essential amino acid metabolism, such as lysine, as well as non-essential amino acids such as glutamine, which may also function as essential amino acids to meet the needs of abnormal proliferation.

Glutamine is the most highly metabolized amino acid in human PDAC. Wang et al. found that tetraspanin CD9 was overexpressed in transformed *LSL-KRas*^{G12D}; *Fbw7*$^{F/F}$; *Ck19-CreER*; *R26-LSL-YFP* (KFCkY) cells by qPCR, with high CD9 expression limited to a subgroup of KFCkY cells, namely CSCs [165]. *In vitro* studies have shown that *LSL-KRas*^{G12D}; *p53* $^{F/F}$; *Pdx1-Cre*; *Rosa26-LSL-YFP* (KPCY) cells with high CD9 expression formed more tumor xenografts than those with CD9 knockdown. Mechanistically, CD9 accelerated CSCs and cancer formation by promoting the plasma membrane localization of the glutamine transporter alanine-serine-cysteine transporter and enhancing glutamine uptake in PDAC cells, thereby enhancing the glutamine metabolism process in PDAC. In a study conducted by Wu et al., it was found that colon CSCs expressed the thrombopoietin (TPO) binding receptor CD110, which played a role in mediating liver metastasis [166]. Building on previous studies, a series of experiments including transcriptome analysis and qPCR on primary xenograft CD110^{+} cancer cells from two CRC liver metastasis cell lines (CRC102-LM and CRC108-LM) revealed increased lysine catabolism of CD110^{+} CSCs in liver metastasis lesions. Mechanistic studies revealed that TPO stimulated the binding of endogenous *MYC* to gene promoters and increased the acetylation of *H3K14* on the promoters of lysine metabolizing genes (*AASS* and *BCKDH*) to promote lysine metabolism. Lysine catabolism generated acetyl-CoA, which was used to activate p300-dependent LRP6 tyrosine phosphorylation, which ultimately activated Wnt signaling to promote self-renewal of CD110^{+} CSCs. Lysine catabolism also produces glutamate, which regulates the redox state of CD110^{+} CSCs and promotes liver colonization and drug resistance.

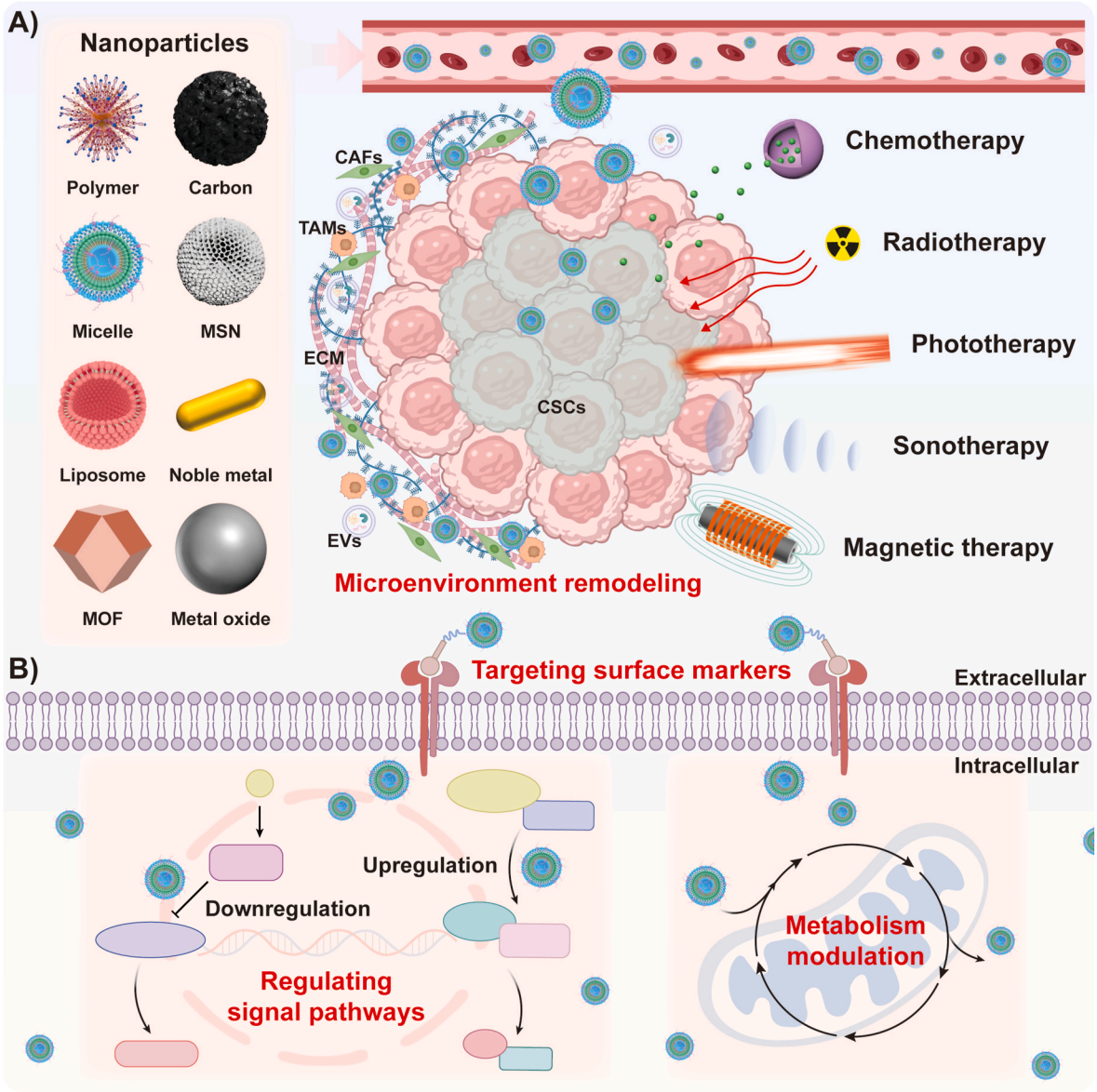

Fig. 5. A) Nanomaterial-based therapeutic strategies. B) Nanotherapeutics targeting the biological characteristics of CSCs, including targeting surface markers, modulating signal pathways, regulating microenvironments, and affecting metabolism. MSN: mesoporous silica nanoparticle; MOF: metal–organic framework.

3. Nanomaterials-based therapeutics for cancer stem cells

The significance of CSCs in cancer therapy cannot be overstated, making it imperative to develop precise strategies to eliminate CSCs and thereby enhance therapeutic outcomes. As mentioned earlier, nanotherapeutic strategies hold promise for eradicating CSCs. To date, several approaches, such as chemotherapy [25,167,168], radiotherapy [22], phototherapy [169,170], sonotherapy [24,171], and magnetic therapy [172,173], based on various NMs including organic (polymers [174], micelles [175], liposomes [176]) and inorganic (carbon [177, 178], silica [179], noble metals [180,181], and metal oxides/sulfides [182–184]) NMs, have been reported for CSC treatment (Fig. 5A). Next, we will explore the research on NMs that target the aforementioned biological characteristics of CSCs to provide insights into biological characteristics-based nanotherapeutic strategies for CSCs (Fig. 5B).

3.1. Targeting surface markers

As previously mentioned, a variety of CSC biomarkers have been identified and can serve as recognition targets for precisely characterizing and eliminating CSC populations through targeted therapies [185]. Taking CD44 as an example, it functions as a receptor for HA, enabling the use of "receptor-ligand" interactions to modify the surface of nanotherapeutics with HA for specific targeting of CD44 on CSCs. Similarly, anti-CD44 Ab can achieve active targeting through specific "antigen-antibody" recognition. The inherent modifiability of nanocarriers makes them exceptionally well-suited for this purpose. Therefore, this section summarizes nanotherapeutic strategies that utilize surface modifications of nanomaterials to actively target CSC surface markers (Table 2), thereby enabling the precise elimination of CSCs.

3.1.1. CD34

LDL is a spherical particle with an average diameter of 22 nm, with a core composed of cholesterol esters and small amounts of triglycerides, and a surface monolayer composed of phospholipid molecules and the receptor protein apolipoprotein B [221], which mediates receptor-dependent uptake in most cells [222,223]. Since Gal et al. demonstrated in 1981 that gynecological cancer cells take up more LDL than normal cells, its use as a drug-targeting vehicle for cancer chemotherapy has been of interest [224]. To determine whether intracellular subtherapeutic drug concentrations can overcome quiescent stem cells in persistent leukemia after targeted administration through the use of synthetic LDL (sLDL) particles, Zhou et al. investigated the cellular uptake of sLDL by leukemia cell lines as well as by stem/progenitor cells from patients with CML [187]. The accumulation level of sLDL was significantly higher in CML $CD34^+$ cells (MFI 148.8 ± 13.7) compared to non-CML $CD34^+$ cells (MFI 61.4 ± 5.1). Furthermore, the presence of sLDL was detected in quiescent stem cells after 72 h of exposure. Thus, drug-loaded sLDL NPs have the potential to eradicate leukemia stem cells from primary CML cells by increasing their intracellular drug concentration.

Tumor cells exhibit higher histone deacetylase (HDAC) levels than normal tissue, producing hypoacetylated nucleosomal histones that repress numerous genes including the cancer suppressor gene [225, 226]. Different from structural abnormalities that lead to irreversible loss of gene function, histone deacetylation-induced genomic silencing can be pharmacologically reversed by HDAC inhibitors (HDACi). Vorinostat (suberoylanilide hydroxamic acid) is the first U.S. Food and Drug Administration (FDA)-approved HDACi for the treatment of patients with progressive, persistent, or recurrent cutaneous T-cell lymphoma [227]. Chandran et al. using human serum albumin in combination with vorinostat developed a protein-vorinostat nanomedicine, which showed selective and superior anti-leukemia activity against heterogeneous AML patient samples and $CD34^+CD38^-$ cell lines (KG-1a) [186]. Nano-vorinostat exhibited enhanced cellular uptake in AML cell lines and patient samples compared to free vorinostat, with more than 90 % of KG-1a cells displaying internalized nano-vorinostat. In addition, nano-vorinostat had a significantly lower IC_{50} (0.5 μM) compared to free vorinostat (1 μM), inducing stronger HDAC inhibition, oxidative damage, cell cycle arrest, and apoptosis. Furthermore, the authors demonstrated the efficacy of nano-vorinostat in LSCs isolated from AML patient samples [228]. Not only did nano-vorinostat successfully ablate $CD34^+CD38^-CD123^+$ LSCs without inducing myelosuppression or hematotoxicity, but it also exerted excellent synergistic killing of leukemic bone marrow cells at a lower concentration (0.1 μM) when combined with the DNA methyltransferase inhibitor decitabine.

3.1.2. CD133

Identified as subpopulation of $CD133^+$/$ALDH1^+$, GSCs are resistant to most chemotherapy and radiotherapy (RT), leading to recurrence in GBM patients [70]. TMZ-mediated chemotherapy has a very limited effect on GBM because of the low penetration of the drugs into the brain cancer due to the presence of the blood-brain barrier (BBB) [229] and blood-brain tumor barrier (BBTB) [230]. Kim et al. developed a dual-targeted immunoliposome encapsulating TMZ (Dual-LP-TMZ) for specific delivery to GSCs using angiopep-2 (An2) peptide and anti-CD133 mAb [190]. Regardless of the TMZ encapsulation, antibody-coupled immunoliposomes showed the highest cellular binding (87.89–91.46 %) in GSCs, resulting in a 425-fold increase in cytotoxicity of Dual-LP-TMZ compared to free TMZ, which significantly increased inhibition of GSCs and reduced drug resistance. *In vivo* studies demonstrated that conjugation of An2 peptide and CD133 mAb was effective in enabling immunoliposomes to penetrate the BBB and deliver encapsulated TMZ to GSCs, resulting in a significant reduction in tumor size of tumor-bearing mice, whose median survival time (MST) was prolonged to 49.2 days. Wang et al. modified SWNTs with CD133 mAb (anti-CD133-SWNTs) for specific targeting and clearance of $CD133^+$ GSCs [189]. Anti-CD133-SWNTs could be internalized in large quantities by $CD133^+$ GBM cells while they were present only in the periphery of $CD133^-$ GBM cells. After irradiation by 808 nm NIR light in a mix-cultured $CD133^+$/$CD133^-$ cells, the $CD133^+$ GBM cells were selectively removed and lost their tumorigenic ability to self-renew and promote GBM growth *in vivo*. O^6-methylguanine-DNA methyltransferase (MGMT) is a repair enzyme that could repair DNA damage caused by TMZ [231], whose level is associated with TMZ resistance in GBM tumors [232,233]. Therefore, effective down-regulation of MGMT activity may be a critical element in overcoming TMZ resistance. Kim et al. developed a tumor-targeting immunoliposome nanocomplex (scL) that could cross the BBB and target delivery of the wild-type (wt) *p53* gene to GBM as well as CSCs [234]. Systemic administration of scL-p53 not only silences MGMT expression (down-regulated by ~95 %) and induces GBM xenografts apoptosis, but also increases TMZ sensitivity and apoptosis in $CD133^+$ CSCs. In addition, the combination with scL-p53 improved the *in vivo* antitumor efficacy of TMZ and prolonged the mice survival of mice with highly TMZ-resistant GBM.

CD133 is also considered as a marker for CSCs in many other tumors. Abou-ElNaga et al. used PLGA NPs as a drug delivery system for PTX, supported by incorporation of folic acid (FA) as the ligand, and found that its IC_{50} against ovarian CSCs was significantly reduced (free PTX was approximately 2.49-fold that of PTX-loaded FA/PLGA NPs) [235]. The expression of chemoresistance genes *ABCG2* and multidrug resistance 1 (*MDR1*) was limited after the application of PTX-loaded PLGA NPs, and the addition of FA as a ligand increased the potential of PLGA NPs to target ovarian CSCs *in vivo* and enhanced the tumor suppression efficiency by inducing apoptosis. Wang et al. loaded 1,4,7,10-tetraazacyclododecane-1,4,7,10-tetraacetic acid (DOTA)-Gd and CD133 mAb onto black titanium dioxide ($bTiO_2$) NPs, and designed a novel $bTiO_2$-Gd-CD133mAb nanoprobe with an r_1 relaxation rate (34.394 mM^{-1} s^{-1}) about 7.5 times higher than that of commercially available Magnevist [188]. Thus, the $bTiO_2$-Gd-CD133mAb nanoprobe exhibited enhanced magnetic resonance imaging (MRI) compared to $bTiO_2$-Gd in CD133-overexpressing pancreatic CSCs model, significantly improving

Table 2
Nanomedicine targeting CSCs surface markers.

Biomarker	Functionalization strategies	Nanocarrier	Size	Cargo	Stimuli	CSC type	Ref
CD34	/	HSA-vorinostat nano-coacervate	~100 nm	vorinostat	/	AML	[186]
	/	synthetic LDL (sLDL)	19 ± 0.7 nm	/	/	CML	[187]
CD133	surface conjugation with anti-CD133 Ab	Fe_3O_4@$mSiO_2$ nanoparticle (NP)	50 ± 10 nm	tirapazamine (TPZ)	alternating magnetic field (AMF)	breast cancer	[172]
	surface conjugation with anti-CD133 mAb	black TiO_2 NP	135 nm	/	near-infrared (NIR) light	pancreatic cancer	[188]
	surface conjugation with anti-CD133 mAb	single-walled carbon nanotube (SWNT)	~233 nm	/	NIR light	glioblastoma	[189]
	conjugation with anti-CD133 mAb	immunoliposome	203.4 nm	temozolomide (TMZ)	/	glioblastoma	[190]
	electrostatic interaction between DOTAP and anti-CD133 mAb	immunoliposome	64.79 nm	LXR inhibitor SR9243	/	CRC	[191]
	self-assembly with CD133 targeting peptides	VPX-CD133/SMOCr nanocomplex	100–120 nm	Smo CRISPR and serine hydroxymethyl transferase 1 (SHMT1) siRNA (*siSHMT1*)	ultraviolet (UV) light	glioblastoma	[192]
	self-assembly with CD133 targeting peptides	CEP-LP@S/D	115 nm	doxorubicin (DOX) and salinomycin (SAL)	glutathione (GSH)	liver cancer	[193]
	surface conjugation with CD133 aptamers	SAL PLGA NP	133.4 nm	SAL	/	osteosarcoma	[194]
	label with CD133 aptamers	SAL-entrapped lipid-polymer NP	98.5 ± 7.8 nm	SAL	/	osteosarcoma	[195]
	/	bovine serum albumin (BSA)-modified gold nanorod (GNR) (GNR-BSA)	32.1 ± 4.6 nm in length, 7.7 ± 1.0 nm in width	/	NIR light	neuroblastoma	[196]
CD44	surface coating with HA	C60@silica NP	~60 nm	DOX and indocyanine green (ICG)	NIR light	breast cancer	[178]
	surface decoration with HA	MSN-Mn	~160 nm	DOX and tariquidar (TQR)	pH; GSH	cervical cancer and lung cancer	[179]
	surface decoration with HA	GNR	39.6 ± 4.1 nm in length, 10.5 ± 2.3 nm in width	diclofenac	NIR light	cervical cancer	[197]
	surface modification of HA by ligand exchange reaction	superparamagnetic iron oxide NP (SPIONP)	114 nm	/	AMF	HNSCC	[198]
	bound HA to the surface by electrostatic interaction	Fe_3O_4@PPr (polypyrrole)	82 nm	Notch inhibitor DAPT	AMF	breast cancer	[199]
	precipitation HA on the surface	conjugated polymer NP	109 nm	/	/	glioblastoma	[200]
	Modifying HA on multiple attachment sites of dendritic polyglycerol (dPG)	gold nanostars (GNSs)-dPG nanoplatform	60.7 nm	retinoic acid (RA)	NIR light	breast cancer	[180]
	integrated HA on the surface of red blood cell membrane	Prussian blue NP	100 nm	/	NIR light	breast cancer	[201]
	grafting PLGA onto the backbone of HA	HA-SS-PLGA NPs	245.3 nm	DOX and cyclopamine (CYC)	D,L-dithiothreitol and GSH	breast cancer	[202]
	conjugation of menthone 1,2-glycerol ketal to the backbone of oligosaccharides of HA	Cur-PTX-NE	120.6 ± 4.5 nm	curcumin (CUR) and paclitaxel (PTX)	pH	breast cancer	[203]
	surface conjugation with chitosan (CHI) and HA	carbon nanotube (CNT)	5–20 μm in length, 1–2 nm in diameter	SAL	pH	gastric cancer	[204]
	self-assembly with CHI	$iPBC_{GC}$ NP	98 nm	gambogic acid and croconium	pH and NIR light	breast cancer	[205]
	Surface-decoration with CHI	nDOX	~250–300 nm at 22 °C, ~20 nm at 37 °C	DOX	pH	breast cancer	[206]
	covalent immobilization of anti-CD44 Ab on the surface	IONP	59 nm	gemcitabine (GEM)	GSH	breast cancer and pancreatic cancer	[207]
	surface modification with anti-CD44 Ab	SPIONP	~100 nm	/	AMF	HNSCC	[182]
	surface modification with anti-CD44 Ab	Fe_3O_4@SiNP	50 nm	heat shock protein 90 (HSP90) inhibitor 17-DMAG	AMF	breast cancer	[208]
	surface conjugation with anti-CD44 Ab	MoS_2 nanosheet	162.4 ± 33.5 nm in length, 103.1 ± 21.9 nm in width	/	NIR light	breast cancer	[184]

(*continued on next page*)

Table 2 (*continued*)

Biomarker	Functionalization strategies	Nanocarrier	Size	Cargo	Stimuli	CSC type	Ref
	surface conjugation with anti-CD44 Ab	SWCNT	250–300 nm	SAL and PTX	pH	breast cancer	[209]
	surface decoration with anti-CD44v6 Fab fragment	polymeric micelle (PM) NP	~23 nm	niclosamide (NCS)	pH	CRC	[210]
CD24	surface conjugation with anti-CD24 Ab	PLGA-PEG NP	~200 nm	docetaxel (DTX)	/	prostate cancer	[211]
CD90	conjugation with anti-CD90 Ab	CD90@TM	130 ± 4.6 nm	/	AMF	liver cancer	[212]
	surface conjugation with anti-CD90 Ab	CdSe quantum dot	/	/	UV light	leukemia	[213]
EpCAM	surface conjugation with anti-EpCAM RNA aptamer	PEG-PLGA nanopolymersome	124 ± 0.9 nm	DOX	pH	breast cancer	[214]
	surface conjugation with EpCAM aptamer	SWNT–PEI–piperazine conjugate	85.08 nm	siRNA	/	breast cancer	[215]
	decoration with EpCAM-targeting RNA aptamer	nanoliposome	84.2 nm	enhanced green fluorescent protein (EGFP) plasmid and siRNA against GFP	pH	breast cancer, and CRC	[216]
	complexed with EpCAM aptamer	PEI:citrate nanocore	156 ± 6.8 nm	EpCAM siRNA	/	breast cancer and retinoblastoma	[217]
	surface conjugation with anti-EpCAM RNA aptamer	PEG–PLGA NP	124 ± 0.9 nm	DOX	/	lung cancer	[20]
	surface decoration with the EpCAM Ab	GNRs@PM	110 ± 0.7 nm	Adriamycin	NIR light	HCC	[218]
	click reaction with between NPs and anti-EpCAM Ab	upconverted NP (UCNP)	45.5 nm	mitoxantrone	NIR light	HCC	[219]
	self-assembly with EpCAM targeting peptides	CEP-LP@S/D	115 nm	DOX and SAL	GSH	liver cancer	[193]
	surface binding with anti-EpCAM Ab	Polymer vesicle	232 nm	DOX and siRNA	/	liver cancer	[220]

the photothermal ablation efficiency to PANC-1 cells. Shahabad et al. investigated the photothermal effect of GNR-BSA to induce autophagy death of human neuroblastoma CSCs [196]. Irradiated by NIR light, GNR-BSA can kill CSCs through the dysregulation of temperature-related autophagic mechanisms. At mild (43 °C) to moderate (46 °C) temperatures, PTT-exposed CSCs died mainly of autophagy and apoptosis. Whereas, higher (49 °C) temperatures resulted in autophagy inhibition and a shift of CSCs death from apoptosis to necrosis. In addition, GNR-BSA-mediated PTT inhibited the clonogenic ability of CSCs, and the number of spherical cell aggregates was significantly reduced, whose formation is a notable feature of CSCs. Liu et al. designed and synthesized a carrier platform with MDR1-targeting siRNA (*siMDR1*) consisting of PEI_{1200}, PEG, and biodegradable lipid cross-linking moieties, which effectively reduced the expression of *MDR1* in human colon CSCs ($CD133^+$-enriched) [236]. The lipid component of nanocomplex plays a key role in transfection, which had the best gene silencing effect with the composition of $PEI\text{-}Lipid_{1:16}$. *siMDR1* silencing dramatically increased the PTX sensitivity of $CD133^+$ cells, synergistically improving the therapeutic efficacy compared to the free PTX. SAL is a polyether ionophore antibiotic that reduces tumor incidence by targeting breast CSCs and is effective against several cancer types [237,238]. Ni et al. prepared SAL-loaded PEGylated PLGA NP coupled with CD133 aptamer (Ap-SAL-NP) and evaluated their targeting and cytotoxicity against $CD133^+$ osteosarcoma CSCs [194]. Ap-SAL-NP could selectively kill osteosarcoma CSCs both *in vitro* and *in vivo*, resulting in a 5-fold reduction in the number of Saos-2 tumorspheres and a significant reduction in the proportion of Saos-2 $CD133^+$ cells compared to the untreated group, showing optimal therapeutic efficacy in Saos-2 xenograft mice. Building on this, the group further developed SAL-entrapped lipid-polymer NPs decorated with CD133 and EGF receptor aptamer (CESP) to simultaneously target osteosarcoma cells and osteosarcoma CSCs for improved therapeutic efficacy [195], and resulted in a 90 % inhibition in tumor volume in osteosarcoma-bearing mice.

3.1.3. CD44

HA has a high binding selectivity to CD44 and has been widely used as a powerful tumor-recognizing fraction in cancer therapy due to its excellent physiological properties and high chemical modification [239,240]. Wang et al. developed a fullerene (C60)-silica NPs system with surface-modified with HA (HC60S), subsequently loaded with DOX and ICG (HC60S-DI), which can be used to achieve combined chemotherapy, photothermal therapy (PTT), and photodynamic therapy (PDT) as a single nanoplatform [178]. The ~60 nm-sized HC60S-DI is suitable for cellular uptake and passive tumor targeting, and can actively target to CD44 overexpressed on breast CSCs *via* HA. In addition, its high drug loading capacity (>90 %) allows for valid drug delivery to CSCs and enables controlled release under NIR light irradiation, which combines with PDT and PTT to effectively destroy breast CSCs. Joseph et al. designed a targeted theranostic nano vehicle (TTNV) using manganese-doped mesoporous silica NPs (MSN-Mn) co-delivery of DOX and drug efflux inhibitor TQR [179]. TTNV could avoid drug leakage by CHI-coated modification, which was subsequently chemically modified with FA and HA to promote folate receptor (FR)-mediated uptake of cancer cells and CD44-mediated uptake of CSCs, respectively. TQR could reverse the biochemical structure of drug-resistant cells, retaining DOX within the cells, achieving sensitization of drug-resistant cells to DOX as well as the precise elimination of CSCs. In addition, the immunostimulatory potential of MSN-Mn selectively enhances the immune response of DOX-exposed cancer cells to the tumor antigens *via* immunogenic cell death (ICD). Ultimately, tumor targeting and synergistic therapy contributed to the appealing tumor elimination on both FR-positive and CD44-positive tumor-bearing mice by TTNV. Hyperthermia therapy (HT) is a cancer therapy strategy that directly kills cells, radiosensitization, and promotes tumor reoxygenation [241,242]. Thapa et al. investigated the cytotoxicity and HT sensitivity of HA-mediated dextran-coated superparamagnetic iron oxide NPs (HA-DESPIONs) in CD44-expressing HNSCC and its CSCs [198], and found that HA-DESPIONs were nontoxic at moderate concentrations (100 μg mL^{-1}) but enhanced the effect of physical HT (≥42 °C) by inducing apoptosis

leading to a decrease in cell survival. Moreover, Rao et al. constructed CHI-decorated DOX-encapsulated polymer NPs (nDOX), enabling specific targeting of the overexpressed CD44 receptor on CSCs [206]. The targeting specificity of nDOX may stem from the shared N-acetyl-D--glucosamine unit between the CHI and HA, which is likely responsible for the interaction with the CD44 receptor. Compared to free DOX, the cytotoxicity of nDOX increased by 6-fold, and it reduced tumor size in an orthotopic xenograft tumor model without significant systemic toxicity.

Antibodies against cancer cell-specific membrane markers are another targeting strategy because of their high affinity for the corresponding antigens. Aires et al. used magnetic iron oxide NPs (MNPs) covalently loaded with GEM and modified with an anti-CD44 antibody (MNP-GEM-antiCD44) for selectively treating $CD44^+$ cancer cells [207]. Anti-CD44 antibody functionalized MNPs could specifically bind to overexpressed CD44 receptors on pancreatic and breast cancer cells, whereas covalently-immobilized GEM on MNPs showed selective and rapid release (96–98 % at 8 h) under intracellular conditions. Therefore, the antitumor efficacy of MNP-GEM-antiCD44 was significantly improved compared to free GEM and MNP-GEM. Further, an anti-CD44 antibody-modified SPIONP (CD44-SPIONP) was prepared for targeted magnetic hyperthermia of CD44 overexpressing CSCs by Su et al. [182] CD44-SPIONPs can target HNSCC and CSCs, and hyperthermia production under the AMF significantly reduces cell viability, leading to programmed death of CSCs. Eventually, CD44-SPIONPs-mediated magnetic hyperthermia significantly inhibited (33.43 %) the growth of the grafted Cal-27 tumors model. A major challenge of magnetic hyperthermia is the overexpression of HSP90, a highly conserved molecular chaperone that protects CSCs from further therapy-induced damage, leading to treatment failure [243,244]. Based on this, Liu et al. utilized silica NPs to encapsulate Fe_3O_4 core and HSP90 inhibitor (HSPI, 17-DMAG) and coated with a specific fluorescent dye conjugated-CD44 antibody, developed a multifunctional CD44-HSPI/Fe_3O_4@SiNP, which was used for CSC-originated cancer therapy by combining thermotherapy and chemotherapy [208]. CD44-HSPI/Fe_3O_4@SiNP is located in the endosomes after entering the cells *via* endocytosis, which is also the transfer location of extracellular HSP90 (eHSP90). Consequently, the treatment can simultaneously inhibit the expression of eHSP90, which in turn eliminates the breast CSCs by attenuating several key signaling pathways (PI3K/Akt, G protein, and Ras signaling). Both *in vitro* and *in vivo* results demonstrated that CD44-HSPI/Fe_3O_4@SiNP-mediated combination therapy effectively reduced breast CSCs, with significantly lower expression of CD44 and CD133 compared to untreated tumors. In this work, the combination therapy of hyperthermia and chemotherapy was also extended to ovarian CSCs and hepatic CSCs, and significantly suppressed the survival of both CSCs. In addition, modification of the silica surface with a lung CSC-specific antibody (CD20) yielded CD20-HSPI&Fe_3O_4@SiNPs that could target and kill lung CSCs, which also significantly inhibited tumor growth and metastasis in lung CSC-initiated tumor-bearing mice model [245]. Dou et al. investigated the efficacy of a mAb against the breast cancer resistance protein ABCG2 in combination with silver NPs (AgNPs) and vincristine (VCR) for the targeted therapy of myeloma CSCs [246]. $CD44^+CD24^-$ cells showed features of CSCs, exhibiting higher proliferation, clonogenicity, migration capacity, and drug resistance, larger side population fraction, and greater carcinogenicity in mice, in addition to significantly upregulating ABCG2 expression. Anti-ABCG2 mAb combination with AgNPs and VCR remarkably induces apoptosis on $CD44^+CD24^-$ by *in vitro*, whose *in vivo* therapeutic effect may be due to the specific action of mAb targeting ABCG2 on CSCs, blocking the efflux of VCR and AgNPs from the cells to produce cytotoxic effects on $CD44^+CD24^-$ CSCs and prolonging the release of VCR. And the results showed that combination therapy effectively inhibited the growth of $CD44^+CD24^-$ cells and prolonged the survival of myeloma-bearing mice. Furthermore, Zhu et al. proposed a cascade-responsive dynamic nano-assembly (named $iPBC_{GC}$) as a photothermal-chemotherapy agent that effectively targeted CSCs for metastasis prevention to achieve the elimination of CSCs in superficial cancers or in post-surgery tissues [205]. $iPBC_{GC}$ was constructed by encapsulating the HSP90 inhibitor gambogic acid and croconium (CR)-based organic photothermal agent (CR_{bio}) in a redox-sensitive CHI matrices and modifying the iRGD cyclic peptide on the surface. iRGD can be rapidly detached under faintly acidic TME, inducing the penetration of NPs into tumors either by themselves or with the help of photothermal effects, promoting the CHI NPs to reach CSCs. Under the synergistic effect of HSP inhibition and chemosensitization, $iPBC_{GC}$ could completely remove $CD44^+CD24^-$ CSCs and non-CSCs by mild PTT. Ultimately, the $iPBC_{GC}$-mediated PTT not only achieved a 76 % tumor inhibition rate in a subcutaneous tumor model but also completely inhibited the lung tumor seeding and effectively suppressed tumor metastasis to the lung and liver, by effectively eradicating CSCs in the tumorspheres.

Differentiation therapy, which converts CSCs from a dedifferentiated high stemness to a differentiated low stemness through the use of small molecules such as second messengers or RA, has recently received a lot of attention [25,247]. Pan et al. developed an RA-loaded GNSs-dPG as a CSC-specific targeting nanoplatform for enhancing the therapeutic effect of PTT on breast CSCs [180]. By modifying HA on multiple attachment sites of dPG, the GNSs-dPG could have multivalent targeting ability through overexpressed CD44 on breast CSCs. RA-induced differentiation of CSCs synergistically with PTT inhibited self-renewal and tumor growth of breast CSCs while significantly down-regulating the expression of stemness genes, such as *OCT4*, *Nanog*, and *SOX2*, and reducing CSC-driven tumorspheres formation. Tumor growth and CSCs *in vivo* were also effectively inhibited and eliminated, thus preventing tumor recurrence. Recently, a differentiation strategy to photothermally attenuate cancer stemness has been reported by Liu et al. by employing CD44-targeted MoS_2 nanosheet to modulate CD44-regulated signaling activities and induce phenotypic converts in cancer cells from mesenchymal (stem-like) to epithelial (less stem-like) [184]. MoS_2 nanosheet, which has good biocompatibility and easy surface modification, was endowed CD44-targeting capability by coating with a mixture of protein A (PA) and BSA on surface (MoS_2@PA), followed by conjugating with CD44 antibody (MoS_2@PA@CD44Ab). Unlike conventional PTT to ablate cancer cells by hyperthermia, MoS_2@PA@CD44Ab-mediated photothermal differentiation modulated CSCs differentiation-involved specific cellular activities through a mild photothermal effect (43 °C), whose feasibility has been demonstrated on TNBC and malignant prostate cancer cell lines. Importantly, the authors revealed the molecular mechanism that reverse the EMT process by MoS_2@CD44Ab and PTT: First, cellular uptake of MoS_2@CD44Ab would deplete membrane CD44, reduce the recruitment of phosphorylated ezrin/radixin/moesin (p-ERM) from the cytoplasm to decrease the formation of the CD44-p-ERM complex and its recruitment to the RhoA inhibitor, RhoGDIα (Rho guanine nucleotide dissociation inhibitor alpha), causing the downregulation of RhoA activation. Subsequently, mild photothermal effects reduced the p-ERM for the formation of the CD44-p-ERM complex by disrupting the ERM phosphorylation, thus further hindering the recruitment of RhoGDIα and the activation of RhoA. These ultimately led to the downregulation of EMT transcription factors, thereby reversing the EMT process. By driving phenotypic changes and differentiation of CSCs, photothermal differentiation attenuated cancer cell stemness, drug resistance, migration, and invasion. Moreover, due to the wide availability of CD44 biomarkers, this approach might be applicable to a variety of cancers.

3.1.4. CD24

Bharali synthesized anti-CD24-modified PLGA-PEG NPs for targeted delivery of encapsulated DTX and evaluated therapeutic efficacy in a prostate cancer mouse model [211]. It can be observed from *in vitro* experiments that the NPs can be efficiently uptake by CD24-overexpressing but not $CD24^-$ cell lines. In the $CD24^+$ PC3M prostate tumor-bearing mice model, anti-CD24-modified NPs preferentially accumulated in tumors 24 h after a single injection, and the

accumulation of DTX was ~10-fold higher compared to non-modified NPs, resulting in reduced tumor mass and tumor viability. Wang et al. encapsulated CUR in stearic acid-g-chitosan oligosaccharide (CSO-SA) micelle to surmount the water insolubility and instability of CUR [248]. CUR-loaded CSO-SA micelles owned excellent cellular uptake to increase the CUR accumulation within cancer cells. It also had a valid antiproliferative effect on primary CRC cells *in vitro*, with a ~6-fold increase in inhibition compared to free CUR with the same concentration. Most of all, CUR-loaded CSO-SA micelle could effectively inhibit subpopulations of $CD44^+/CD24^+$ cells both *in vitro* and *in vivo*, indicating its potential to eliminate colorectal CSCs. Atkinson et al. identified gold nanoshells as thermal-enhanced radiosensitizers that greatly reduced the radioresistance of an enriched subpopulation of $Lin^-CD29^HCD24^H$ CSCs [22]. CSC subpopulations are more resistant to treatment with 6 Gy ionizing radiation (IR) than most other cancer cells, resulting in an increase in proportion 48–72 h after RT. Whereas, HT could sensitize CSCs to IR, which achieves a greater reduction in tumor volume without increasing the proportion. Gold nanoshell-mediated IR plus HT not only reduced the oncogenicity of residual cancer cells but also caused them to exhibit more differentiated phenotypes, achieving a better RT prognosis. In addition, IR + HT-mediated thermal radiosensitization prevented DNA repair in CSC subpopulations, probably through thermal effect on nucleoprotein unfolding, inhibiting radiation-induced double-strand breaks (DSBs) repair, or altering how DSBs are recognized or processed [249]. Ultimately, even in highly resistant TNBC, moderate HT could be effective in increasing the sensitivity of resistant CSCs to IR.

3.1.5. CD90

Zheng et al. adopted different antibody-modified PEG immunoliposomes loaded with TGF-β inhibitors and compared the effects on targeting T cells *via* CD90 (internalizing receptor) or CD45 (non-internalizing receptor) [250]. When directly applied liposomal TGF-β inhibitors with two targeting ligands to lymphocytes *in vivo*, adoptive cell therapy with melanoma-specific $CD8^+$ T-cells supported by repeated injections of anti-CD90-targeted liposomes slowed tumor growth and significantly improved survival more than anti-CD45-targeted liposomes. Yang et al. reported thermosensitive magnetoliposomes (TMs) containing magnetic Fe_3O_4 and CD90 (CD90@TMs) for the targeting and elimination of $CD90^+$ liver CSCs [212]. After effectively targeting to $CD90^+$ liver CSCs, CD90@TMs showed significantly lower IC_{50} (3.7 ± 0.2 μg mL^{-1}) than the control group (15.7 ± 3 μg mL^{-1}) and TMs group (7.8 ± 1.1 μg mL^{-1}) in the presence of AMF. By reducing the number of $CD90^+$ liver CSCs, the CD90@TMs-triggered magnetic hyperthermia could inhibit the growth rate of tumors in liver CSC-bearing mice. Zou et al. encapsulated two types of silica NPs with significantly different stiffness in mesenchymal stem cell (MSC) membranes (MSC membrane-coated silica NPs, MCSNs) and found that compared to the rigid MCSN (Young's modulus 2.3 GPa), the uptake rate of soft MCSN (Young's modulus 44.0 MPa) was much lower by macrophages, but significantly higher by cancer cells [251]. This phenomenon was attributed to the soft MCSN can form a membrane coating enriched with proteins, particularly containing high levels of MSC chemokine factor CXCR4 and MSC surface marker CD90. Consequently, the soft MCSN enhanced cancer cell uptake *via* the CD90/integrin receptor-mediated pathway and the CXCR4/SDF-1 pathway. Additionally, Bakalova et al. modified CdSe quantum dots with anti-CD90 antibodies for targeting $CD90^+$ leukemia cells to sensitize them to ultraviolet light irradiation and enhanced the PDT effect of the photosensitizer [213].

3.1.6. EpCAM

Aptamer-coupled NPs are delivery systems capable of enhancing cellular uptake through specific binding to cancer cells. EpCAM, as a marker of CSCs, is highly expressed in a variety of adenocarcinoma cell lines and minimally expressed in normal cells, enabling it a versatile target for nucleic acid aptamer-based therapies for CSCs. Moitra et al. developed an EpCAM-targeting RNA aptamer (named $[C5C]_8$-D_{24}-T_1) and doped it into the hydrophobic layer of a pH-responsive cationic co-liposome to selectively deliver genes to EpCAM-overexpressing CSCs [216]. The aptamer is integrated into the bilayer assembly by linking to the cholesterol and labeled with the DY647 fluorescent dye to facilitate monitoring of their internalization pathway, which directs pH-responsive co-liposomes to efficiently and selectively deliver EGFP plasmid and GFP-against siRNA to the cancer site. Subramanian et al. investigated target-specific delivery of DOX using RNA aptamer against EpCAM in retinoblastoma cells [252]. The authors synthesized DOX conjugate of chimeric EpCAM aptamer (EpDT3-Dox) and scrambled aptamer (Scr-EpDT3-Dox), respectively, and validated targeting and efficacy on Y79, WERI-Rb1, and Müller glial cells. In contrast to noncancerous Müller glial cells, EpDT3-Dox could specifically target CSCs and cause cytotoxicity, whereas Scr-EpDT3-Dox showed no significant binding or subsequent cytotoxicity in either cell line. Alibolandi et al. covalently coupled EpCAM aptamer to DOX-loaded nanopolymersomes by the pH gradient method to prepare EpCAM-targeted PEG-PLGA nanopolymersomes [20,214]. Targeted nanopolymersomes exhibited efficient cellular uptake and controlled release, with significantly higher cytotoxicity against $EpCAM^+$ cancer cells than non-targeted nanopolymersomes, improving the therapeutic index. Analogously, Subramanian et al. employing EpCAM aptamer and EpCAM siRNA developed an aptamer-PEI-siRNA nanocomplex for EpCAM targeting to deliver siRNA and silence target genes [217]. In EpCAM-positive cancer cells, the nanocomplex inhibited more cell proliferation than scrambled aptamer-loaded nanocomplexes and showed potential for possible EpCAM targeting *in vivo*. Since EpCAM is the CSC marker, this aptamer-based targeted drug delivery system would prevent the adverse effects of nonspecific drug activity and precisely kill CSCs.

In addition to aptamer, there are also other strategies being developed for targeting EpCAM. Wang et al. reported a redox-responsive dual-targeting liposome for co-delivery of DOX and SAL (CEP-LP@S/D) for synergistic therapy of liver CSCs [193]. Based on the Y-shaped ligands formed by the binding of CD133-and EpCAM-targeting peptides (CEP) and anchored to the surface of liposomes, CEP-LP@S/D can selectively target $CD133^+$ $EpCAM^+$ liver CSCs. After endocytosis into the cytoplasm, the high-concentration GSH will break the disulfide bonds in the liposome, inducing a fast release of DOX and SAL, which synergistically inhibiting tumor growth and reducing CSC stemness. In addition, this GSH-responsive co-delivery system also eliminated non-CSC subpopulations, showing high antitumor efficacy both *in vitro* and *in vivo*. Chen et al. designed an anti-EpCAM mAb-labeled CSC-targeting polymersome as a nanocarrier for anticancer drug and siRNA to surmount the drug resistance of CSCs by silencing the oncogenes [220]. As the polymersome was labeled by CSC-specific EpCAM-mAb, it had a high delivery efficiency for both DOX and siRNA. The fluorescence intensity of DOX within the $EpCAM^+$ CSCs increased from 110.6 ± 9.9 to 182.3 ± 4.1 compared to the unlabeled one, and the relative level of the target gene (*miR-429*) decreased to 22 % of the untreated group, as well as being more pronounced than that of the non-targeted vesicle. Therefore, the IC_{50} value of DOX-loaded CSC-targeted polymersome (0.051 μg mL^{-1}) was only one-fifth of the non-targeted vesicle (0.241 μg mL^{-1}), showing better CSC killing and tumor growth inhibition ability. Similarly, anti-EpCAM antibodies have been used to modify GNRs [218] and up-conversion NPs [219] for targeted combination therapy against CSCs.

3.2. Regulating signal pathways

The Wnt, Hh, and Notch signaling pathways play critical roles in various CSCs, making them promising targets for CSC-directed therapies [253]. Additionally, small-molecule compounds such as sulforaphane [254] and CUR [255] have demonstrated potent CSC-targeting and killing effects. However, inhibitors of these pathways or small-molecule

drugs often face significant challenges, including poor stability, low solubility, rapid systemic clearance, short half-life, and limited cellular uptake. For instance, Hh pathway inhibitor CYC [256] exhibits poor water solubility, which severely restricts its clinical application. The initial application of nanomaterials in cancer therapy stemmed from their ability to improve the pharmacokinetics and toxicity profiles of drugs and enhance their accumulation in tumors [257]. Following the discussion in the previous section on how nanocarriers enhance CSC targeting through surface modifications, this section will focus on the use of nanocarriers to deliver inhibitors or drugs for the modulation of CSC-related signaling pathways.

3.2.1. *Wnt/β-catenin signaling pathway*

The Wnt/β-catenin signaling pathway is highly associated with the development of various cancers, and targeting this signaling pathway is a promising approach for cancer therapy [258,259]. Feng et al. synthesized dual stimulus-responsive nanotheranostics (OBX-MMNs) consisting of melanin-coated magnetic NPs (MMNs) and a Wnt signaling inhibitor obatoclax (OBX), for multimodal imaging-guided mild hyperthermia-enhanced chemotherapy [260]. OBX-MMNs enable drug release in response to pH/light dual stimulation, which increases 2.7-fold of OBX accumulation in cancer cells and enhances the inhibition of the Wnt/β-catenin signaling pathway. The use of light as an exogenous stimulus to promote drug release and cellular uptake allows spatiotemporal control of the therapeutic effect and significantly reduces the systemic toxicity of chemotherapeutic agents. In addition, MMNs can be used as MRI and photoacoustic imaging (PAI) contrast agents, thus OBX-MMNs-mediated photothermal-chemical combination therapy guided by dual-modality imaging could achieve complete tumor elimination and 80 % of mice survived longer than 42 days. CD44v6 is a biomarker for advanced CRC and CSCs, Andrade et al. developed amphiphilic polymeric micelles chemically modified with an antibody fragment against CD44v6 (Fab-CD44v6) and loaded with the Wnt/β-catenin pathway inhibitor NCS, termed PM-NCS:Fab, for the treatment of colorectal CSCs and circulating cancer cells [210]. The Fab-CD44v6-modified polymer micelles could effectively target the $CD44v6^+$ subpopulation (CSCs), exhibiting significant NCS toxicity against colonspheres, and reducing circulating cancer cells in tumor-bearing mice.

BCL9l/BCL9 is a member of the nuclear complex that triggers the transcription of classical Wnt target genes, and BCL9l is also one of the major factors regulating the switch between the adhesion and transcriptional functions of β-catenin [261,262]. Thereafter, Mohammadi et al. physically attached an RNA aptamer against EpCAM (EpDT3) to a SWNT-coupled piperazine-PEI derivative based on SWNT to deliver siRNA targeting BCL9l to $EpCAM^+$ cells for gene therapy of breast cancer [215]. The vector-aptamer/siRNA nanocomplex specifically induced more than 20 % apoptosis in EpCAM-positive cell lines compared to EpCAM-negative cells. Moreover, the nanocomplex could inhibit BCL9l expression in $EpCAM^+$ cells through aptamer-mediated specific binding to EpCAM on the cell surface. The reduction of BCL9l protein levels in MCF-7 cells detected by Western blot indicates that the nanocomplex has targeted silencing activity. Consequently, the induction of apoptosis and the reduction of BCL9l protein levels suggest that this vector-aptamer/siRNA delivery system has good potential for targeted gene delivery. DOX-resistant tumors expressed higher levels of CSC biomarkers, CD44, Wnt and its receptors LRP5/6. Therefore, Miller-Kleinhenz et al. conjugated the ATF_{24} peptide with three histidine residues onto nitrilotriacetic acid-copper (NTA-Cu)-modified and amphiphilic polymer-coated iron oxide NPs (IONP) with dual targeting of Wnt/LRP5/6 and urokinase plasminogen activator (uPA) receptor (uPAR), to effectively treat resistant tumors [263]. Overexpression of uPAR in breast cancer induces CSC-like properties and leads to activation of the Wnt/β-catenin pathway [264], thus inhibition of uPAR could decrease the genes expression that activate Wnt/β-catenin signaling. Results showed that dual-targeted IONPs descend breast cancer cell invasion through simultaneous binding to LRP5/6 and uPAR, and distinctly inhibited Wnt/β-catenin signaling and the stemness phenotype of cancer cells. Systemically administered dual-targeted IONPs delivered DOX to a breast cancer PDX model with greater inhibition of tumor growth than non-targeted or single-targeted IONP-DOX.

3.2.2. *Hh signaling pathway*

Inhibiting the Hh signaling pathway with *Smo* inhibitors has been demonstrated to significantly suppress tumor proliferation [265], and various inhibitors have been tested in preclinical models targeting a variety of solid tumors [266]. Hu et al. utilized an amphiphilic polymer, HA-SS-PLGA, to simultaneously deliver DOX and the *Smo* inhibitor CYC with diverse solubility into CD44-overexpressing breast CSCs [202]. The dual-drug nano-delivery system exhibited redox-responsive drug release characteristics, releasing 66.9 % of DOX and 74.6 % of CYC in a reducing environment within 42 h. In addition, HA showed targeted effects on breast CSCs, which could effectively reduce the number and size of tumorspheres. The *in vivo* combination therapy further showed significant synergistic antitumor effects, achieving complete tumor suppression and prolonged survival in an orthotopic mammary fat pad tumor model compared to single-drug group treatment. However, CYC is a teratogen with low bioavailability, short half-life, and chemical instability, making it ineffective as a therapeutic drug. Utilizing site-specific gene editing therapy to inhibit Smo from the source of mutations can reduce chemotherapy-related side effects. Pandey et al. linked CD133 peptide to a penetration active vitamin B_6-coupled polydixylitol vector (VPX-CD133) for targeted delivery of Smo CRISPR/Cas9 plasmid to inhibit the Hh pathway in GSCs, thereby negatively impacting its growth [192]. Compared to VPX complexes, VPX-CD133 nanocomplexes significantly targeted and transfected GSCs *in vitro* and subcutaneous tumors. Simultaneously, using *siSHMT1* to inhibit SHMT1-driven thymidylate biosynthesis pathway to suppress the proliferation of non-GSCs. In xenograft mice, VPX-CD133 delivered SMO-CRISPR to CSCs while VPX delivered *siSHMT1* to non-GSCs, inducing massive apoptosis and resulting in a significant reduction in tumor volume by up to 81 %.

Since *Gli* transcription factors would be activated after the activation of *Smo* to induce gene transcription [267,268], inhibiting Gli can also block the Hh signaling pathway. Anthothecol is an antimalarial drug, which was discovered its potential as a Gli inhibitor by Verma et al. [269] They encapsulated anthothecol into PLGA NPs to form Antho-NPs, which were found to inhibit cell proliferation and colony formation, induce apoptosis in pancreatic CSCs, and suppress cancer cell migration and invasion by upregulating E-cadherin as well as inhibiting N-cadherin and Zeb1. Importantly, Antho-NPs disrupted the binding between Gli and DNA, thereby inhibiting Gli transcription and its target genes. Therefore, Antho-NPs can inhibit the growth of CSCs by suppressing the Hh signaling pathway.

3.2.3. *Notch signaling pathway*

N-[N-(3,5-Difluorophenacetyl-L-alanyl)]-S-phenylglycinetbutylester (DAPT) could effectively suppress γ-secretase activity and reduce CSCs by inhibiting the Notch signaling pathway [270], but its biodistribution and efficacy are hampered by the aggregation of the molecules in the physiological environment due to its hydrophobicity [271]. Tang et al. fabricated magnetic Fe_3O_4@PPr@HA hybrid NPs (h-NPs) to deliver the hydrophobic DAPT to synergistically eliminate CSCs [199]. The hydrophobic properties and π-π stacking of PPr enhanced DAPT loading, while HA ligands greatly increased the accumulation of h-NPs in CSCs. In addition, both the hyaluronidase in TME and the magnetothermal effect of the Fe_3O_4 core accelerated the release of DAPT at the tumor site, further enhancing the capacity of the combination of magneto-hyperthermia therapy (MHT) and chemotherapy to eliminate CSCs. Thus, under the PPr-mediated PAI-guided and Fe_3O_4-mediated MRI-guided synergy therapy, DAPT@h-NPs effectively inhibited tumor growth *in vivo* and reduced the proportion of CSCs in tumor tissues. Sun

et al. analyzed 226 samples from glioma patients and found that the expression of tumor vascular laminin-411 (α4β1γ1) was clinically correlated with the expression of CSC markers and with higher tumor grade [272]. The data suggest that laminin-411 interacts with integrins containing the β1 chain, affecting glioblastoma migration, invasion, and Notch signaling. Therefore, they designed a poly(β-l-malic acid) (PMLA)/PEG/trileucine (LLL)/anti-murine transferrin receptor (muTfR)/chimeric anti-human TfR (huTfRch)/antisense oligonucleotides (AON, α4β1) nanobioconjugate to inhibit laminin-411 for GBM therapy [272]. Treatment with the nanobioconjugate in LN229 xenograft mice prolonged animal survival (MST of 77 days vs. 36 days in the PBS group) while inhibiting Notch family members, including Notch ligand delta-like 4 (Dll4), Notch-1, and Notch-3 in residual tumors. In addition, the dramatic decrease of other CSC markers (Nestin, CD133, and *c-Myc*) after inhibition of laminin-411 suggested the effective elimination of CSCs by the nanobioconjugate. The aforementioned differentiation therapy is also one of the strategies for eliminating GSCs in the treatment of GBM. Liu et al. identified zinc finger protein 117 (*ZNF117*) as a major calibrator of GSC differentiation, wherein its downregulation reduced *JAG2* expression, inhibited the Notch pathway, and caused GSC differentiation towards the oligodendroglial lineage, resulting in suppression of glioblastoma advance [273]. Moreover, *ZNF117* can be targeted through targeted delivery of CRISPR machinery *via* NPs. Therefore, the authors employed their previously designed liposome-templated hydrogel NPs (LHNPs) [274] to encapsulate ribonucleoprotein (RNP) complexes of Cas9 protein and single guide RNA targeting *ZNF117*, and modified it with iRGD and lexiscan (a small molecule that can transiently open the BBB) for targeted therapy of GBM in a mouse xenograft model. The *ZNF117* expression in PS30 and GS5 cells was significantly reduced when being treated with LHNPs loaded with *ZNF117*-targeted RNP compared to that loaded with GFP-targeted RNP. Moreover, the MST of the treatment group was 48 days, significantly longer than that of the control LHNPs group (33 days) and PBS group (32 days). Additionally, immunostaining results from the treatment group showed a significant reduction of $Nestin^{+}$, along with an enrichment of $GalC^{+}$ cells, indicating the validity of the differentiation of *ZNF117*.

3.2.4. TGF-β signaling pathway

Zuo et al. demonstrated that tumor penetration of siRNA-carrying PEG-PLGA NPs (NP_{siRNA}) can be facilitated by inhibiting the TGF-β signaling pathway, which is beneficial for CSCs therapy [275]. NP_{siRNA} delivered siRNA more efficiently into $ALDH^{high}$ MDA-MB-231 CSCs compared with free siRNA, with about a 4-fold enhancement of intracellular fluorescence intensity. Selecting polo-like kinase 1 (Plk1) as a therapeutic target for CSCs, the authors observed that NP_{siPlk1} effectively kills breast CSCs *in vitro*, which is sequestered in the vessel after *in vivo* administration. In contrast, treatment with TGF-β receptor inhibitor LY364947 increased NP_{siPlk1} extravasation from the tumor vasculature, which resulted in a 1.5-fold and 2.1-fold in the accumulation of NP_{siPlk1} in cancer cells and CSCs, respectively, and ultimately improved *in vivo* transfection efficiency of CSCs. MDA-MB-231 xenograft-bearing mice treated with a combination of TGF-β signaling pathway inhibition and NP_{siPlk1} showed significant tumor regression and a decrease in CSCs percentage. Liu et al. reported a metallofullerenol nanomedicine $Gd@C_{82}(OH)_{22}$, which eliminated breast CSCs by blocking EMT, thereby preventing tumorigenesis and metastasis [276]. The Gd atom in $Gd@C_{82}(OH)_{22}$ is encapsulated by a carbon cage composed of 82 carbon atoms, whose surface is modified by 22 hydroxyl groups to form a viral morphology. In normoxic conditions, TGF-β was diminished at both the mRNA and protein levels with $Gd@C_{82}(OH)_{22}$ treatment, which affected EMT by blocking TGF-β signaling to achieve a significant decrease in the CSC population in TNBC. In contrast, under the hypoxia of TME, cellular uptake of $Gd@C_{82}(OH)_{22}$ is facilitated, resulting in inhibition of the EMT phenotype and functionally remarkable inhibition of cell migration and invasion. Moreover, $Gd@C_{82}(OH)_{22}$ acted as a dual inhibitor of HIF-1α and TGF-β activities, enhancing the elimination of CSCs under hypoxia.

3.2.5. JAK/STAT3 signaling pathway

As_2O_3 (ATO) has been approved by the FDA as a first-line therapeutic for acute promyelocytic leukemia [277], but is unsatisfactory in the treatment of solid tumors *in vivo* [278]. Shan et al. developed novel ATO-based $ZnAs@SiO_2$ NPs for targeting liver CSCs [279]. Compared with ATO, $ZnAs@SiO_2$ promoted apoptosis in MHCC97L and Hep3b cells, and significantly suppressed tumor growth by 2.2-fold and inhibited HCC cell metastasis by 3.5-fold. Colony formation assay showed that $ZnAs@SiO_2$ reduced the number of colonies in MHCC97L and Hep3b cells by 84.18 ± 7.36 % and 79.17 ± 3.75 %, respectively. $ZnAs@SiO_2$ can also inhibit tumorsphere formation *in vitro* and tumorigenesis *in vivo*, and modulate the expression of stemness markers (CD133, *SOX2*, and *OCT4*) and EMT markers (E-cadherin, Vimentin, and *Slug*) both *in vitro* and *in vivo*. In terms of molecular mechanism, $ZnAs@SiO_2$ upregulated Src homology region 2 (SH2)-containing protein tyrosine phosphatase 1 (SHP-1) and inhibited the phosphorylation of JAK2/STAT3, thus the inhibitory effect on stemness and EMT was mediated by the SHP-1/JAK2/STAT3 signaling pathway, which made $ZnAs@SiO_2$ an effective agent to restrain the malignancy of HCC cells, resulting in a 2.2-fold delay in tumor growth *in vivo* compared with ATO.

3.2.6. NF-κB signaling pathway

Disulfiram (DS) is a drug with strong NF-κB inhibition and anti-CSC activity, therefore, Kannappan et al. detected the *in vitro* anti-GSC activity of DS and the *in vivo* anti-GBM effect of DS-encapsulated PLGA NPs (DS-PLGA) [280]. The authors found that NF-κB is at a higher hierarchical location than HIFs in the hypoxia regulatory network and plays a key role in hypoxia-induced GSCs characterization. Meanwhile, DS could inhibit the expression of NF-κBp65 and target to GSCs, which selectively poisoned GBM cells, rooted out GSCs, and prevented their migration and invasion. Subsequently, the authors developed DS-PLGA to overcome the limitation of the short half-life of DS, which increased the half-life to 13.4 min, and effectively inhibited subcutaneous and orthotopic GBM xenograft mice model without toxicity to major organs. Wang et al. utilizing GNRs loaded with DTX and siRNA-p65 developed a host-guest nanoplatform (GDTX/p65) for the synergistic therapy of metastatic breast cancer with chemotherapy, RNA interference (RNAi) and PTT [281]. GDTX/p65 was obtained by coating cyclodextrin-grafted PEI on the surface of GNRs and loading DTX and siRNA by host-guest interaction with cyclodextrin and electrostatic interaction with PEI, respectively. Under NIR light irradiation, the photothermal effect generated by GNRs triggers more than 70 % of DTX release, as well as intracellular release of siRNA. DTX inhibited tumor growth by suppressing mitosis in cancer cells, while *siRNA-p65* blocked the NF-κB pathway and downregulated MMP-9 and Bcl2 to synergistically inhibit cancer cell proliferation and metastasis. GDTX/p65 in combination with NIR light irradiation not only significantly suppressed the growth of 4T1 breast tumors, achieving 84.5 % tumor inhibition rate, but also validly prevented the lung metastasis, with a large decrease in average metastatic lung nodules (1.4 ± 0.9) compared to the DTX treatment (21.0 ± 3.2).

3.3. Microenvironment remodeling

The TME plays a crucial role in the formation and maintenance of CSCs. Thereinto, TAMs and CAFs secrete cytokines and chemokines that induce and sustain the stem-like properties of cancer cells. Additionally, CSCs can regulate stemness through the secretion of EVs, while hypoxia further supports the CSC niche [282]. Therefore, an ideal strategy to combat CSCs should simultaneously target both CSCs and their microenvironments. Nanotherapeutic can exert microenvironmental regulatory through directly deplete TAMs [283] or reprogramming M2-phentype TAMs to M1-phentype [284], as well as blocking related signaling pathways to inhibit cytokine secretion [285] to suppress CSCs.

3.3.1. Tumor-associated macrophages

Wang et al. demonstrated, for the first time, that ZnO NPs can simultaneously target cancer cells, CSCs, and TAMs, and perform multiple critical functions including inhibiting cancer proliferation, sensitizing drug-resistant cancers, preventing cancer recurrence and metastasis, and restoring cancer immunosurveillance [286]. DOX-loaded ZnO NPs (ZnO/DOX) had a 4-time higher uptake than that of free DOX by MDR cancer cells and penetrated 3D tumorspheres more effectively. It is important that ZnO NPs could effectively reduce the stemness of CSCs that lead to the sensitization of CSCs to DOX, inhibiting the adhesion and migration of cancer cells and preventing the formation of tumorspheres. In addition, ZnO NPs could act as an immunomodulator to protect macrophages from DOX-induced toxicity and promote TAM polarization toward the M1 phenotype, enhancing DOX immunogenicity and anticancer activity. Jin et al. developed a TME-activated multifunctional liposome for the co-delivery of simvastatin (SV) and PTX by modifying the liposome with a cell-penetrating peptide [287]. SV was able to repolarize the TAM, promote the M2-to-M1 phenotypic transition through cholesterol-related LXR/ABCA1 regulation, upregulate TNF-α and downregulates TGF-β, which in turn remodels TME and inhibits EMT, achieving complete tumor suppression in the A549T-xenograft resistance model. Zhang et al. designed and synthesized a dihydroxyl-containing boron-dipyrromethene (BODIPY) monomer and formed a biodegradable polymer (P^{PDT}) by polycondensation, followed by further encapsulation of the cyclooxygenase 2 (COX-2) inhibitor celecoxib (CXB) to form NP^{PDT}@CXB, which was used for tumor photodynamic immunotherapy by PDT-induced ICD under NIR light [288]. Prostaglandin E2 (PGE_2) synthesized and released by cancer cells not only activates the proliferation of quiescent CSCs but also promotes the non-CSC-to-CSC transformation [289], whereas NP^{PDT}@CXB + L can effectively downregulate the stemness of CSCs by inhibiting PGE_2 synthesis, with an 80.8 % decrease of CD44. It has also been reported recently that ROS can facilitate the polarization of TAMs from M2 to M1 phenotype [290,291]. The results showed that beside the PGE_2, NP^{PDT}@CXB + L also reduced the synthesis of IL-10 and IL-12, thereby reprogramming M2-like TAMs to M1-like and reversing immunosuppressive TME. Ultimately, NP^{PDT}@CXB + L achieved 96.7 % tumor inhibition in the K7M2 solid tumor-bearing mouse model and significantly suppressed the growth of both primary and distant tumors in the bilateral tumor model.

3.3.2. Cancer-associated fibroblasts

ECM proteins, cytokines, and growth factors secreted by overactivated CAFs in the TME create an aberrant tumor mechanical microenvironment (TMME), which creates an advantageous ecological niche for CSCs, severely limiting the antitumor effects of predrug nanomedicines [292]. Wang et al. prepared nanomedicines (FDINs) with carbamate disulfide-bridged DOX dimer precursors (DOX-SS-DOX) as pharmaceutical components, IR780 iodides as photothermal agents, and hydroxyethyl starch-FA (HES-FA) conjugates as amphiphilic surfactants, to effectively scavenge CSCs by disrupting their unique ecological niche [293]. FDINs can actively target TNBC tumor tissues to achieve reduction-responsive drug release at high GSH concentrations in cancer cells and CSCs. In addition to directly leading to cancer cell damage and chemotherapeutic sensitization, the photothermal effect mediated by FDINs modulates abnormal TMME by reducing CAFs and depleting ECM proteins, thereby normalizing the structure and function of tumor vessels to facilitate drug and oxygen delivery. After remodeling TMME, FDINs-mediated PTT resulted in a 25.1 % and 27.9 % decrease in the proportion of $CD133^+$ CSCs and $CD44^+$ CSCs, respectively. Eventually, eliminating CSCs by disrupting their specific ecological niche and depleting intracellular GSH, FDINs-mediated PTT significantly inhibited tumor growth in subcutaneous and orthotopic 4T1 tumor models, achieving 81.4 % and 52.2 % tumor inhibition rates, respectively.

CXCL13 produced by CAFs could recruit B cells to the TME and differentiate them into regulatory B cells (Bregs), which may impair antitumor immune responses [294]. More seriously, CXCL13 can also promote the EMT of cancer cells, thus discouraging the activity of CXCL13 within TME may limit B cell infiltration, suppress tumor development, and regulate the EMT of CSCs, thereby restraining tumor metastasis [295]. Shen et al. designed an affinity protein called nano trap to bind with CXCL13 and adopted lipid-protamine-DNA (LPD) NPs to deliver plasmid DNA encoding CXCL13 trap for inhibiting the growth of desmoplastic tumor models [296]. Localized transient delivery of CXCL13 trap provided higher efficacy than anti-CXCL13 mAb while reducing the autoimmune risks. Not only did the CXCL13 trap reduce IL-10-generating Bregs to decrease PI3K-γ production and alter antineoplastic immunosuppressive cell populations, but it can also modulate the suppressive TME, activate dendritic cells (DCs), suppress the differentiation of CSCs through Lgr5 regulation, and inhibited metastasis. In pancreatic cancer, *BRAF*-mutant melanoma, and TNBC models, the CXCL13 trap effectively inhibited tumor growth and significantly prolonged the survival of the host.

3.3.3. Extracellular vesicle

sEVs are critical mediators of intercellular communication between cancer cells and M2-TAM by transferring lncRNA, and can play a messenger role by transferring proteins and RNA [297,298]. Wu et al. reported that miR-134 could block the expression of its targeting LAMC2 through the PI3K/Akt pathway and inhibit the migration and invasion of OSCC CSCs [299]. Thereafter, they uncovered that sEVs derived from OSCC CSCs (OSCC-CSC-sEVs) could transfer lncRNA urothelial carcinoma associated 1 by targeting LAMC2 to promote TAMs polarization toward M2 phenotype, inhibiting $CD4^+$ T cell proliferation and IFN-γ generation, which promote tumor progression and immunosuppression [124]. This finding provides new perspectives into the mechanisms of OSCC CSCs and suggests that CSC-sEVs and M2-TAMs could be potential targets for OSCC therapy. During migration from GBM origins, CSCs can maintain quiescent stage (G0) and thus resistance to TMZ, disrupting the cell cycle-induced cell death [26], which is mediated by the activation of protein tyrosine phosphatase receptor β/ζ (PTPRZ1) on CSC membranes, and thus inhibition of PTPRZ1 signaling is considered a promising therapeutic strategy to awaken and kill CSCs from the G0 phase after TMZ exposure. Yoon et al. employed the nanovesicles (NVs) of GSCs (CSC-NVs) conjugated with anti-PTPRZ1 peptide (PT-PEG) and loaded TMZ to obtain a nano-awakener (CSC-NV-PT-TMZ), which kills the CSCs after tracking and waking up them [26]. CSC-NVs can enhance cancer-specific therapeutic efficacy while minimizing side effects on normal cells by eliminating the functional features of cancer cells while retaining only the interactions between cell membranes [300]. Compared with liposomes, peptide-free CSC-NVs, and scramble peptide CSC-NVs, CSC-NVs with PT-PEG exhibited higher targeting efficiency and activated the S-phase process in quiescent CSCs, which induced sensitization to TMZ treatment and significantly reduced the survival of CSCs.

Tumor-derived exosomes (EXOs) are nanoscale vesicles (30–140 nm) that provide the TME and pre-metastatic ecological niche for tumor progression, metastasis, and immune escape [301,302]. Yong et al. developed tumor EXOs bionic porous silicon NPs (E-PSiNPs) and used them as the DOX delivery vehicle (DOX@E-PSiNPs) for tumor targeting therapy [303]. H22 cell-derived DOX@E-PSiNPs not only possessed homologous targeting properties that could be efficiently uptake by H22 CSCs, with intracellular DOX concentrations 2.1-fold and 1.7-fold higher than those of free DOX and DOX@PSiNPs, respectively, but also exhibited cross-reactive cellular uptake behaviors in melanoma B16F10 CSCs, which were significantly higher than those of free DOX and DOX@PSiNPs in the internalization value. Thereby, DOX@E-PSiNPs remarkably suppressed the formation of H22 tumorspheres and exhibited strong cytotoxicity against B16F10 CSCs *in vitro*. After intravenous (*i.v.*) administration, DOX@E-PSiNPs showed highly effective tumor targeting, with accumulative dose about 2.5- and 2.3-fold that of free DOX and DOX@PSiNPs, respectively. Hence, DOX@E-PSiNPs showed

efficient antitumor performance in the subcutaneous H22 tumor model (91 %), orthotopic 4T1 tumor model (68 %), and B16F10 lung metastatic tumor model, as well as CSC reduction activity, and significantly extended survival. CSC-derived DCs (CSC-DCs) vaccines could compete with CSCs by inducting cytotoxic T cells, thereby inhibiting tumor growth and recurrence [304,305]. However, identifying the adequate antigen source is a main challenge in programming DC-based therapeutics against CSCs. Naseri et al. investigated the effectiveness of DCs loaded with CSC-enriched tumorsphere-derived EXOs (CSC_{enr}-EXOs) in activating CSC-specific T-cell responses in *in vitro* model of HT-29 CRC [306]. CSC_{enr}-EXOs did not inhibit the maturation of DCs, while significantly increasing the IL-12/IL-10 ratio in the supernatant of mature DCs similarly to CSC_{enr} lysate. Furthermore, DCs loaded with CSC_{enr}-EXOs effectively promoted T cell proliferation with CSC-directed cytotoxicity.

3.3.4. Hypoxia

Extremely hypoxic CSCs in specific TME may remain an "invisible status" that allows CSCs to evade immune system surveillance and resist cancer therapy [27,307], thus eradication of hypoxia is a great challenge to develop strategies against CSCs to overcome immune system escape and drug resistance. CSCs would maintain a lower ROS level to protect themselves from DNA, lipid, and protein damage for resisting chemotherapy and RT [308], thus ROS-related therapeutics may be a potentially effective option for eradicating CSCs. Our research team constructed manganese oxide-loaded polydopamine (MnO_x/PDA) nanobombs that can generate ROS through chemodynamic therapy (CDT) and PDT dual-pathways to simultaneously resistant CSCs and non-CSCs [23]. Except for generating ROS, MnO_x/PDA can also consume overexpressed GSH in the TME and release manganese ions to mediate a Fenton-like reaction, generating large amounts of oxygen to alleviate tumor hypoxia. By downregulating HIF-1α, MnO_x/PDA reduces the stemness and self-renewal ability of CSCs, thereby weakening their carcinogenicity. What's more, macrophage cell membrane coating enhanced the tumor-targeting ability of MnO_x/PDA by 1.9 times, achieving a tumor inhibition rate of 70.8 % in a CRC-bearing mice model. Tumor-associated enzyme carbonic anhydrase (CA) IX is overexpressed exclusively in the hypoxic regions of various cancers [309], providing a therapeutic target for hypoxic tumors [310]. Wang et al. discovered that hypoxic CSCs highly express the CAIX on the cell membrane, and constructed a peptide-based spherical nanostructure (CA-Pt) with cisplatin as a model drug to target CAIX to overcome the RT resistance of hypoxic CSCs [21]. CA-Pt can be enriched into tumor tissue through the enhanced permeability and retention effect and released CAIX-targeted peptide monomers with deep penetration after responding to the overexpressed MMP-2, which tended to move toward the tumor center and localize on the surface of CSCs. Whereafter, the supramolecular nanofibers generated by surface-induced *in situ* self-assembly amplify the consequence of CAIX inhibitors, which subsequently induced the differentiation of CSCs by decreasing the expression of HIF-1α and the production of hydrogen protons, and inhibited the proliferation of CSCs in response to RT stress. In addition, CAIX-mediated endocytosis promotes the CSCs' uptake of radiosensitizers, thereby enhancing the DNA-damaging of cisplatin to contribute to RT and eliminating differentiated CSCs. In the CSC-enriched subcutaneous NCI-H1975 tumor model, the combination of CA-Pt and RT effectively inhibited tumor growth, achieving a tumor inhibition rate of 86.02 % and significantly reducing the percentage of CSCs. Further, in a zebrafish embryo model, the combined therapy strategy was effective in preventing tumor invasion and metastasis, with the metastatic ability of CSCs in the control group being 4.73 times that in the CA-Pt + IR group.

Hypoxia-activated prodrugs are another therapeutic approach that targets tumor hypoxia. TPZ is a typical hypoxia-activated prodrug, which can produce highly cytotoxic free radicals in hypoxic environments, resulting in intracellular DNA breakage and cell death, showing 300 times higher cytotoxicity in normoxic environments [311]. Li et al. designed a multistage drug delivery nanosystem (CD133/TAT/TPZ--Fe_3O_4@$mSiO_2$) with thermal-triggered targeting and drug release to eradicate breast CSCs by combining magnetothermal therapy and hypoxia-activated chemotherapy [172]. The outermost azo linker conjugated anti-CD133 antibody allows CD133/TAT/TPZ-Fe_3O_4@$mSiO_2$ to active transport to tumor tissue and enhanced internalization of CSCs. After entry into the CSCs, AMF was employed to stimulate azo bond breaking to expose the secondary TAT peptide for CSC-nucleus targeting, thereby exerting the effects of loaded TPZ, which exhibits significant selective toxicity to hypoxic CSCs. The magnetothermal generated by the innermost Fe_3O_4 NPs core under AMF could strengthen the chemosensitivity and enable CSC-targeted MHT and chemotherapy to reverse resistance. By downregulating the HIF-1α signaling pathway, CD133/TAT/TPZ-Fe_3O_4@$mSiO_2$ could effectively eliminate hypoxic CSCs, and achieved a 95.64 % inhibition of cancer xenograft growth in the breast CSCs xenograft nude mice model, without significant side effects during the treatment. Shen et al. selected all-trans RA (ATRA) and camptothecin (CPT) to develop differentiation-regulated micellar NPs (ATRA/CPT-NPs) for overcoming therapeutic barriers posed by CSC-derived heterogeneity [25]. After being uptake by CSCs, ATRA/CPT-NPs rapidly released ATRA through hypoxia-induced changes in hydrophobic properties, which induced differentiation of CSCs, decreased the $CD44^+/CD24^-$ cell ratio, and significantly down-regulated stemness-associated transcription factors, such as *OCT4*, *SOX2*, and *Nanog*. Elevated ROS levels in differentiated non-CSCs lead to CPT release and subsequent cell death. In addition, the released CPT could alleviate tumor hypoxia by inhibiting HIF-1α, thereby augmenting the chemotherapeutic response. This on-demand release strategy of ATRA and CPT in CSCs reduces stemness-related drug resistance, which enabled ATRA/CPT-NPs to achieve the highest tumor suppression efficiency on the orthotopic breast CSC-enriched tumor mouse models and effectively prevented tumor recurrence and metastasis after surgery.

3.3.5. Cytokines

Conventional chemotherapeutic agents are difficult to eradicate CSCs and may instead create an inhibitory immune microenvironment for the initiation and proliferation of CSCs [312,313]. Guan et al. conjugated CPT with the indoleamine 2,3-dioxygenase (IDO) inhibitor NLG919 to develop a reduction-responsive prodrug, CPT-SS-NLG919 (CN), which effectively inhibited CSCs by modulating their ecological niche [314]. CN could induce ICD after intratumoral administration and exhibited ~2-fold greater ability than CPT to promote DCs maturation and antigen presentation, which in turn activated memory T cells, achieving 85 % tumor suppression in a subcutaneous 4T1 tumor model. The increase in tryptophan, and the decrease in cytokines such as IL-6, IL-13, TGF-β, and Tregs, suggesting effective suppression of IDO, further attenuated the negative regulation of the immune process. And by decreasing the ratio of G0/G1 phase (0.56 %) and (G0-G1)/S of $CD133^+$ CSCs, and significantly increasing the ratio of Sub-G0 (97.93 %), CN could convert more CSCs from dormant to re-proliferative phases, making them more susceptible to the chemotherapeutic agent CPT. Using polylactic acid (PLA)-HES-FA (PHF) load CN to obtain nanoformulation CN@PHF, which could effectively target tumor tissues after tail vein administration. By alleviating the cell cycle blockade of CSCs to reverse the TME into a hostile environment for CSCs and non-CSCs, CN@PHF could make them more vulnerable to antitumor immune cells and chemotherapeutic agents, and ultimately induce effective tumor suppression in an orthotopic 4T1 tumor model.

3.3.6. Angiogenesis

VM is a vessel-like structure formed by cancer cells, whereby nutrients and blood could be transported to the hypoxic and ischemic regions of the tumor tissue, and thus, disruption of VM would improve antitumor efficacy [315,316]. By conjugating cRGD to the cell-penetrating peptide octa-arginine (R8) to endow R8 with the integrin $\alpha_v\beta_3$ binding

affinity, Liu et al. developed multifunctional R8-cRGD-modified liposomes loaded with PTX (PTX-R8-cRGD-Lip) for disrupting VM channels and gliomas therapy [317]. PTX-R8-cRGD-Lip exhibited the strongest targeting ability to brain CSCs *in vitro*, with almost 20-fold higher cellular uptake than PEG-Lip. In addition to inhibiting VM channel formation, PTX-R8-cRGD-Lip treatment exhibited efficient inhibition of brain CSCs, with the highest late apoptosis rate of 64.45 ± 4.60 %. Accordingly, in intracranial C6-bearing mice, the PTX-R8-cRGD-Lip group displayed the most potent anti-glioma effect, with a mean survival time of 43 days, which was prolonged by 79 % compared to the control group (24 days). Wang et al. proposed a self-assembling peptide-based transformable dual-inhibition system (TDS) to *in situ* construct a nanofiber barrier on cell membranes, which aided in reducing endothelial permeability and angiogenesis, and inhibit stemness and metastasis of renal CSCs [318]. CD105 is a specific biomarker for both tumor neovascular endothelial cells and CSCs [319], which could be intended to modulate both cells for cancer therapy. However, TDS could specifically target overexpressed CD105, inducing a transformation *via* ligand-receptor interaction that constructed a barrier on the cell membrane. For vascular endothelium, vascular permeability and angiogenesis were decreased to 67.0 % ± 4.7 % and 62.0 % ± 4.0 % by TDS, respectively, thereby preventing metastasis. Furthermore, TDS also inhibited stemness by suppressing endogenous miR-19b and its transport in human-derived CSCs, leading to increased expression of the protein tyrosine phosphatase gene and subsequently inhibiting CSC-mediated metastasis. In PDX mice, TDS shrank tumor volume to 24.3 % ± 7.4 % and markedly inhibited angiogenesis compared to the control group, which also reduced metastatic nodules in the lungs by 5.0-fold. Zhao's research team systematically mapped the cell-type-specific gene expression of chemotherapy-resistant osteosarcoma using single-cell transcriptomics and discovered that the combination of VEGFR2 inhibitor (Apa) and Jumonji domain containing 3 (JMJD3) inhibitor (J4) synergistically hindered the proliferation of osteosarcoma cells and the tumor growth [168]. Therefore, the authors developed L-cysteine-based polydisulfide NPs (Cys-PDSA) loaded with J4 and Apa (NP_{J4+Apa}). Through dual targeting of VEGFR2 and JMJD3, they achieved effective eradication of chemotherapy-resistant osteosarcoma CSC-/progenitor cell-derived tumors.

3.3.7. Extracellular matrix

The tumor stromal microenvironment (TSM), consisting of stromal cells and the ECM, forms a barrier that hinders the accessibility of NPs to cancer cells, greatly compromising their antitumor effectiveness [320,321]. Illuminated by the composition and biological properties of high-density lipoprotein (HDL), Tan et al. synthesized a bioinspired lipoprotein (bLP) using dimyristoyl phosphatidylcholine, dioleoyl phosphatidylethanolamine, and apolipoprotein A1-mimetic peptides, loading photothermal agent $DiOC_{18}(7)$ (DiR) (named as D-bLP) to induce efficient photothermal effect for remodeling the TSM, which improved the accessibility of subsequent mertansine-loaded bLP (M-bLP) to cancer cells or CSCs, enabling satisfactory curative effect [176]. D-bLP-mediated photothermal effect significantly disrupted a variety of stromal cells in TSM, such as CAFs and TAMs, especially the ECM component, with collagen and fibronectin reduced by 93.7 % and 84.3 %, respectively. As a result, the penetration depth of the second M-bLP throughout the tumor tissues was enhanced, with a 4.27-fold improvement in tumor accumulation and a 27.0-fold increase in accessibility to cancer cells. Ultimately, this bLP-mediated TSM remodeling for enhanced cancer cell accessibility strategy had eminent tumor growth inhibition, achieving 95.9 % tumor suppression in a lung-metastatic 4T1 model and a reduction of 97.4 % of metastatic lung nodules, in addition to almost complete tumor ablation (99.4 %) in the MCF-7 model.

3.4. Metabolism modulation

CSCs exhibit diverse metabolic phenotypes, including glycolysis, OXPHOS, lipid and amino acid metabolism. And they adapt to microenvironmental pressures by dynamically switching between glycolysis and OXPHOS, which regulated by signaling pathways and the TME [7]. Metabolism-directed nanotherapeutic strategies can precisely target metabolic nodes or deliver drugs to CSC mitochondria, such as inhibiting GLUT1, disrupting the mitochondrial electron transport chain or regulating the rate-limiting enzyme HK2 in glycolysis, thereby influencing CSC metabolism to enhance therapeutic efficacy.

3.4.1. Glycolysis

As a metabolite of glycolysis in CSCs, lactate with elevated concentrations might create an immune environment conducive to tumor growth, so targeting the lactate oxidation process is beneficial to the inhibition of glycolysis and tumor growth [322]. Yang et al. assembled LDHA inhibitor (Mn-DOX) with BSA (Mn-D@B) and modified with PEG-FA (Mn-D@BP), followed by binding it to GAG-containing sequence and matching with GLUT1 recognition aptamer, to obtain a photo-driven lactate attenuator (Mn-D@BPFe-A) for HIF-1 inhibition in synergistic cancer phototherapy [323]. Mn-D@BPFe-A had obvious tumor-targeting properties due to the GLUT1 acceptor-induced accumulation, and the Mn and DOX levels in tumor tissues increased gradually with time after *i.v.* injection and reached 23.4 μg g^{-1} and 34.9 μg g^{-1} after 12 h, respectively. Under LED red light irradiation, Mn-D@BPFe-A could oxidize water to hydroxyl radical, which converts lactate to pyruvate and causes mitochondrial dysfunction. Besides, Mn-D@BPFe-A could also reduce the expression of HIF-1α and GLUT1 in HepG-2 cells, which effectively inhibited tumor growth in HepG-2 tumor-bearing nude mice. Chen et al. decorated GNR with a functional polymer containing an HA-targeting section and a GLUT1 inhibitor, diclofenac, to obtain a GNR/HA-DC nanosystem that selectively sensitized tumor to PTT by hindering anaerobic glycolysis [197]. GNR/HA-DC could specifically target to CD44 positive cancer cell lines and sequentially release diclofenac triggered by hyaluronidase overexpressed in the TME. The released diclofenac could consume GLUT1 and exert a cascade effect on cellular metabolism *via* glucose uptake inhibition, glycolysis block, ATP levels reduction, and HSPs (HSP70/90) down-expression. Thanks to the sensitization of GNR/HA-DC, the PTT efficiency in tumor-bearing mice was significantly improved, achieving an 83 % tumor inhibition rate. Besides, the combined treatment of diclofenac and PTT significantly decreased the percentage of CSCs, which also contributed to the antitumor effect.

Pan et al. simultaneously conjugated the HK2 inhibitor 3-bromopyruvate (3BP), the mitochondria-targeting molecule triphenylphosphine (TPP), and HA onto gold nanostars-dendritic polyglycerol (GNSs-dPG) NPs to develop GNSs-dPG-3BP,TPP,HA nanocomposites for combined metabolism inhibition and targeted PTT for CSCs [181]. GNSs-dPG-3BP, TPP,HA exhibited excellent photothermal properties, whose solution temperature was apparently increased to 74.5 °C within 5 min under NIR laser irradiation. Because of the presence of TPP and HA, the cellular accumulation of GNSs-dPG-3BP, TPP, and HA in mammosphere cells was 4-fold higher than that of GNSs-dPG. After targeting to mitochondria, GNSs-dPG-3BP,TPP,HA displayed superior HK2 binding ability *via* 3BP to inhibit metabolism, which ulteriorly induced apoptosis by releasing cytochrome *c*, achieving 73.7 % of killing effect in mammosphere cells after combined PTT and minimizing the percentage of $ALDH^+$ CSCs (0.5 %). In addition, the self-renewal of breast CSCs was inhibited, stemness gene (*SOX2*, *Nanog*, *OCT4*) expression was significantly downregulated, and CSC-driven mammosphere formation was apparently reduced after synergistic therapy, which also effectively removed CSCs and inhibited the tumor growth in tumor-bearing mice.

3.4.2. Oxidative phosphorylation

Shen et al. developed the NPs form of ^{188}Re-Liposome by conjugating

^{188}Re to a N,N-bis(2-mercaptoethyl)-N9,N9-diethylethylenediamine (BMEDA) chelator (^{188}Re-BMEDA) and embedding in liposomes, and investigated its therapeutic effects on radioresistant ovarian cancer cells by *i.v.* or intraperitoneal (*i.p.*) administration of either the ^{188}Re-Liposome or ^{188}Re-BMEDA [324]. The authors found that the metabolic pathway of radioresistant ovarian cancer cells was glycolysis, whereas *i.p.* injection of ^{188}Re-Liposome could decrease the expression of stemness markers, reduce the cellular subpopulation of CSCs, and restore metabolism to OXPHOS. Furthermore, *i.p.* administration of ^{188}Re-Liposome was able to block EMT and reactivate *p53* function, inhibiting stemness and metabolic characteristics. Therefore, in the orthotopic radioresistant ovarian cancer model, *i.p.* administration of ^{188}Re-Liposome had a strongest tumor-killing effect that remarkably eradicated tumor compared with *i.v.* and *i.p.* administration of ^{188}Re-BMEDA or with *i.v.* injections of ^{188}Re-Liposome.

3.4.3. Metabolic adaptation

The HIF-induced metabolic reprogramming from OXPHOS to glycolysis is one of the major metabolic adaptations in cancer cells [325,326], which would support rapid tumor growth and proliferation [327]. Multiple catabolic pathways in gliomas not only generate energy but are also associated with anabolic pathways that support cellular function. For instance, glycolysis and pentose phosphate pathway (PPP) support energy production as well as offering carbon skeleton for nucleic acid synthesis. Sridharan et al. reported that cerium oxide NPs (CNPs) can regulate gene expression of metabolic pathways with therapeutic potential for GBMs [328]. 6-nm-sized CNPs (CNP-6) showed 24-h short-term alleviation of ROS levels and reduced the IC_{50} of TMZ in TME conditions. Since ROS could inhibit glycolytic enzymes and thus promote PPP, cells pre-treated with CNP-6 before exposure to TME were significantly up-regulated the glycolysis markers [GLUT1, GLUT3, MCT1, MCT4, PKM, and phosphofructokinase (PFKP)] expression, while down-regulated the PPP markers [glucose-6 phosphate dehydrogenase (G6PD) and transketolase-like-1 (TKTL1)] expression. Consequently, CNPs would have the potential for GBM therapy by modulating ROS levels, chemosensitivity, and metabolic gene expression profiles of cancer cells. Yang et al. prepared nano-realgar by nano-grinding the crude realgar powder and formulated it into nano-realgar solution (NRS) for antitumor studies with metabolic reprogramming [329]. NRS can not only inhibit the viability of lung CSCs, but also suppress glucose metabolism by down-regulating the expression of metabolic reprogramming-associated regulatory factors [GLUT1, pyruvate dehydrogenase kinase (PDK) 1, PKM2, and LDH], which resulted in a reduction of glucose consumption by lung CSCs. Through molecular mechanism research, the authors found that the above metabolic reprogramming may be related to the down-regulation of HIF-1α by NRS *via* the PI3K/Akt/mTOR pathway both *in vitro* and *in vivo*. And 60 mg kg^{-1} of NRS could significantly inhibit tumor growth in lung CSCs xenograft mice after *in vivo* intervention. Ascorbate (AA) can deplete GSH, leading to an elevation in ROS levels within cancer cells, thereby inactivating glyceraldehyde 3-phosphate dehydrogenase (GAPDH) and inhibiting glycolysis [330]. Jiang et al. discovered that CSCs respond to AA treatment by transiting their metabolic pathways to OXPHOS for energy supply [174]. However, this led to changes in mitochondrial dynamics, resulting in the inhibition of CSC self-renewal and increased sensitivity to chemotherapy. The authors coordinated Zn^{2+} with carboplatin (Carb) or oxaliplatin (OX) prodrugs, further modifying them with a lipid bilayer containing cholesterol-DTX or cholesterol-SN38 conjugates to form core-shell structures of Carb/DTX or OX/SN38 nanoscale coordination polymers (NCPs) particles for combined chemotherapy with AA [174]. The results showed that AA enhanced the antitumor effects of NCPs and reduced the stemness of cancer cells *in vivo*. Compared to Carb/DTX, the combination treatment of AA and Carb/DTX led to a significant reduction in the expression of *SOX2*, *OCT4*, and *Nanog* by 63.0 ± 13.8 %, 63.7 ± 23.0 %, and 47.5 ± 12.1 %, respectively. Furthermore, due to the elimination of CSCs, the combined therapy of AA and OX/SN38 completely suppressed the recurrence of a CRC resection model, with an MST exceeding 100 days. And the combination treatment of AA and Carb/DTX significantly reduced systemic metastasis in an orthotopic 4T1 model.

3.4.4. Lipid metabolism

Lipid metabolism plays a crucial role in EMT, hereby, Jin et al. developed a TME-activated multifunctional liposome for co-delivery of the cholesterol-lowering drugs SV and PTX to reverse EMT-associated drug resistance through lipid metabolism [287]. SV could destroy cholesterol-rich domains (lipid rafts), downregulate integrin β3, and inhibit focal adhesion formation, thereby suppressing the FAK signaling pathway and re-sensitizing drug-resistance of cancer cells to PTX. LXR signaling regulates metabolism in various cancers, thereunder Dianat-Moghadam et al. developed anti-CD133 mAb-decorated immunoliposomes for specific delivery of the LXR inhibitor (SR9243, SR) to $CD133^+$ CSCs and inducing their functional effects [191]. CD133-targeted immunoliposomes showed significantly higher SR accumulation in $CD133^+$ CSCs and exhibited ~1.57-fold more potent cytotoxicity compared to non-targeted liposomes. Notably, immunoliposomal SR treatment significantly down-regulated the expression of stearoyl-CoA desaturase-1 and fatty acid synthase and suppressed the stemness and clonogenic capacity of CSCs by modulating their lipid metabolism phenotype, which additionally promoted ROS generation and induced more early apoptosis in CSCs (65.3 %) compared with that by free SR (50.2 %).

3.4.5. Amino acid metabolism

The function of the cystine/glutamate transporter (Xc-) system is regulated by glutamate levels, as glutamate is exchanged for cystine by the Xc-system in a 1:1 ratio. Thus, high extracellular concentrations of glutamate block the activity of the Xc-system, inhibit cystine uptake, and lead to ferroptosis [331,332], which is a potential strategy for cancer therapy [333]. Ni et al. loaded atranorin onto SPION to construct Atranorin@SPION complexes for inhibiting key molecule expression in the Xc-/glutathione peroxidase 4 (GPX4) axis and inducing ferroptosis in gastric CSCs [334]. Atranorin@SPION not only directly inhibited the viability of $CD44^+/CD24^+$ gastric CSCs, but also decreased the expression of stemness markers (*OCT4* and CD44), which reduced their proliferation, invasion, angiogenesis, and carcinogenicity *in vitro*. Importantly, Atranorin@SPION markedly inhibited the expression levels of Xc-/GPX4 and Tet methylcytosine dioxygenase (TET) family proteins, which led to ferroptosis in gastric CSCs by reducing the 5-hydroxymethylcytosine modification of mRNAs, and by promoting the accumulation of lipid peroxides and the expression of ferroptosis-related genes. Eventually, the *in vivo* carcinogenicity of gastric CSCs was also suppressed, and the tumor volume of the Atranorin@SPION-treated group was significantly smaller than that of the SPION-treated group.

4. Conclusion and perspectives

In-depth research on CSCs has not only revealed their roles in cancer progression but has also inspired the development of a series of nanotherapeutic strategies targeting their biological characteristics, including targeting surface markers, regulating signaling pathways and the microenvironment, influencing metabolism, and have achieved encouraging results, advancing cancer therapy. Currently, there is only one clinical trial of gold nanoparticles based on CD24-conjugated gold nanocomposite (CD24-AuNC) for biomarker-based diagnosis of CSCs in salivary gland tumors (NCT04907422) [335], which demonstrated that CD24-AuNC exhibited high sensitivity and promising potential for diagnosing and predicting the prognosis of salivary gland tumors. Other clinical trials of nanomedicine for cancer treatment include the TNF-bound colloidal gold (CYT-6091) nanomedicine for the treatment of advanced solid tumors (NCT00356980) [336]; magnetic IONPs (NanoTherm®) for localized intracranial magnetic hyperthermia for

glioblastoma [337], along with a new clinical trial based on NanoTherm® ASI for recurrent GBM (NCT06271421); the radiation sensitizer NBTXR3, based on functionalized hafnium oxide NPs, has completed Phase I clinical trials for the treatment of soft tissue sarcoma (NCT01433068, NCT02379845) and is currently being investigated in clinical trials to enhance radiotherapy in combination with other treatments for various cancers, including pancreatic cancer (NCT04484909), NSCLC (NCT04505267), HNSCC (NCT04862455, NCT04892173) [338], esophageal cancer (NCT04615013), and other advanced malignant tumors (NCT03589339, NCT05039632). For nanomedicines that have completed or are undergoing clinical trials, their safety has either been validated (NCT01946867) [339] or can be further enhanced through PEGylation to improve biocompatibility [336]. Given the high modifiability of nanomedicine, various functional modifications can be employed to enhance safety while achieving CSC targeting. Moreover, chemotherapy, hyperthermia, and radiotherapy strategies based on nanomedicine have also demonstrated efficacy against CSCs. Therefore, nanomedicine holds promise not only as an effective adjunct to existing treatment strategies but also as a driving force for the development of therapies specifically targeting CSCs. However, to effectively eradicate CSCs and achieve satisfactory treatment outcomes in clinical trials, it is crucial to overcome the numerous limitations of CSCs nanotherapeutic strategies.

4.1. Cancer stem cells

CSCs constitute a small proportion within tumor tissues, making precise and effective identification and isolation of CSCs a major challenge in CSC research [340]. Specific surface markers of CSCs are commonly used methods for identification and isolation, however, only a few CSC-specific surface markers have been identified and validated currently, many of which are shared with normal stem cells [341], thus requiring improvements in specificity and sensitivity. Further research aims to identify specific surface markers distinct from normal stem cells or the combined use of multiple surface markers, offering promising approaches for more accurate sorting and identification of CSCs. Besides, CSCs are a highly heterogeneous subpopulation of cells within tumors and a major cause of intra-tumor heterogeneity [12], which promote tumor initiation and exacerbate the malignancy of tumors by enhancing their metastasis, recurrence, and drug resistance. Interactions among various components within tumors can induce different metabolic phenotypes in CSCs and alter the TME heterogeneity. Environmental pressures on CSCs can induce adaptive changes in their phenotypic characteristics. Additionally, the aberrant activation or suppression of different cellular signaling pathways within tumors also contributes to the heterogeneity of CSCs [12]. Therefore, identifying common mechanisms and regulatory molecules underlying CSC heterogeneity could further elucidate the molecular mechanisms of cell-to-cell interactions that maintain tumor heterogeneity, and hold promise for preventing the formation and progression of tumor heterogeneity. The advancement of artificial intelligence (AI) has enabled more efficient and precise detection of CSCs. Chambost et al. developed a convolutional neural network (CNN) integrated with a microfluidics-based high-throughput single-cell imaging system, achieving 91.2 % accuracy in discriminating CSCs from non-CSCs while enabling real-time monitoring and analysis of CSC behavioral dynamics [342]. In another study, Zhang et al. employed a conditional generative adversarial network (CGAN) to identify CSCs through phase-contrast imaging and established an AI workflow based on CGAN-mediated image transformation for CSC prediction [343]. In a separate approach, Ji et al. correlated mRNA expression profiles with an mRNA stemness index (mRNAsi) derived from a univariate logistic regression (OCLR) machine-learning algorithm [344]. This led to the development of an mRNA-based breast CSC signature capable of identifying and quantifying CSCs in primary breast cancer patient samples, while also elucidating the roles of polyamine anabolism and HIF-1 signaling in breast CSC enrichment. Therefore, future research could not only enhance CSC detection accuracy through multimodal data integration but also decipher CSC heterogeneity at the subpopulation level, providing novel insights for developing targeted nanotheranostic strategies. Furthermore, AI-powered real-time monitoring of CSC adaptive evolution under therapeutic pressure may uncover unprecedented drug resistance mechanisms, enabling the design of smart nano-delivery systems capable of modulating the drug-resistant microenvironment to achieve precision-targeted therapeutic intervention.

4.2. Nanomedicine

The general safety issues of nanotherapeutics have hindered clinical studies on NMs targeting CSCs. The high stability of many inorganic NMs makes them difficult to metabolize and eliminate from the body after exerting their effects, leading to accumulation toxicity [345,346]. Developing biodegradable nanotherapeutics may be a feasible strategy, as they degrade after exerting therapeutic effects, metabolizing out of the body through urine or feces to avoid unpredictable toxicity [347]. Additionally, constructing nanotherapeutics on a biogenic matrix base, such as protein NPs or liposomes/lipid NPs, may provide another effective approach, but it faces challenges in scale-up production and cost control [348]. Upon entering the body, extraneous nanomedicine would rapidly adsorb endogenous proteins onto the surface to form protein corona [349], which enhances cellular uptake and phagocytosis by the reticuloendothelial system (RES) [350], leading to high accumulation in organs causing organ damage, and reducing targeting efficiency to the tumor increasing off-target toxicity. When targeting lesions outside the RES, strategies such as inhibiting protein adsorption or recruiting endogenous proteins for targeting could be employed to prevent the formation of the protein corona [350]. For instance, PEG, as one of the most commonly used nonionic hydrophilic polymers, can be grafted onto NM surfaces to minimize nonspecific interactions with blood components, thereby suppressing protein adsorption and protein corona formation [351]. Other zwitterionic coatings, such as glycosylated polyhydroxy polymers, have also demonstrated comparable efficacy [352]. On the other hand, nanotherapeutics in anti-tumor applications typically involve passive targeting based on the EPR effect [353], along with active targeting based on interactions such as antigen-antibody [190], and ligand-receptor [263], and cell membrane [354]. Further development of nanotherapeutics with targeting specificity not only enhances therapeutic efficiency but also addresses off-target toxicity of NMs. Moreover, the broad-spectrum therapeutic effects of nanotherapeutics, such as hyperthermia [355–357] and ROS [358–360], ensure effective cancer suppression but inevitably cause side effects in adjacent normal tissues [345,346]. Improving the therapeutic specificity of nanotherapeutics aims to maximize therapeutic effects while minimizing damage to normal tissues, thereby reducing patient suffering and improving prognosis.

The clinical translation of nanomedicine necessitates the establishment of a systematic evaluation framework addressing safety concerns, including *in vivo* degradation/metabolism, off-target toxicity, and potential immune-related risks such as cytokine storms. Recent studies have elucidated correlations between fundamental physicochemical properties of NMs and their biodistribution patterns, immune interactions, and biocompatibility [361,362]. Among them, the surface charge modulates cellular uptake efficiency and receptor-binding specificity [363]; the morphology governs vascular extravasation dynamics and immune recognition patterns [364]; while surface modification strategies critically determine targeting accuracy and circulation half-life [365]. To advance CSC-targeted nanotherapeutics, cross-disciplinary comparative studies should establish standardized guidelines encompassing material preparation, structural characterization, immune regulation mechanisms, and metabolic fate analysis. Beyond safety considerations, the scalability of NM production remains a critical bottleneck for clinical implementation. Ensuring

batch-to-batch consistency and pharmaceutical-grade stability requires developing rigorous quality control protocols through comprehensive regulatory systems. Although the European Union's relevant regulations state that products containing NMs must obtain authorization under current laws and undergo additional nano-specific risk assessments to ensure their safety for human and environmental use [366], updated policies indicate that the FDA and European Commission-Joint Research Centre exempt toxicity testing for nanoscale additives derived from proven safe substance [367,368]. Additionally, the current regulatory landscapes remain rudimentary for the lack of component-specific toxicity profiling for engineered NMs. Therefore, the regulatory policies need to keep pace with the times and tiered safety evaluation criteria for distinct NM categories should be incorporated.

4.3. Interaction between cancer stem cells and nanotherapeutics

Through the precise design of NMs including size, charge, hydrophilic and hydrophobic properties, and surface modification groups, they can specifically recognize and bind to surface markers of CSCs, which allows for precise control of their CSC-targeting and biological activity *in vivo*. By elucidating the structure-efficacy relationship of NMs on CSCs, tailored nanotherapeutics can be designed based on the characteristics of CSCs to avoid off-target toxicity and side effects. The survival and proliferation of CSCs depend on specific microenvironmental conditions, and NMs have shown great potential in regulating the TME [369,370]. By designing nanotherapeutics with specific physicochemical properties, it is possible to effectively interfere with and alter the CSCs microenvironment, thereby inhibiting their growth and metastasis. In recent years, the deep integration of AI and nanomedicine has opened new avenues for precision-targeted therapies against tumors and CSCs. In the realm of nanomaterial design, Wei et al. employed a fully connected deep neural network-based model to accurately analyze the relationship between particles and their properties through machine learning, thereby achieving both classification and quantitative prediction of the enzyme-like activities of nanozymes [371]. Jiang et al. utilized edge-transitive nets to map the complex structures of multicomponent MOFs, providing algorithmic support for the design of novel NMs [372]. GNoME (graph networks for materials exploration) model of Google DeepMind and the MatterGen model reported by Zeni et al. have respectively established extensive candidate libraries of novel crystalline materials and inorganic material generation systems, significantly enhancing the stability and diversity of newly generated NMs [373,374]. The latest MatterChat model further guides material synthesis by predicting critical physical properties [375]. In terms of predicting the targeting efficiency of NPs, Wang et al. accelerated the screening and design of ionizable lipids and targeted lipid NPs (LNPs) through AI models [376], while May et al. utilized supervised machine learning to analyze vascular and TAM density data, proposing a biomarker scoring system to differentiate the accumulation of nanomedicines within tumors [377]. Moreover, AI has demonstrated tremendous potential in structure-activity relationship predictions. Deng et al. developed the DeepNano-seq tool, which predicts nanoantibody-antigen interactions based on protein sequence information and exhibits excellent cross-species generalization and virtual screening performance [378]. Chen et al. raised TopoFormer model could convert the three-dimensional structures of protein-ligand complexes into one-dimensional topological sequences to capture fundamental interactions across spatial scales [379], thereby providing a theoretical basis for designing NMs that target CSC surface markers. Overall, the application of AI in predicting nanomaterial structures, synthesis processes, targeting efficiency, and structure-activity relationships not only provides a vast repository of candidate materials and design tools for the field of nanomedicine but also lays a solid foundation for developing personalized treatment strategies targeting CSCs.

In summary, the development of nanotechnology and the advancement of nanotherapeutic strategies have brought new hope for clinical cancer treatment by specifically targeting and eliminating CSCs. The progress in cancer cell and molecular biology has promoted interdisciplinary research and the development of cancer treatment. It is anticipated that by gradually addressing the existing issues related to CSCs and NMs, safer and more effective nanotherapeutics will emerge in the future, enabling precise cancer treatment by specifically targeting CSCs.

CRediT authorship contribution statement

Hongyu Wang: Writing – review & editing, Writing – original draft, Visualization, Validation, Investigation. **Wenjing Zhang:** Writing – review & editing, Writing – original draft, Validation, Investigation. **Yun Sun:** Writing – review & editing, Visualization. **Xican Xu:** Writing – review & editing. **Xiaoyang Chen:** Writing – review & editing. **Kexu Zhao:** Writing – review & editing. **Zhao Yang:** Writing – review & editing, Supervision, Resources, Project administration, Funding acquisition. **Huiyu Liu:** Writing – review & editing, Supervision, Resources, Project administration, Funding acquisition, Conceptualization.

Ethics approval and consent to participate

This review article does not require any ethical approval or allied consents for publication.

Declaration of competing interest

The authors declare that they have no known competing financial interests or personal relationships that could have appeared to influence the work reported in this paper.

Acknowledgements

H.W and W.Z contributed equally to this work. This work was supported by the National Natural Science Foundation of China (Nos. 22325801, U21A2085, 92359202), National Key Research and Development Program of China (Nos. 2021YFC2102900, 2022YFC2603900, 2023YFC2604600), Beijing Nova Program (No. 20220484168), Fundamental Research Funds for the Central Universities (Nos. QNTD2023-01, buctrc201915), "Open Competition to Select the Best Candidates" Key Technology Program for Nucleic Acid Drugs of NCTIB (NCTIB2022HS01016), Joint Project of Biomedical Translational Engineering Research Center of Beijing University of Chemical Technology-China-Japan Friendship Hospital (XK2023-21), and Open Foundation of State Key Laboratory of Organic-Inorganic Composites, Beijing University of Chemical Technology (No. OIC-202201010).

References

[1] G.R. Dagenais, D.P. Leong, S. Rangarajan, F. Lanas, P. Lopez-Jaramillo, R. Gupta, R. Diaz, A. Avezum, G.B.F. Oliveira, A. Wielgosz, S.R. Parambath, P. Mony, K. F. Alhabib, A. Temizhan, N. Ismail, J. Chifamba, K. Yeates, R. Khatib, O. Rahman, K. Zatonska, K. Kazmi, L. Wei, J. Zhu, A. Rosengren, K. Vijayakumar, M. Kaur, V. Mohan, A. Yusufali, R. Kelishadi, K.K. Teo, P. Joseph, S. Yusuf, Variations in common diseases, hospital admissions, and deaths in middle-aged adults in 21 countries from five continents (PURE): a prospective cohort study, Lancet 395 (2020) 785–794, https://doi.org/10.1016/S0140-6736(19)32007-0.

[2] F. Bray, M. Laversanne, H. Sung, J. Ferlay, R.L. Siegel, I. Soerjomataram, A. Jemal, Global cancer statistics 2022: GLOBOCAN estimates of incidence and mortality worldwide for 36 cancers in 185 countries, CA Cancer J. Clin. 74 (2024) 229–263, https://doi.org/10.3322/caac.21834.

[3] R.B. Mokhtari, T.S. Homayouni, N. Baluch, E. Morgatskaya, S. Kumar, B. Das, H. Yeger, Combination therapy in combating cancer, Oncotarget 8 (2017) 38022–38043, https://doi.org/10.18632/oncotarget.16723.

[4] D.A. Jaffray, Image-guided radiotherapy: from current concept to future perspectives, Nat. Rev. Clin. Oncol. 9 (2012) 688–699, https://doi.org/10.1038/nrclinonc.2012.194.

[5] N. André, M. Carré, E. Pasquier, Metronomics: towards personalized chemotherapy? Nat. Rev. Clin. Oncol. 11 (2014) 413–431, https://doi.org/10.1038/nrclinonc.2014.89.

[6] D.N. Khalil, E.L. Smith, R.J. Brentjens, J.D. Wolchok, The future of cancer treatment: immunomodulation, CARs and combination immunotherapy, Nat. Rev. Clin. Oncol. 13 (2016) 273–290, https://doi.org/10.1038/nrclinonc.2016.25.

[7] T. Huang, X. Song, D. Xu, D. Tiek, A. Goenka, B. Wu, N. Sastry, B. Hu, S.-Y. Cheng, Stem cell programs in cancer initiation, progression, and therapy resistance, Theranostics 10 (2020) 8721–8743, https://doi.org/10.7150/thno.41648.

[8] M. Erkisa, D. Karakas, E. Ulukaya, Cancer stem cells: root of the evil, Crit. Rev. Oncog. 24 (2019) 69–87, https://doi.org/10.1615/CritRevOncog.2019029512.

[9] N.K. Lytle, A.G. Barber, T. Reya, Stem cell fate in cancer growth, progression and therapy resistance, Nat. Rev. Cancer 18 (2018) 669–680, https://doi.org/10.1038/s41568-018-0056-x.

[10] R. Bjerkvig, B.B. Tysnes, K.S. Aboody, J. Najbauer, A.J.A. Terzis, The origin of the cancer stem cell: current controversies and new insights, Nat. Rev. Cancer 5 (2005) 899–904, https://doi.org/10.1038/nrc1740.

[11] J.-J. Loh, S. Ma, Hallmarks of cancer stemness, Cell Stem Cell 31 (2024) 617–639, https://doi.org/10.1016/j.stem.2024.04.004.

[12] F. Naz, M. Shi, S. Sajid, Z. Yang, C. Yu, Cancer stem cells: a major culprit of intra-tumor heterogeneity, Am. J. Cancer Res. 11 (2021) 5782–5811.

[13] M.M. Gottesman, T. Fojo, S.E. Bates, Multidrug resistance in cancer: role of ATP–dependent transporters, Nat. Rev. Cancer 2 (2002) 48–58, https://doi.org/10.1038/nrc706.

[14] M. Diehn, R.W. Cho, N.A. Lobo, T. Kalisky, M.J. Dorie, A.N. Kulp, D. Qian, J. S. Lam, L.E. Ailles, M. Wong, B. Joshua, M.J. Kaplan, I. Wapnir, F.M. Dirbas, G. Somlo, C. Garberoglio, B. Paz, J. Shen, S.K. Lau, S.R. Quake, J.M. Brown, I. L. Weissman, M.F. Clarke, Association of reactive oxygen species levels and radioresistance in cancer stem cells, Nature 458 (2009) 780–783, https://doi.org/10.1038/nature07733.

[15] J. Han, M. Won, J.H. Kim, E. Jung, K. Min, P. Jangili, J.S. Kim, Cancer stem cell-targeted bio-imaging and chemotherapeutic perspective, Chem. Soc. Rev. 49 (2020) 7856–7878, https://doi.org/10.1039/D0CS00379D.

[16] F.-Y. Du, Q.-F. Zhou, W.-J. Sun, G.-L. Chen, Targeting cancer stem cells in drug discovery: current state and future perspectives, World J. Stem Cells 11 (2019) 398–420, https://doi.org/10.4252/wjsc.v11.i7.398.

[17] F. Ju, M.M. Atyah, N. Horstmann, S. Gul, R. Vago, C.J. Bruns, Y. Zhao, Q.-Z. Dong, N. Ren, Characteristics of the cancer stem cell niche and therapeutic strategies, Stem Cell Res. Ther. 13 (2022) 233, https://doi.org/10.1186/s13287-022-02904-1.

[18] V.K. Singh, A. Saini, R. Chandra, The implications and future perspectives of nanomedicine for cancer stem cell targeted therapies, Front. Mol. Biosci. 4 (2017) 52, https://doi.org/10.3389/fmolb.2017.00052.

[19] W.-D. Wang, Y.-Y. Guo, Z.-L. Yang, G.-L. Su, Z.-J. Sun, Sniping cancer stem cells with nanomaterials, ACS Nano 17 (2023) 23262–23298, https://doi.org/10.1021/acsnano.3c07828.

[20] M. Alibolandi, M. Ramezani, K. Abnous, F. Sadeghi, F. Atyabi, M. Asouri, A. A. Ahmadi, F. Hadizadeh, In vitro and in vivo evaluation of therapy targeting epithelial-cell adhesion-molecule aptamers for non-small cell lung cancer, J. Controlled Release 209 (2015) 88–100, https://doi.org/10.1016/j.jconrel.2015.04.026.

[21] Q. Wang, H. Cao, X. Hou, D. Wang, Z. Wang, Y. Shang, S. Zhang, J. Liu, C. Ren, J. Liu, Cancer stem-like cells-oriented surface self-assembly to conquer radioresistance, Adv. Mater. 35 (2023) 2302916, https://doi.org/10.1002/adma.202302916.

[22] R.L. Atkinson, M. Zhang, P. Diagaradjane, S. Peddibhotla, A. Contreras, S. G. Hilsenbeck, W.A. Woodward, S. Krishnan, J.C. Chang, J.M. Rosen, Thermal enhancement with optically activated gold nanoshells sensitizes breast cancer stem cells to radiation therapy, Sci. Transl. Med. 2 (2010) 55ra79, https://doi.org/10.1126/scitranslmed.3001447.

[23] S. Liu, T. Zhang, S. Li, Q. Wu, K. Wang, X. Xu, M. Lu, R. Shao, W. Zhao, H. Liu, Biomimetic nanobomb for synergistic therapy with inhibition of cancer stem cells, Small 19 (2023) 2206503, https://doi.org/10.1002/smll.202206503.

[24] Y. Jiang, X. Liao, W. Tang, C. Huang, Y. Pan, S. Ning, Platelet membrane biomimetic manganese carbonate nanoparticles promote breast cancer stem cell clearance for sensitized radiotherapy, Int. J. Nanomed. 19 (2024) 1699–1707, https://doi.org/10.2147/IJN.S450018.

[25] S. Shen, X. Xu, S. Lin, Y. Zhang, H. Liu, C. Zhang, R. Mo, A nanotherapeutic strategy to overcome chemotherapeutic resistance of cancer stem-like cells, Nat. Nanotechnol. 16 (2021) 104–113, https://doi.org/10.1038/s41565-020-00793-0.

[26] S.-J. Yoon, S. Baek, S.E. Yu, E. Jo, D. Lee, J.-K. Shim, R.J. Choi, J. Park, J. H. Moon, E.-H. Kim, J.H. Chang, J.B. Lee, J.-S. Park, H.-J. Sung, S.-G. Kang, Tissue niche miniature of glioblastoma patient treated with nano-awakeners to induce suicide of cancer stem cells, Adv. Healthcare Mater. 11 (2022) 2201586, https://doi.org/10.1002/adhm.202201586.

[27] H. Lopez-Bertoni, K.L. Kozielski, Y. Rui, B. Lal, H. Vaughan, D.R. Wilson, N. Mihelson, C.G. Eberhart, J. Laterra, J.J. Green, Bioreducible polymeric nanoparticles containing multiplexed cancer stem cell regulating miRNAs inhibit glioblastoma growth and prolong survival, Nano Lett. 18 (2018) 4086–4094, https://doi.org/10.1021/acs.nanolett.8b00390.

[28] P. Xia, Surface markers of cancer stem cells in solid tumors, Curr. Stem Cell Res. Ther. 9 (2014) 102–111.

[29] Z. Kozovska, V. Gabrisova, L. Kucerova, Malignant melanoma: diagnosis, treatment and cancer stem cells, Neoplasma 63 (2016) 510–517, https://doi.org/10.4149/neo_2016_403.

[30] M. Grimm, M. Krimmel, J. Polligkeit, D. Alexander, A. Munz, S. Kluba, C. Keutel, J. Hoffmann, S. Reinert, S. Hoefert, ABCB5 expression and cancer stem cell hypothesis in oral squamous cell carcinoma, Eur. J. Cancer 48 (2012) 3186–3197, https://doi.org/10.1016/j.ejca.2012.05.027.

[31] P. Jongkhajornpong, T. Nakamura, C. Sotozono, M. Nagata, T. Inatomi, S. Kinoshita, Elevated expression of ABCB5 in ocular surface squamous neoplasia, Sci. Rep. 6 (2016) 20541, https://doi.org/10.1038/srep20541.

[32] A.S. Köseer, S. Di Gaetano, C. Arndt, M. Bachmann, A. Dubrovska, Immunotargeting of cancer stem cells, Cancers 15 (2023) 1608, https://doi.org/10.3390/cancers15051608.

[33] V. Cardinale, A. Renzi, G. Carpino, A. Torrice, M.C. Bragazzi, F. Giuliante, A. M. De Rose, A. Fraveto, P. Onori, C. Napoletano, A. Franchitto, A. Cantafora, G. Grazi, N. Caporaso, G. D'Argenio, G. Alpini, L.M. Reid, E. Gaudio, D. Alvaro, Profiles of cancer stem cell subpopulations in cholangiocarcinomas, Am. J. Pathol. 185 (2015) 1724–1739, https://doi.org/10.1016/j.ajpath.2015.02.010.

[34] Y.-C. Liu, C.-T. Yeh, K.-H. Lin, Cancer stem cell functions in hepatocellular carcinoma and comprehensive therapeutic strategies, Cells 9 (2020) 1331, https://doi.org/10.3390/cells9061331.

[35] Y. Li, J. Shi, Z. Liu, Y. Lin, A. Xie, W. Sun, J. Liu, J. Liang, Regulation of the migration of colorectal cancer stem cells via the TLR4/MyD88 signaling pathway by the novel surface marker CD14 following LPS stimulation, Oncol. Lett. 27 (2024) 1–9, https://doi.org/10.3892/ol.2023.14194.

[36] L. Wei, J. Meng, D. Xiang, Q. Yang, Y. Zhou, L. Xu, J. Chen, Y. Han, The pan-cancer analysis uncovers the prognostic and immunotherapeutic significance of CD19 as an immune marker in tumor, Int. J. Gen. Med. 17 (2024) 2593–2612, https://doi.org/10.2147/IJGM.S459914.

[37] Q. Yin, X. Shi, S. Lan, H. Jin, D. Wu, Effect of melanoma stem cells on melanoma metastasis, Oncol. Lett. 22 (2021) 566, https://doi.org/10.3892/ol.2021.12827.

[38] F.J. Suárez-Sánchez, P. Lequerica-Fernández, J.P. Rodrigo, F. Hermida-Prado, J. Suárez-Canto, T. Rodríguez-Santamarta, F. Domínguez-Iglesias, J.M. García-Pedrero, J.C. de Vicente, Tumor-infiltrating CD20+ B lymphocytes: significance and prognostic implications in oral cancer microenvironment, Cancers 13 (2021) 395, https://doi.org/10.3390/cancers13030395.

[39] Y. Wang, H. Yu, M. Yu, H. Liu, B. Zhang, Y. Wang, S. Zhao, Q. Xia, CD24 blockade as a novel strategy for cancer treatment, Int. Immunopharmacol. 121 (2023) 110557, https://doi.org/10.1016/j.intimp.2023.110557.

[40] S. Davies, A. Beckenkamp, A. Buffon, CD26 a cancer stem cell marker and therapeutic target, Biomed. Pharmacother. 71 (2015) 135–138, https://doi.org/10.1016/j.biopha.2015.02.031.

[41] T. Lapidot, C. Sirard, J. Vormoor, B. Murdoch, T. Hoang, J. Caceres-Cortes, M. Minden, B. Paterson, M.A. Caligiuri, J.E. Dick, A cell initiating human acute myeloid leukaemia after transplantation into SCID mice, Nature 367 (1994) 645–648, https://doi.org/10.1038/367645a0.

[42] S. Kapoor, S.P. Shenoy, B. Bose, CD34 cells in somatic, regenerative and cancer stem cells: developmental biology, cell therapy, and omics big data perspective, J. Cell. Biochem. 121 (2020) 3058–3069, https://doi.org/10.1002/jcb.29571.

[43] W. Szlasa, J. Czarny, N. Sauer, K. Rakoczy, N. Szymańska, J. Stecko, M. Kołodziej, M. Kaźmierczak, E. Barg, Targeting CD38 in neoplasms and non-cancer diseases, Cancers 14 (2022) 4169, https://doi.org/10.3390/cancers14174169.

[44] S.S. Skandalis, T.T. Karalis, A. Chatzopoulos, N.K. Karamanos, Hyaluronan-CD44 axis orchestrates cancer stem cell functions, Cell. Signal. 63 (2019) 109377, https://doi.org/10.1016/j.cellsig.2019.109377.

[45] A.A. Gómez-Gallegos, L. Ramírez-Vidal, J. Becerril-Rico, E. Pérez-Islas, Z. J. Hernandez-Peralta, M.E. Toledo-Guzmán, A. García-Carrancá, E. Langley, A. Hernández-Guerrero, F. López-Casillas, R. Herrera-Goepfert, L.F. Oñate-Ocaña, E. Ortiz-Sánchez, CD24+CD44+CD54+EpCAM+ gastric cancer stem cells predict tumor progression and metastasis: clinical and experimental evidence, Stem Cell Res. Ther. 14 (2023) 16, https://doi.org/10.1186/s13287-023-03241-7.

[46] C. Li, S. Liu, R. Yan, N. Han, K.-K. Wong, L. Li, CD54-NOTCH1 axis controls tumor initiation and cancer stem cell functions in human prostate cancer, Theranostics 7 (2017) 67–80, https://doi.org/10.7150/thno.16752.

[47] R. Bharti, G. Dey, F. Lin, J. Lathia, O. Reizes, CD55 in cancer: complementing functions in a non-canonical manner, Cancer Lett. 551 (2022) 215935, https://doi.org/10.1016/j.canlet.2022.215935.

[48] P.-K. Lo, D. Kanojia, X. Liu, U.P. Singh, F.G. Berger, Q. Wang, H. Chen, CD49f and CD61 identify Her2/neu-induced mammary tumor-initiating cells that are potentially derived from luminal progenitors and maintained by the integrin–TGFβ signaling, Oncogene 31 (2012) 2614–2626, https://doi.org/10.1038/onc.2011.439.

[49] X. Guan, Y. Lu, C. Wang, P. Zhan, Z. Chen, Role of CD61+ low-density neutrophils in promoting hepatocellular carcinoma metastasis through CCDC25 upregulation, Int. Immunopharmacol. 134 (2024) 112272, https://doi.org/10.1016/j.intimp.2024.112272.

[50] W. Huang, S. Zhao, W. Xu, Z. Zhang, X. Ding, J. He, W. Liang, Presence of intra-tumoral CD61+ megakaryocytes predicts poor prognosis in non-small cell lung cancer, Transl. Lung Cancer Res. 8 (2019) 323–331, https://doi.org/10.21037/tlcr.2019.08.23.

[51] A. Ammothumkandy, T.T. Maliekal, M.V. Bose, T. Rajkumar, S. Shirley, B. Thejaswini, V.G. Giri, S. Krishna, CD66 and CD49f expressing cells are associated with distinct neoplastic phenotypes and progression in human cervical cancer, Eur. J. Cancer 60 (2016) 166–178, https://doi.org/10.1016/j.ejca.2016.03.072.

[52] M.V. Shaikh, M. Kala, M. Nivsarkar, CD90 a potential cancer stem cell marker and a therapeutic target, Cancer Biomarkers 16 (2016) 301–307, https://doi.org/10.3233/CBM-160590.

[53] W. Gao, L. Chen, Z. Ma, Z. Du, Z. Zhao, Z. Hu, Q. Li, Isolation and phenotypic characterization of colorectal cancer stem cells with organ-specific metastatic potential, Gastroenterology 145 (2013) 636–646, https://doi.org/10.1053/j.gastro.2013.05.049.

[54] P.E. Zage, S.B. Whittle, J.M. Shohet, CD114: a new member of the neural crest-derived cancer stem cell marker family, J. Cell. Biochem. 118 (2017) 221–231, https://doi.org/10.1002/jcb.25656.

[55] B.M. Foster, D. Zaidi, T.R. Young, M.E. Mobley, B.A. Kerr, CD117/c-kit in cancer stem cell-mediated progression and therapeutic resistance, Biomedicines 6 (2018) 31, https://doi.org/10.3390/biomedicines6010031.

[56] Z. Li, CD133: a stem cell biomarker and beyond, Exp. Hematol. Oncol. 2 (2013) 17, https://doi.org/10.1186/2162-3619-2-17.

[57] F. Ferragut, V.S. Vachetta, M.F. Troncoso, G.A. Rabinovich, M.T. Elola, ALCAM/CD166: a pleiotropic mediator of cell adhesion, stemness and cancer progression, Cytokine Growth Factor Rev. 61 (2021) 27–37, https://doi.org/10.1016/j.cytogfr.2021.07.001.

[58] O.A. Elkashty, G. Abu Elghanam, X. Su, Y. Liu, P.J. Chauvin, S.D. Tran, Cancer stem cells enrichment with surface markers CD271 and CD44 in human head and neck squamous cell carcinomas, Carcinogenesis 41 (2020) 458–466, https://doi.org/10.1093/carcin/bgz182.

[59] F. Islam, V. Gopalan, R. Wahab, R.A. Smith, A.K.-Y. Lam, Cancer stem cells in oesophageal squamous cell carcinoma: identification, prognostic and treatment perspectives, Crit. Rev. Oncol. Hematol. 96 (2015) 9–19, https://doi.org/10.1016/j.critrevonc.2015.04.007.

[60] N. Lyu, B. Pedersen, E. Shklovskaya, H. Rizos, M.P. Molloy, Y. Wang, SERS characterization of colorectal cancer cell surface markers upon anti-EGFR treatment, Exploration 2 (2022) 20210176, https://doi.org/10.1002/EXP.20210176.

[61] M. Kim, L. Bakyt, A. Akhmetkaliyev, D. Toktarkhanova, D. Bulanin, Re-sensitizing cancer stem cells to conventional chemotherapy agents, Int. J. Mol. Sci. 24 (2023) 2122, https://doi.org/10.3390/ijms24032122.

[62] H.-Z. Cao, X.-F. Liu, W.-T. Yang, Q. Chen, P.-S. Zheng, LGR5 promotes cancer stem cell traits and chemoresistance in cervical cancer, Cell Death Dis. 8 (2017), https://doi.org/10.1038/cddis.2017.393 e3039–e3039.

[63] M. Shimokawa, Y. Ohta, S. Nishikori, M. Matano, A. Takano, M. Fujii, S. Date, S. Sugimoto, T. Kanai, T. Sato, Visualization and targeting of LGR5+ human colon cancer stem cells, Nature 545 (2017) 187–192, https://doi.org/10.1038/nature22081.

[64] H. Xu, W. Li, X. Song, H. Zhang, H. Wang, J. Wang, L. Hu, H. Li, X. Sun, D. Wang, Expression and prognostic value of Lgr5 in patients with recurrent nasopharyngeal carcinoma, Int. J. Gen. Med. 16 (2023) 2023–2034, https://doi.org/10.2147/IJGM.S408991.

[65] T. Ishiwata, Y. Matsuda, H. Yoshimura, N. Sasaki, S. Ishiwata, N. Ishikawa, K. Takubo, T. Arai, J. Aida, Pancreatic cancer stem cells: features and detection methods, Pathol. Oncol. Res. 24 (2018) 797–805, https://doi.org/10.1007/s12253-018-0420-x.

[66] Q.-L. Tang, Y. Liang, X.-B. Xie, J.-Q. Yin, C.-Y. Zou, Z.-Q. Zhao, J.-N. Shen, J. Wang, Enrichment of osteosarcoma stem cells by chemotherapy, Chin. J. Cancer 30 (2011) 426–432, https://doi.org/10.5732/cjc.011.10127.

[67] F.M. Uckun, H. Sather, G. Reaman, J. Shuster, V. Land, M. Trigg, R. Gunther, L. Chelstrom, A. Bleyer, P. Gaynon, W. Crist, Leukemic cell growth in SCID mice as a predictor of relapse in high-risk B-lineage acute lymphoblastic leukemia, Blood 85 (1995) 873–878, https://doi.org/10.1182/blood.V85.4.873.bloodjournal854873.

[68] S.C. Park, N.T. Nguyen, J.R. Eun, Y. Zhang, Y.J. Jung, B. Tschudy-Seney, A. Trotsyuk, A. Lam, R. Ramsamooj, Y. Zhang, N.D. Theise, M.A. Zern, Y. Duan, Identification of cancer stem cell subpopulations of CD34+ PLC/PRF/5 that result in three types of human liver carcinomas, Stem Cells Dev. 24 (2015) 1008–1021, https://doi.org/10.1089/scd.2014.0405.

[69] A. Weigmann, D. Corbeil, A. Hellwig, W.B. Huttner, Prominin, a novel microvilli-specific polytopic membrane protein of the apical surface of epithelial cells, is targeted to plasmalemmal protrusions of non-epithelial cells, Proc. Natl. Acad. Sci. USA 94 (1997) 12425–12430, https://doi.org/10.1073/pnas.94.23.12425.

[70] S.K. Singh, C. Hawkins, I.D. Clarke, J.A. Squire, J. Bayani, T. Hide, R. M. Henkelman, M.D. Cusimano, P.B. Dirks, Identification of human brain tumour initiating cells, Nature 432 (2004) 396–401, https://doi.org/10.1038/nature03128.

[71] S. Mersakova, K. Janikova, M. Kalman, J. Marcinek, M. Grendar, M. Vojtko, R. Kycina, M. Pindura, J. Janik, P. Mikolajcik, E. Gabonova, L. Laca, E. Mejstrikova, E. Halasova, J. Strnadel, Z. Lasabova, Cancer stem cell marker expression and methylation status in patients with colorectal cancer, Oncol. Lett. 24 (2022) 1–13, https://doi.org/10.3892/ol.2022.13352.

[72] S. Attia, N. Atwan, M. Arafa, R.A. Shahin, Expression of CD133 as a cancer stem cell marker in invasive gastric carcinoma, Pathologica 111 (2019) 18–23, https://doi.org/10.32074/1591-951X-51-18.

[73] C.B. Underhill, A.L. Thurn, B.E. Lacy, Characterization and identification of the hyaluronate binding site from membranes of SV-3T3 cells, J. Biol. Chem. 260 (1985) 8128–8133, https://doi.org/10.1016/S0021-9258(17)39573-X.

[74] M. Al-Hajj, M.S. Wicha, A. Benito-Hernandez, S.J. Morrison, M.F. Clarke, Prospective identification of tumorigenic breast cancer cells, Proc. Natl. Acad. Sci. USA 100 (2003) 3983–3988, https://doi.org/10.1073/pnas.0530291100.

[75] J. Kim, K.-W. Choi, J. Lee, J. Lee, S. Lee, R. Sun, J. Kim, Wnt/β-catenin signaling inhibitors suppress the tumor-initiating properties of a CD44+CD133+ subpopulation of caco-2 cells, Int. J. Biol. Sci. 17 (2021) 1644–1659, https://doi.org/10.7150/ijbs.58612.

[76] Z. Yang, C. Li, Z. Fan, H. Liu, X. Zhang, Z. Cai, L. Xu, J. Luo, Y. Huang, L. He, C. Liu, S. Wu, Single-cell sequencing reveals variants in *ARID1A, GPRC5A* and *MLL2* driving self-renewal of human bladder cancer stem cells, Eur. Urol. 71 (2017) 8–12, https://doi.org/10.1016/j.eururo.2016.06.025.

[77] F.M. Hofman, E. Yanagihara, B. Byrne, R. Billing, S. Baird, D. Frisman, C. R. Taylor, Analysis of B-cell antigens in normal reactive lymphoid tissue using four B-cell monoclonal antibodies, Blood 62 (1983) 775–783, https://doi.org/10.1182/blood.V62.4.775.775.

[78] J. Dou, M. Pan, P. Wen, Y. Li, Q. Tang, L. Chu, F. Zhao, C. Jiang, W. Hu, K. Hu, N. Gu, Isolation and identification of cancer stem-like cells from murine melanoma cell lines, Cell. Mol. Immunol. 4 (2007) 467–472.

[79] A. Ooki, C.J. VandenBussche, M. Kates, N.M. Hahn, A. Matoso, D.J. McConkey, T. J. Bivalacqua, M.O. Hoque, CD24 regulates cancer stem cell (CSC)-like traits and a panel of CSC-related molecules serves as a non-invasive urinary biomarker for the detection of bladder cancer, Br. J. Cancer 119 (2018) 961–970, https://doi.org/10.1038/s41416-018-0291-7.

[80] J.B. Overdevest, S. Thomas, G. Kristiansen, D.E. Hansel, S.C. Smith, D. Theodorescu, CD24 offers a therapeutic target for control of bladder cancer metastasis based on a requirement for lung colonization, Cancer Res. 71 (2011) 3802–3811, https://doi.org/10.1158/0008-5472.CAN-11-0519.

[81] A.E. Reif, J.M.V. Allen, The akr thymic antigen and its distribution in leukemias and nervous tissues, J. Exp. Med. 120 (1964) 413–433, https://doi.org/10.1084/jem.120.3.413.

[82] Z.F. Yang, D.W. Ho, M.N. Ng, C.K. Lau, W.C. Yu, P. Ngai, P.W.K. Chu, C.T. Lam, R. T.P. Poon, S.T. Fan, Significance of CD90+ cancer stem cells in human liver cancer, Cancer Cell 13 (2008) 153–166, https://doi.org/10.1016/j.ccr.2008.01.013.

[83] X. Shu, H. Liu, Y. Pan, L. Sun, L. Yu, L. Sun, Z. Yang, Y. Ran, Distinct biological characterization of the CD44 and CD90 phenotypes of cancer stem cells in gastric cancer cell lines, Mol. Cell. Biochem. 459 (2019) 35–47, https://doi.org/10.1007/s11010-019-03548-1.

[84] Z. Liu, M. Bai, J. Li, Correlation between inflammatory cytokines and liver cancer stem cell markers in DEN-induced liver cancer rats, Eur. Rev. Med. Pharmacol. Sci. 25 (2021) 710–721, https://doi.org/10.26355/eurrev_202101_24632.

[85] Y. Liu, Y. Wang, S. Sun, Z. Chen, S. Xiang, Z. Ding, Z. Huang, B. Zhang, Understanding the versatile roles and applications of EpCAM in cancers: from bench to bedside, Exp. Hematol. Oncol. 11 (2022) 97, https://doi.org/10.1186/s40164-022-00352-4.

[86] D. Herlyn, M. Herlyn, Z. Steplewski, H. Koprowski, Monoclonal antibodies in cell-mediated cytotoxicity against human melanoma and colorectal carcinoma, Eur. J. Immunol. 9 (1979) 657–659, https://doi.org/10.1002/eji.1830090817.

[87] H.S. Hwang, J.E. Yoo, D.H. Han, J.S. Choi, J.G. Lee, D.J. Joo, M.S. Kim, S.I. Kim, G.H. Choi, Y.N. Park, Circulating cancer stem cells expressing EpCAM/CD90 in hepatocellular carcinoma: a pilot study for predicting tumor recurrence after living donor liver transplantation, Gut Liver 16 (2022) 443–455, https://doi.org/10.5009/gnl210162.

[88] T. Mederer, F. Elsner, T. Robold, C. Großer, R. Neu, M. Ried, S. Bleicher, T. Schamberger, I. Blochberger, H.-S. Hofmann, C.A. Klein, EpCAM-positive disseminated cancer cells in bone marrow impact on survival of early-stage NSCLC patients, Lung Cancer 167 (2022) 73–77, https://doi.org/10.1016/j.lungcan.2022.02.008.

[89] L. Yang, P. Shi, G. Zhao, J. Xu, W. Peng, J. Zhang, G. Zhang, X. Wang, Z. Dong, F. Chen, H. Cui, Targeting cancer stem cell pathways for cancer therapy, Signal Transduct. Targeted Ther. 5 (2020) 1–35, https://doi.org/10.1038/s41392-020-0110-5.

[90] G. Babaei, S.G.-G. Aziz, N.Z.Z. Jaghi, EMT, cancer stem cells and autophagy; the three main axes of metastasis, Biomed. Pharmacother. 133 (2021) 110909, https://doi.org/10.1016/j.biopha.2020.110909.

[91] R. Nusse, H.E. Varmus, Many tumors induced by the mouse mammary tumor virus contain a provirus integrated in the same region of the host genome, Cell 31 (1982) 99–109, https://doi.org/10.1016/0092-8674(82)90409-3.

[92] H. Clevers, R. Nusse, Wnt/β-Catenin signaling and disease, Cell 149 (2012) 1192–1205, https://doi.org/10.1016/j.cell.2012.05.012.

[93] L.F. Ng, P. Kaur, N. Bunnag, J. Suresh, I.C.H. Sung, Q.H. Tan, J. Gruber, N. S. Tolwinski, WNT signaling in disease, Cells 8 (2019) 826, https://doi.org/10.3390/cells8080826.

[94] Y. He, X. Jiang, L. Duan, Q. Xiong, Y. Yuan, P. Liu, L. Jiang, Q. Shen, S. Zhao, C. Yang, Y. Chen, LncRNA PKMYT1AR promotes cancer stem cell maintenance in non-small cell lung cancer via activating Wnt signaling pathway, Mol. Cancer 20 (2021) 156, https://doi.org/10.1186/s12943-021-01469-6.

[95] T. Tang, C. Guo, T. Xia, R. Zhang, K. Zen, Y. Pan, L. Jin, LncCCAT1 promotes breast cancer stem cell function through activating WNT/β-catenin signaling, Theranostics 9 (2019) 7384–7402, https://doi.org/10.7150/thno.37892.

[96] C. Nüsslein-Volhard, E. Wieschaus, Mutations affecting segment number and polarity in Drosophila, Nature 287 (1980) 795–801, https://doi.org/10.1038/287795a0.

[97] X. Zheng, W. Zeng, X. Gai, Q. Xu, C. Li, Z. Liang, H. Tuo, Q. Liu, Role of the Hedgehog pathway in hepatocellular carcinoma, Oncol. Rep. 30 (2013) 2020–2026, https://doi.org/10.3892/or.2013.2690.

[98] C. Li, Y. Du, Z. Yang, L. He, Y. Wang, L. Hao, M. Ding, R. Yan, J. Wang, Z. Fan, GALNT1-Mediated glycosylation and activation of sonic hedgehog signaling maintains the self-renewal and tumor-initiating capacity of bladder cancer stem cells, Cancer Res. 76 (2016) 1273–1283, https://doi.org/10.1158/0008-5472.CAN-15-2309.

[99] X. Sun, J. Song, E. Li, H. Geng, Y. Li, D. Yu, C. Zhong, Cigarette smoke supports stemness and epithelial-mesenchymal transition in bladder cancer stem cells through SHH signaling, Int. J. Clin. Exp. Pathol. 13 (2020) 1333–1348.
[100] L.W. Ellisen, J. Bird, D.C. West, A.L. Soreng, T.C. Reynolds, S.D. Smith, J. Sklar, TAN-1, the human homolog of the Drosophila Notch gene, is broken by chromosomal translocations in T lymphoblastic neoplasms, Cell 66 (1991) 649–661, https://doi.org/10.1016/0092-8674(91)90111-B.
[101] A. Joutel, E. Tournier-Lasserve, Notch signalling pathway and human diseases, Semin. Cell Dev. Biol. 9 (1998) 619–625, https://doi.org/10.1006/scdb.1998.0261.
[102] J.A. Clara, C. Monge, Y. Yang, N. Takebe, Targeting signalling pathways and the immune microenvironment of cancer stem cells — a clinical update, Nat. Rev. Clin. Oncol. 17 (2020) 204–232, https://doi.org/10.1038/s41571-019-0293-2.
[103] L. Yi, X. Zhou, T. Li, P. Liu, L. Hai, L. Tong, H. Ma, Z. Tao, Y. Xie, C. Zhang, S. Yu, X. Yang, Notch1 signaling pathway promotes invasion, self-renewal and growth of glioma initiating cells via modulating chemokine system CXCL12/CXCR4, J. Exp. Clin. Cancer Res. 38 (2019) 339, https://doi.org/10.1186/s13046-019-1319-4.
[104] L. Jing, Z. Ruan, H. Sun, Q. Li, L. Han, L. Huang, S. Yu, Y. Wang, H. Guo, M. Jiao, Epithelial–mesenchymal transition induced cancer-stem-cell-like characteristics in hepatocellular carcinoma, J. Cell. Physiol. 234 (2019) 18448–18458, https://doi.org/10.1002/jcp.28480.
[105] B. Schmierer, C.S. Hill, TGFβ–SMAD signal transduction: molecular specificity and functional flexibility, Nat. Rev. Mol. Cell Biol. 8 (2007) 970–982, https://doi.org/10.1038/nrm2297.
[106] H. Zhao, J. Wei, J. Sun, Roles of TGF-β signaling pathway in tumor microenvirionment and cancer therapy, Int. Immunopharmacol. 89 (2020) 107101, https://doi.org/10.1016/j.intimp.2020.107101.
[107] X. Wang, J. Wang, Y.-M. Tsui, C. Shi, Y. Wang, X. Zhang, Q. Yan, M. Chen, C. Jiang, Y.-F. Yuan, C.-M. Wong, M. Liu, Z. Feng, H. Chen, I.O.L. Ng, L. Jiang, X.-Y. Guan, RALYL increases hepatocellular carcinoma stemness by sustaining the mRNA stability of TGF-β2, Nat. Commun. 12 (2021) 1518, https://doi.org/10.1038/s41467-021-21828-7.
[108] W. Yuan, J. Ji, Y. Shu, J. Chen, S. Liu, L. Wu, Z. Zhou, Z. Liu, Q. Tang, X. Zhang, X. Shu, Downregulation of DAPK1 promotes the stemness of cancer stem cells and EMT process by activating ZEB1 in colorectal cancer, J. Mol. Med. 97 (2019) 89–102, https://doi.org/10.1007/s00109-018-1716-8.
[109] J. Huynh, N. Etemadi, F. Hollande, M. Ernst, M. Buchert, The JAK/STAT3 axis: a comprehensive drug target for solid malignancies, Semin. Cancer Biol. 45 (2017) 13–22, https://doi.org/10.1016/j.semcancer.2017.06.001.
[110] P.M. Nguyen, T.L. Putoczki, M. Ernst, STAT3-Activating cytokines: a therapeutic opportunity for inflammatory bowel disease? J. Interferon Cytokine Res. 35 (2015) 340–350, https://doi.org/10.1089/jir.2014.0225.
[111] D.A. Almiron Bonnin, M.C. Havrda, M.C. Lee, H. Liu, Z. Zhang, L.N. Nguyen, L. X. Harrington, S. Hassanpour, C. Cheng, M.A. Israel, Secretion-mediated STAT3 activation promotes self-renewal of glioma stem-like cells during hypoxia, Oncogene 37 (2018) 1107–1118, https://doi.org/10.1038/onc.2017.404.
[112] T. Wang, J.F. Fahrmann, H. Lee, Y.-J. Li, S.C. Tripathi, C. Yue, C. Zhang, V. Lifshitz, J. Song, Y. Yuan, G. Somlo, R. Jandial, D. Ann, S. Hanash, R. Jove, H. Yu, JAK/STAT3-Regulated fatty acid β-oxidation is critical for breast cancer stem cell self-renewal and chemoresistance, Cell Metab. 27 (2018) 136–150, https://doi.org/10.1016/j.cmet.2017.11.001.
[113] X. Dolcet, D. Llobet, J. Pallares, X. Matias-Guiu, NF-kB in development and progression of human cancer, Virchows Arch. 446 (2005) 475–482, https://doi.org/10.1007/s00428-005-1264-9.
[114] K. Vazquez-Santillan, J. Melendez-Zajgla, L. Jimenez-Hernandez, G. Martínez-Ruiz, V. Maldonado, NF-κB signaling in cancer stem cells: a promising therapeutic target? Cell. Oncol. 38 (2015) 327–339, https://doi.org/10.1007/s13402-015-0236-6.
[115] M. Yamamoto, Y. Taguchi, T. Ito-Kureha, K. Semba, N. Yamaguchi, J. Inoue, NF-κB non-cell-autonomously regulates cancer stem cell populations in the basal-like breast cancer subtype, Nat. Commun. 4 (2013) 2299, https://doi.org/10.1038/ncomms3299.
[116] A.L. Harris, Hypoxia — a key regulatory factor in tumour growth, Nat. Rev. Cancer 2 (2002) 38–47, https://doi.org/10.1038/nrc704.
[117] B.A. Webb, M. Chimenti, M.P. Jacobson, D.L. Barber, Dysregulated pH: a perfect storm for cancer progression, Nat. Rev. Cancer 11 (2011) 671–677, https://doi.org/10.1038/nrc3110.
[118] A. Barker, J. Dombrosky, D. Chaput, B. Venables, S. Wolverton, S.M. Stevens, Validation of a non-targeted LC-MS approach for identifying ancient proteins: method development on bone to improve artifact residue analysis, Ethnobiol. Lett. 6 (2015) 162–174.
[119] K.E. de Visser, J.A. Joyce, The evolving tumor microenvironment: from cancer initiation to metastatic outgrowth, Cancer Cell 41 (2023) 374–403, https://doi.org/10.1016/j.ccell.2023.02.016.
[120] P. Nallasamy, R.K. Nimmakayala, S. Parte, A.C. Are, S.K. Batra, M.P. Ponnusamy, Tumor microenvironment enriches the stemness features: the architectural event of therapy resistance and metastasis, Mol. Cancer 21 (2022) 225, https://doi.org/10.1186/s12943-022-01682-x.
[121] L. Cassetta, J.W. Pollard, A timeline of tumour-associated macrophage biology, Nat. Rev. Cancer 23 (2023) 238–257, https://doi.org/10.1038/s41568-022-00547-1.
[122] Y. Zheng, Y. Han, Q. Sun, Z. Li, Harnessing anti-tumor and tumor-tropism functions of macrophages via nanotechnology for tumor immunotherapy, Exploration 2 (2022) 20210166, https://doi.org/10.1002/EXP.20210166.
[123] Y. Pan, Y. Yu, X. Wang, T. Zhang, Tumor-associated macrophages in tumor immunity, Front. Immunol. 11 (2020) 583084, https://doi.org/10.3389/fimmu.2020.583084.
[124] L. Wu, S. Ye, Y. Yao, C. Zhang, W. Liu, Oral cancer stem cell-derived small extracellular vesicles promote M2 macrophage polarization and suppress $CD4^+$ T-cell activity by transferring UCA1 and targeting LAMC2, Stem Cells Int. 2022 (2022) e5817684, https://doi.org/10.1155/2022/5817684.
[125] H.-C. Wang, L.-Y. Haung, C.-J. Wang, Y.-J. Chao, Y.-C. Hou, C.-J. Yen, Y.-S. Shan, Tumor-associated macrophages promote resistance of hepatocellular carcinoma cells against sorafenib by activating CXCR2 signaling, J. Biomed. Sci. 29 (2022) 99, https://doi.org/10.1186/s12929-022-00881-4.
[126] Z. Liao, Z.W. Tan, P. Zhu, N.S. Tan, Cancer-associated fibroblasts in tumor microenvironment – accomplices in tumor malignancy, Cell. Immunol. 343 (2019) 103729, https://doi.org/10.1016/j.cellimm.2017.12.003.
[127] Z. Zhao, Y. Zhang, E. Guo, Y. Zhang, Y. Wang, Periostin secreted from podoplanin-positive cancer-associated fibroblasts promotes metastasis of gastric cancer by regulating cancer stem cells via AKT and YAP signaling pathway, Mol. Carcinog. 62 (2023) 685–699, https://doi.org/10.1002/mc.23517.
[128] R. Pradhan, S. Paul, B. Das, S. Sinha, S.R. Dash, M. Mandal, C.N. Kundu, Resveratrol nanoparticle attenuates metastasis and angiogenesis by deregulating inflammatory cytokines through inhibition of CAFs in oral cancer by CXCL-12/IL-6-dependent pathway, J. Nutr. Biochem. 113 (2023) 109257, https://doi.org/10.1016/j.jnutbio.2022.109257.
[129] J.I. Erices, I. Niechi, A. Uribe-Ojeda, M. de los Á. Toro, N. García-Romero, J. Carrión-Navarro, Á. Monago-Sánchez, Á. Ayuso-Sacido, R.S. Martin, C. Quezada-Monrás, The low affinity A2B adenosine receptor enhances migratory and invasive capacity in vitro and angiogenesis in vivo of glioblastoma stem-like cells, Front. Oncol. 12 (2022) 969993, https://doi.org/10.3389/fonc.2022.969993.
[130] C. Ye, H. Li, Y. Li, Y. Zhang, G. Liu, H. Mi, H. Li, Q. Xiao, L. Niu, X. Yu, Hypoxia-induced HMGB1 promotes glioma stem cells self-renewal and tumorigenicity via RAGE, iScience 25 (2022) 104872, https://doi.org/10.1016/j.isci.2022.104872.
[131] H. Dai, Q. Fan, C. Wang, Recent applications of immunomodulatory biomaterials for disease immunotherapy, Exploration 2 (2022) 20210157, https://doi.org/10.1002/EXP.20210157.
[132] M.G. Scioli, S. Terriaca, E. Fiorelli, G. Storti, G. Fabbri, V. Cervelli, A. Orlandi, Extracellular vesicles and cancer stem cells in tumor progression: new therapeutic perspectives, Int. J. Mol. Sci. 22 (2021) 10572, https://doi.org/10.3390/ijms221910572.
[133] I. Cifola, F. Fratini, B. Cardinali, V. Palmieri, G. Gatti, T. Selmi, S. Donzelli, A. Sacconi, V. Cesarini, H.E. Marei, M. Papi, G. Blandino, C. Cenciarelli, G. Falcone, I. D'Agnano, miRNome and proteome profiling of small extracellular vesicles secreted by human glioblastoma cell lines and primary cancer stem cells, Biomedicines 10 (2022) 1886, https://doi.org/10.3390/biomedicines10081886.
[134] W.-M. Chung, R.D. Molony, Y.-F. Lee, Non-stem bladder cancer cell-derived extracellular vesicles promote cancer stem cell survival in response to chemotherapy, Stem Cell Res. Ther. 12 (2021) 533, https://doi.org/10.1186/s13287-021-02600-6.
[135] C. Clemente-González, A. Carnero, Role of the hypoxic-secretome in seed and soil metastatic preparation, Cancers 14 (2022) 5930, https://doi.org/10.3390/cancers14235930.
[136] F. Hajizadeh, I. Okoye, M. Esmaily, M. Ghasemi Chaleshtari, A. Masjedi, G. Azizi, M. Irandoust, G. Ghalamfarsa, F. Jadidi-Niaragh, Hypoxia inducible factors in the tumor microenvironment as therapeutic targets of cancer stem cells, Life Sci. 237 (2019) 116952, https://doi.org/10.1016/j.lfs.2019.116952.
[137] Y.S. Ko, T. Rugira, H. Jin, Y.N. Joo, H.J. Kim, Radiotherapy-resistant breast cancer cells enhance tumor progression by enhancing premetastatic niche formation through the HIF-1α-LOX Axis, Int. J. Mol. Sci. 21 (2020) 8027, https://doi.org/10.3390/ijms21218027.
[138] S. Ghosh, S.K. Juin, S. Bhattacharyya Majumdar, S. Majumdar, Crucial role of glucosylceramide synthase in the regulation of stem cell-like cancer cells in B16F10 murine melanoma, Mol. Carcinog. 60 (2021) 840–858, https://doi.org/10.1002/mc.23347.
[139] F. Li, J. Xu, S. Liu, Cancer stem cells and neovascularization, Cells 10 (2021) 1070, https://doi.org/10.3390/cells10051070.
[140] D. Zhao, C. Pan, J. Sun, C. Gilbert, K. Drews-Elger, D.J. Azzam, M. Picon-Ruiz, M. Kim, W. Ullmer, D. El-Ashry, C.J. Creighton, J.M. Slingerland, VEGF drives cancer-initiating stem cells through VEGFR-2/Stat3 signaling to upregulate Myc and Sox2, Oncogene 34 (2015) 3107–3119, https://doi.org/10.1038/onc.2014.257.
[141] M.A. Nengroo, A. Verma, D. Datta, Cytokine chemokine network in tumor microenvironment: impact on CSC properties and therapeutic applications, Cytokine 156 (2022) 155916, https://doi.org/10.1016/j.cyto.2022.155916.
[142] Y. Brown, S. Hua, P.S. Tanwar, Extracellular matrix-mediated regulation of cancer stem cells and chemoresistance, Int. J. Biochem. Cell Biol. 109 (2019) 90–104, https://doi.org/10.1016/j.biocel.2019.02.002.
[143] W. He, Q. Wang, X. Tian, G. Pan, Recapitulating dynamic ECM ligand presentation at biomaterial interfaces: molecular strategies and biomedical prospects, Exploration 2 (2022) 20210093, https://doi.org/10.1002/EXP.20210093.
[144] G. Biondani, K. Zeeberg, M.R. Greco, S. Cannone, I. Dando, E. Dalla Pozza, M. Mastrodonato, S. Forciniti, V. Casavola, M. Palmieri, S.J. Reshkin, R. A. Cardone, Extracellular matrix composition modulates PDAC parenchymal and stem cell plasticity and behavior through the secretome, FEBS J. 285 (2018) 2104–2124, https://doi.org/10.1111/febs.14471.

[145] S. Papadaki, A. Magklara, Regulation of metabolic plasticity in cancer stem cells and implications in cancer therapy, Cancers 14 (2022) 5912, https://doi.org/10.3390/cancers14235912.
[146] O. Warburg, F. Wind, E. Negelein, The metabolism of tumors in the body, J. Gen. Physiol. 8 (1927) 519–530, https://doi.org/10.1085/jgp.8.6.519.
[147] P.P. Hsu, D.M. Sabatini, Cancer cell metabolism: Warburg and beyond, Cell 134 (2008) 703–707, https://doi.org/10.1016/j.cell.2008.08.021.
[148] Q. Guo, Y. Qiu, Y. Liu, Y. He, G. Zhang, Y. Du, C. Yang, F. Gao, Cell adhesion molecule CD44v10 promotes stem-like properties in triple-negative breast cancer cells via glucose transporter GLUT1-mediated glycolysis, J. Biol. Chem. 298 (2022) 102588, https://doi.org/10.1016/j.jbc.2022.102588.
[149] H.-J. Lee, C.-F. Li, D. Ruan, J. He, E.D. Montal, S. Lorenz, G.D. Girnun, C.-H. Chan, Non-proteolytic ubiquitination of Hexokinase 2 by HectH9 controls tumor metabolism and cancer stem cell expansion, Nat. Commun. 10 (2019) 2625, https://doi.org/10.1038/s41467-019-10374-y.
[150] N. Wang, T. Ma, B. Yu, Targeting epigenetic regulators to overcome drug resistance in cancers, Signal Transduct. Targeted Ther. 8 (2023) 1–24, https://doi.org/10.1038/s41392-023-01341-7.
[151] N.T.B. Nguyen, S. Gevers, R.N.U. Kok, L.M. Burgering, H. Neikes, N. Akkerman, M.A. Betjes, M.C. Ludikhuize, C. Gulersonmez, E.C.A. Stigter, Y. Vercoulen, J. Drost, H. Clevers, M. Vermeulen, J.S. Van Zon, S.J. Tans, B.M.T. Burgering, M. J. Rodríguez Colman, Lactate controls cancer stemness and plasticity through epigenetic regulation, Cell Metab. 0 (2025) S1550413125000026, https://doi.org/10.1016/j.cmet.2025.01.002.
[152] D. Guo, Y. Tong, X. Jiang, Y. Meng, H. Jiang, L. Du, Q. Wu, S. Li, S. Luo, M. Li, L. Xiao, H. He, X. He, Q. Yu, J. Fang, Z. Lu, Aerobic glycolysis promotes tumor immune evasion by hexokinase2-mediated phosphorylation of IκBα, Cell Metab. 34 (2022) 1312–1324.e6, https://doi.org/10.1016/j.cmet.2022.08.002.
[153] J. Wang, F. Shao, Y. Yang, W. Wang, X. Yang, R. Li, H. Cheng, S. Sun, X. Feng, Y. Gao, J. He, Z. Lu, A non-metabolic function of hexokinase 2 in small cell lung cancer: promotes cancer cell stemness by increasing USP11-mediated CD133 stability, Cancer Commun. 42 (2022) 1008–1027, https://doi.org/10.1002/cac2.12351.
[154] G.E. Thomas, G. Egan, L. García-Prat, A. Botham, V. Voisin, P.S. Patel, F.W. Hoff, J. Chin, B. Nachmias, K.B. Kaufmann, D.H. Khan, R. Hurren, X. Wang, M. Gronda, N. MacLean, C. O'Brien, R.P. Singh, C.L. Jones, S.M. Harding, B. Raught, A. Arruda, M.D. Minden, G.D. Bader, R. Hakem, S. Kornblau, J.E. Dick, A. D. Schimmer, The metabolic enzyme hexokinase 2 localizes to the nucleus in AML and normal haematopoietic stem and progenitor cells to maintain stemness, Nat. Cell Biol. 24 (2022) 872–884, https://doi.org/10.1038/s41556-022-00925-9.
[155] X. Yang, F. Shao, D. Guo, W. Wang, J. Wang, R. Zhu, Y. Gao, J. He, Z. Lu, WNT/β-catenin-suppressed FTO expression increases m6A of c-Myc mRNA to promote tumor cell glycolysis and tumorigenesis, Cell Death Dis. 12 (2021) 1–14, https://doi.org/10.1038/s41419-021-03739-z.
[156] K. Lee, J.M. Giltnane, J.M. Balko, L.J. Schwarz, A.L. Guerrero-Zotano, K. E. Hutchinson, M.J. Nixon, M.V. Estrada, V. Sánchez, M.E. Sanders, T. Lee, H. Gómez, A. Lluch, J.A. Pérez-Fidalgo, M.M. Wolf, G. Andrejeva, J.C. Rathmell, S.W. Fesik, C.L. Arteaga, MYC and MCL1 cooperatively promote chemotherapy-resistant breast cancer stem cells via regulation of mitochondrial oxidative phosphorylation, Cell Metab. 26 (2017) 633–647, https://doi.org/10.1016/j.cmet.2017.09.009.
[157] S. Liu, H. Zhao, Y. Hu, C. Yan, Y. Mi, X. Li, D. Tao, J. Qin, Lactate promotes metastasis of normoxic colorectal cancer stem cells through PGC-1α-mediated oxidative phosphorylation, Cell Death Dis. 13 (2022) 1–12, https://doi.org/10.1038/s41419-022-05111-1.
[158] U.P. Yadav, T. Singh, P. Kumar, P. Sharma, H. Kaur, S. Sharma, S. Singh, S. Kumar, K. Mehta, Metabolic adaptations in cancer stem cells, Front. Oncol. 10 (2020) 1010, https://doi.org/10.3389/fonc.2020.01010.
[159] S. Liu, Y. Cong, D. Wang, Y. Sun, L. Deng, Y. Liu, R. Martin-Trevino, L. Shang, S. P. McDermott, M.D. Landis, S. Hong, A. Adams, R. D'Angelo, C. Ginestier, E. Charafe-Jauffret, S.G. Clouthier, D. Birnbaum, S.T. Wong, M. Zhan, J.C. Chang, M.S. Wicha, Breast cancer stem cells transition between epithelial and mesenchymal states reflective of their normal counterparts, Stem Cell Rep. 2 (2014) 78–91, https://doi.org/10.1016/j.stemcr.2013.11.009.
[160] M. Janiszewska, M.L. Suvà, N. Riggi, R.H. Houtkooper, J. Auwerx, V. Clément-Schatlo, I. Radovanovic, E. Rheinbay, P. Provero, I. Stamenkovic, Imp2 controls oxidative phosphorylation and is crucial for preserving glioblastoma cancer stem cells, Genes Dev. 26 (2012) 1926–1944, https://doi.org/10.1101/gad.188292.112.
[161] X. Li, J.B. Wu, Q. Li, K. Shigemura, L.W.K. Chung, W.-C. Huang, SREBP-2 promotes stem cell-like properties and metastasis by transcriptional activation of c-Myc in prostate cancer, Oncotarget 7 (2016) 12869–12884, https://doi.org/10.18632/oncotarget.7331.
[162] C.-L. Chen, H. Tsukamoto, J.-C. Liu, C. Kashiwabara, D. Feldman, L. Sher, S. Dooley, S.W. French, L. Mishra, L. Petrovic, J.H. Jeong, K. Machida, Reciprocal regulation by TLR4 and TGF-β in tumor-initiating stem-like cells, J. Clin. Investig. 123 (2013) 2832–2849, https://doi.org/10.1172/JCI65859.
[163] C.-L. Chen, D.B. Uthaya Kumar, V. Punj, J. Xu, L. Sher, S.M. Tahara, S. Hess, K. Machida, NANOG metabolically reprograms tumor-initiating stem-like cells through tumorigenic changes in oxidative phosphorylation and fatty acid metabolism, Cell Metab. 23 (2016) 206–219, https://doi.org/10.1016/j.cmet.2015.12.004.
[164] H. Li, J. Song, Y. He, Y. Liu, Z. Liu, W. Sun, W. Hu, Q. Lei, X. Hu, Z. Chen, X. He, CRISPR/Cas9 screens reveal that hexokinase 2 enhances cancer stemness and tumorigenicity by activating the ACSL4-fatty acid β-oxidation pathway, Adv. Sci. 9 (2022) 2105126, https://doi.org/10.1002/advs.202105126.
[165] V.M.-Y. Wang, R.M.M. Ferreira, J. Almagro, T. Evan, N. Legrave, M. Zaw Thin, D. Frith, J. Carvalho, D.J. Barry, A.P. Snijders, E. Herbert, E.L. Nye, J.I. MacRae, A. Behrens, CD9 identifies pancreatic cancer stem cells and modulates glutamine metabolism to fuel tumour growth, Nat. Cell Biol. 21 (2019) 1425–1435, https://doi.org/10.1038/s41556-019-0407-1.
[166] Z. Wu, D. Wei, W. Gao, Y. Xu, Z. Hu, Z. Ma, C. Gao, X. Zhu, Q. Li, TPO-induced metabolic reprogramming drives liver metastasis of colorectal cancer CD110+ tumor-initiating cells, Cell Stem Cell 17 (2015) 47–59, https://doi.org/10.1016/j.stem.2015.05.016.
[167] X. Wang, X.C. Low, W. Hou, L.N. Abdullah, T.B. Toh, M. Mohd Abdul Rashid, D. Ho, E.K.-H. Chow, Epirubicin-adsorbed nanodiamonds kill chemoresistant hepatic cancer stem cells, ACS Nano 8 (2014) 12151–12166, https://doi.org/10.1021/nn503491e.
[168] L. Wang, X. Huang, X. You, T. Yi, B. Lu, J. Liu, G. Lu, M. Ma, C. Zou, J. Wu, W. Zhao, Nanoparticle enhanced combination therapy for stem-like progenitors defined by single-cell transcriptomics in chemotherapy-resistant osteosarcoma, Signal Transduct. Targeted Ther. 5 (2020) 196, https://doi.org/10.1038/s41392-020-00248-x.
[169] D. Zhang, S. Tian, Y. Liu, M. Zheng, X. Yang, Y. Zou, B. Shi, L. Luo, Near infrared-activatable biomimetic nanogels enabling deep tumor drug penetration inhibit orthotopic glioblastoma, Nat. Commun. 13 (2022) 6835, https://doi.org/10.1038/s41467-022-34462-8.
[170] Y. Yu, X. Yang, S. Reghu, S.C. Kaul, R. Wadhwa, E. Miyako, Photothermogenetic inhibition of cancer stemness by near-infrared-light-activatable nanocomplexes, Nat. Commun. 11 (2020) 4117, https://doi.org/10.1038/s41467-020-17768-3.
[171] W. Lv, H. Wu, Y. Zhang, H. Li, H. Shu, C. Su, Y. Zhu, T. Wang, F. Nie, cRGD-targeted gold-based nanoparticles overcome EGFR-TKI resistance of NSCLC *via* low-temperature photothermal therapy combined with sonodynamic therapy, Biomater. Sci. 11 (2023) 1677–1691, https://doi.org/10.1039/D2BM01825J.
[172] H. Li, W. Yan, X. Suo, H. Peng, X. Yang, Z. Li, J. Zhang, D. Liu, Nucleus-targeted nano delivery system eradicates cancer stem cells by combined thermotherapy and hypoxia-activated chemotherapy, Biomaterials 200 (2019) 1–14, https://doi.org/10.1016/j.biomaterials.2019.01.048.
[173] D. Liu, Y. Hong, Y. Li, C. Hu, T.-C. Yip, W.-K. Yu, Y. Zhu, C.-C. Fong, W. Wang, S.-K. Au, S. Wang, M. Yang, Targeted destruction of cancer stem cells using multifunctional magnetic nanoparticles that enable combined hyperthermia and chemotherapy, Theranostics 10 (2020) 1181–1196, https://doi.org/10.7150/thno.38989.
[174] X. Jiang, J. Liu, J. Mao, W. Han, Y. Fan, T. Luo, J. Xia, M.J. Lee, W. Lin, Pharmacological ascorbate potentiates combination nanomedicines and reduces cancer cell stemness to prevent post-surgery recurrence and systemic metastasis, Biomaterials 295 (2023) 122037, https://doi.org/10.1016/j.biomaterials.2023.122037.
[175] F. Andrade, D. Rafael, M. Vilar-Hernández, S. Montero, F. Martínez-Trucharte, J. Seras-Franzoso, Z.V. Díaz-Riascos, A. Boullosa, N. García-Aranda, P. Cámara-Sánchez, D. Arango, M. Nestor, I. Abasolo, B. Sarmento, S. Schwartz, Polymeric micelles targeted against CD44v6 receptor increase niclosamide efficacy against colorectal cancer stem cells and reduce circulating tumor cells *in vivo*, J. Controlled Release 331 (2021) 198–212, https://doi.org/10.1016/j.jconrel.2021.01.022.
[176] T. Tan, H. Hu, H. Wang, J. Li, Z. Wang, J. Wang, S. Wang, Z. Zhang, Y. Li, Bioinspired lipoproteins-mediated photothermia remodels tumor stroma to improve cancer cell accessibility of second nanoparticles, Nat. Commun. 10 (2019) 3322, https://doi.org/10.1038/s41467-019-11235-4.
[177] M. Fiorillo, A.F. Verre, M. Iliut, M. Peiris-Pagés, B. Ozsvari, R. Gandara, A. R. Cappello, F. Sotgia, A. Vijayaraghavan, M.P. Lisanti, Graphene oxide selectively targets cancer stem cells, across multiple tumor types: implications for non-toxic cancer treatment, via "differentiation-based nano-therapy,", Oncotarget 6 (2015) 3553–3562, https://doi.org/10.18632/oncotarget.3348.
[178] H. Wang, P. Agarwal, S. Zhao, J. Yu, X. Lu, X. He, Combined cancer therapy with hyaluronan-decorated fullerene-silica multifunctional nanoparticles to target cancer stem-like cells, Biomaterials 97 (2016) 62–73, https://doi.org/10.1016/j.biomaterials.2016.04.030.
[179] M.M. Joseph, A.N. Ramya, V.M. Vijayan, J.B. Nair, B.T. Bastian, R.K. Pillai, S. T. Therakathinal, K.K. Maiti, Targeted theranostic nano vehicle endorsed with self-destruction and immunostimulatory features to circumvent drug resistance and wipe-out tumor reinitiating cancer stem cells, Small 16 (2020) 2003309, https://doi.org/10.1002/smll.202003309.
[180] Y. Pan, X. Ma, C. Liu, J. Xing, S. Zhou, B. Parshad, T. Schwerdtle, W. Li, A. Wu, R. Haag, Retinoic acid-loaded dendritic polyglycerol-conjugated gold nanostars for targeted photothermal therapy in breast cancer stem cells, ACS Nano 15 (2021) 15069–15084, https://doi.org/10.1021/acsnano.1c05452.
[181] Y. Pan, S. Zhou, C. Liu, X. Ma, J. Xing, B. Parshad, W. Li, A. Wu, R. Haag, Dendritic polyglycerol-conjugated gold nanostars for metabolism inhibition and targeted photothermal therapy in breast cancer stem cells, Adv. Healthcare Mater. 11 (2022) 2102272, https://doi.org/10.1002/adhm.202102272.
[182] Z. Su, D. Liu, L. Chen, J. Zhang, L. Ru, Z. Chen, Z. Gao, X. Wang, CD44-Targeted magnetic nanoparticles kill head and neck squamous cell carcinoma stem cells in an alternating magnetic field, Int. J. Nanomed. 14 (2019) 7549–7560, https://doi.org/10.2147/IJN.S215087.
[183] Y. Wang, Q.-W. Yang, Q. Yang, T. Zhou, M.-F. Shi, C.-X. Sun, X.-X. Gao, Y.-Q. Cheng, X.-G. Cui, Y.-H. Sun, Cuprous oxide nanoparticles inhibit prostate cancer by attenuating the stemness of cancer cells via inhibition of the Wnt signaling pathway, Int. J. Nanomed. 12 (2017) 2569–2579, https://doi.org/10.2147/IJN.S130537.

[184] J. Liu, S. Smith, C. Wang, Photothermal attenuation of cancer cell stemness, chemoresistance, and migration using CD44-targeted MoS2 nanosheets, Nano Lett. 23 (2023) 1989–1999, https://doi.org/10.1021/acs.nanolett.3c00089.
[185] X. Chu, W. Tian, J. Ning, G. Xiao, Y. Zhou, Z. Wang, Z. Zhai, G. Tanzhu, J. Yang, R. Zhou, Cancer stem cells: advances in knowledge and implications for cancer therapy, Signal Transduct. Targeted Ther. 9 (2024) 170, https://doi.org/10.1038/s41392-024-01851-y.
[186] P. Chandran, A. Kavalakatt, G.L. Malarvizhi, D.R.V.N. Vasanthakumari, A. P. Retnakumari, N. Sidharthan, K. Pavithran, S. Nair, M. Koyakutty, Epigenetics targeted protein-vorinostat nanomedicine inducing apoptosis in heterogeneous population of primary acute myeloid leukemia cells including refractory and relapsed cases, Nanomed. Nanotechnol. Biol. Med. 10 (2014) 721–732, https://doi.org/10.1016/j.nano.2013.09.008.
[187] P. Zhou, S. Hatziieremia, M.A. Elliott, L. Scobie, C. Crossan, A.M. Michie, T. L. Holyoake, G.W. Halbert, H.G. Jørgensen, Uptake of synthetic Low Density Lipoprotein by leukemic stem cells — a potential stem cell targeted drug delivery strategy, J. Controlled Release 148 (2010) 380–387, https://doi.org/10.1016/j.jconrel.2010.09.016.
[188] S. Wang, W. Ren, J. Wang, Z. Jiang, M. Saeed, L. Zhang, A. Li, A. Wu, Black TiO_2-based nanoprobes for T_1-weighted MRI-guided photothermal therapy in CD133 high expressed pancreatic cancer stem-like cells, Biomater. Sci. 6 (2018) 2209–2218, https://doi.org/10.1039/C8BM00454D.
[189] C.-H. Wang, S.-H. Chiou, C.-P. Chou, Y.-C. Chen, Y.-J. Huang, C.-A. Peng, Photothermolysis of glioblastoma stem-like cells targeted by carbon nanotubes conjugated with CD133 monoclonal antibody, Nanomed. Nanotechnol. Biol. Med. 7 (2011) 69–79, https://doi.org/10.1016/j.nano.2010.06.010.
[190] J.S. Kim, D.H. Shin, J.-S. Kim, Dual-targeting immunoliposomes using angiopep-2 and CD133 antibody for glioblastoma stem cells, J. Controlled Release 269 (2018) 245–257, https://doi.org/10.1016/j.jconrel.2017.11.026.
[191] H. Dianat-Moghadam, S. Abbasspour-Ravasjani, H. Hamishehkar, R. Rahbarghazi, M. Nouri, LXR inhibitor SR9243-loaded immunoliposomes modulate lipid metabolism and stemness in colorectal cancer cells, Med. Oncol. 40 (2023) 156, https://doi.org/10.1007/s12032-023-02027-4.
[192] S. Pandey, M. Lee, J. Lim, S. Park, Y.-H. Choung, J.E. Kim, P. Garg, J.H. Chung, SMO-CRISPR-mediated apoptosis in CD133-targeted cancer stem cells and tumor growth inhibition, J. Controlled Release 357 (2023) 94–108, https://doi.org/10.1016/j.jconrel.2023.03.023.
[193] Z. Wang, M. Sun, W. Li, L. Fan, Y. Zhou, Z. Hu, A novel CD133- and EpCAM-targeted liposome with redox-responsive properties capable of synergistically eliminating liver cancer stem cells, Front. Chem. 8 (2020) 649, https://doi.org/10.3389/fchem.2020.00649.
[194] M. Ni, M. Xiong, X. Zhang, G. Cai, H. Chen, Q. Zeng, Z. Yu, Poly(lactic-co-glycolic acid) nanoparticles conjugated with CD133 aptamers for targeted salinomycin delivery to CD133+ osteosarcoma cancer stem cells, Int. J. Nanomed. 10 (2015) 2537–2554, https://doi.org/10.2147/IJN.S78498.
[195] F. Chen, Y. Zeng, X. Qi, Y. Chen, Z. Ge, Z. Jiang, X. Zhang, Y. Dong, H. Chen, Z. Yu, Targeted salinomycin delivery with EGFR and CD133 aptamers based dual-ligand lipid-polymer nanoparticles to both osteosarcoma cells and cancer stem cells, Nanomed. Nanotechnol. Biol. Med. 14 (2018) 2115–2127, https://doi.org/10.1016/j.nano.2018.05.015.
[196] Z.A. Shahabad, C.B. Avci, F. Bani, A. Zarebkohan, M. Sadeghizadeh, R. Salehi, M. Ghafarkhani, R. Rahbarghazi, B.G. Bagca, N.P. Ozates, Photothermal effect of albumin-modified gold nanorods diminished neuroblastoma cancer stem cells dynamic growth by modulating autophagy, Sci. Rep. 12 (2022) 11774, https://doi.org/10.1038/s41598-022-15660-2.
[197] W.-H. Chen, G.-F. Luo, Q. Lei, S. Hong, W.-X. Qiu, L.-H. Liu, S.-X. Cheng, X.-Z. Zhang, Overcoming the heat endurance of tumor cells by interfering with the anaerobic glycolysis metabolism for improved photothermal therapy, ACS Nano 11 (2017) 1419–1431, https://doi.org/10.1021/acsnano.6b06658.
[198] R. Thapa, S. Galoforo, S.M. Kandel, M.H. El-dakdouki, T.G. Wilson, X. Huang, B. J. Roth, G.D. Wilson, Radiosensitizing and hyperthermic properties of hyaluronan conjugated, dextran-coated ferric oxide nanoparticles: implications for cancer stem cell therapy, J. Nanomater. 2015 (2015) 1–11, https://doi.org/10.1155/2015/840594.
[199] J. Tang, H. Zhou, J. Liu, J. Liu, W. Li, Y. Wang, F. Hu, Q. Huo, J. Li, Y. Liu, C. Chen, Dual-mode imaging-guided synergistic chemo- and magnetohyperthermia therapy in a versatile nanoplatform to eliminate cancer stem cells, ACS Appl. Mater. Interfaces 9 (2017) 23497–23507, https://doi.org/10.1021/acsami.7b06393.
[200] D. Lubanska, S. Alrashed, G.T. Mason, F. Nadeem, A. Awada, M. DiPasquale, A. Sorge, A. Malik, M. Kojic, M.A.R. Soliman, A.C. deCarvalho, A. Shamisa, S. Kulkarni, D. Marquardt, L.A. Porter, S. Rondeau-Gagné, Impairing proliferation of glioblastoma multiforme with CD44+ selective conjugated polymer nanoparticles, Sci. Rep. 12 (2022) 12078, https://doi.org/10.1038/s41598-022-15244-0.
[201] B. Liu, W. Wang, J. Fan, Y. Long, F. Xiao, M. Daniyal, C. Tong, Q. Xie, Y. Jian, B. Li, X. Ma, W. Wang, RBC membrane camouflaged prussian blue nanoparticles for gamabutolin loading and combined chemo/photothermal therapy of breast cancer, Biomaterials 217 (2019) 119301, https://doi.org/10.1016/j.biomaterials.2019.119301.
[202] K. Hu, H. Zhou, Y. Liu, Z. Liu, J. Liu, J. Tang, J. Li, J. Zhang, W. Sheng, Y. Zhao, Y. Wu, C. Chen, Hyaluronic acid functional amphipathic and redox-responsive polymer particles for the co-delivery of doxorubicin and cyclopamine to eradicate breast cancer cells and cancer stem cells, Nanoscale 7 (2015) 8607–8618, https://doi.org/10.1039/C5NR01084E.
[203] D. Chen, G. Wang, W. Song, Q. Zhang, Novel CD44 receptor targeting multifunctional "nano-eggs" based on double pH-sensitive nanoparticles for co-delivery of curcumin and paclitaxel to cancer cells and cancer stem cells, J. Nanoparticle Res. 17 (2015) 421, https://doi.org/10.1007/s11051-015-3217-9.
[204] H. Yao, Y. Zhang, L. Sun, Y. Liu, The effect of hyaluronic acid functionalized carbon nanotubes loaded with salinomycin on gastric cancer stem cells, Biomaterials 35 (2014) 9208–9223, https://doi.org/10.1016/j.biomaterials.2014.07.033.
[205] X. Zhu, L. Li, J. Tang, C. Yang, H. Yu, K. Liu, Z. Zheng, X. Gu, Q. Yu, F.-J. Xu, Z. Gan, Cascade-responsive nano-assembly for efficient photothermal-chemo synergistic inhibition of tumor metastasis by targeting cancer stem cells, Biomaterials 280 (2022) 121305, https://doi.org/10.1016/j.biomaterials.2021.121305.
[206] W. Rao, H. Wang, J. Han, S. Zhao, J. Dumbleton, P. Agarwal, W. Zhang, G. Zhao, J. Yu, D.L. Zynger, X. Lu, X. He, Chitosan-decorated doxorubicin-encapsulated nanoparticle targets and eliminates tumor reinitiating cancer stem-like cells, ACS Nano 9 (2015) 5725–5740, https://doi.org/10.1021/nn506928p.
[207] A. Aires, S.M. Ocampo, B.M. Simões, M. Josefa Rodríguez, J.F. Cadenas, P. Couleaud, K. Spence, A. Latorre, R. Miranda, Á. Somoza, R.B. Clarke, J. L. Carrascosa, A.L. Cortajarena, Multifunctionalized iron oxide nanoparticles for selective drug delivery to CD44-positive cancer cells, Nanotechnology 27 (2016) 065103, https://doi.org/10.1088/0957-4484/27/6/065103.
[208] Y. Liu, X. Suo, H. Peng, W. Yan, H. Li, X. Yang, Z. Li, J. Zhang, D. Liu, Multifunctional magnetic nanoplatform eliminates cancer stem cells via inhibiting the secretion of extracellular heat shock protein 90, Adv. Healthcare Mater. 8 (2019) 1900160, https://doi.org/10.1002/adhm.201900160.
[209] A. Al Faraj, A.S. Shaik, E. Ratemi, R. Halwani, Combination of drug-conjugated SWCNT nanocarriers for efficient therapy of cancer stem cells in a breast cancer animal model, J. Controlled Release 225 (2016) 240–251, https://doi.org/10.1016/j.jconrel.2016.01.053.
[210] F. Andrade, D. Rafael, M. Vilar-Hernández, S. Montero, F. Martínez-Trucharte, J. Seras-Franzoso, Z.V. Díaz-Riascos, A. Boullosa, N. García-Aranda, P. Cámara-Sánchez, D. Arango, M. Nestor, I. Abasolo, B. Sarmento, S. Schwartz, Polymeric micelles targeted against CD44v6 receptor increase niclosamide efficacy against colorectal cancer stem cells and reduce circulating tumor cells *in vivo*, J. Controlled Release 331 (2021) 198–212, https://doi.org/10.1016/j.jconrel.2021.01.022.
[211] D.J. Bharali, T. Sudha, H. Cui, B.M. Mian, S.A. Mousa, Anti-CD24 nano-targeted delivery of docetaxel for the treatment of prostate cancer, Nanomed. Nanotechnol. Biol. Med. 13 (2017) 263–273, https://doi.org/10.1016/j.nano.2016.08.017.
[212] R. Yang, L.Y. An, Q.F. Miao, F.M. Li, Y. Han, H.X. Wang, D.P. Liu, R. Chen, S. Q. Tang, Effective elimination of liver cancer stem-like cells by CD90 antibody targeted thermosensitive magnetoliposomes, Oncotarget 7 (2016) 35894–35916, https://doi.org/10.18632/oncotarget.9116.
[213] R. Bakalova, H. Ohba, Z. Zhelev, T. Nagase, R. Jose, M. Ishikawa, Y. Baba, Quantum dot anti-CD conjugates: are they potential photosensitizers or potentiators of classical photosensitizing agents in photodynamic therapy of cancer? Nano Lett. 4 (2004) 1567–1573, https://doi.org/10.1021/nl049627w.
[214] M. Alibolandi, M. Ramezani, F. Sadeghi, K. Abnous, F. Hadizadeh, Epithelial cell adhesion molecule aptamer conjugated PEG–PLGA nanopolymersomes for targeted delivery of doxorubicin to human breast adenocarcinoma cell line in vitro, Int. J. Pharm. 479 (2015) 241–251, https://doi.org/10.1016/j.ijpharm.2014.12.035.
[215] M. Mohammadi, Z. Salmasi, M. Hashemi, F. Mosaffa, K. Abnous, M. Ramezani, Single-walled carbon nanotubes functionalized with aptamer and piperazine–polyethylenimine derivative for targeted siRNA delivery into breast cancer cells, Int. J. Pharm. 485 (2015) 50–60, https://doi.org/10.1016/j.ijpharm.2015.02.031.
[216] P. Moitra, S.K. Misra, K. Kumar, P. Kondaiah, P. Tran, W. Duan, S. Bhattacharya, Cancer stem cell-targeted gene delivery mediated by aptamer-decorated pH-sensitive nanoliposomes, ACS Biomater. Sci. Eng. 7 (2021) 2508–2519, https://doi.org/10.1021/acsbiomaterials.1c00110.
[217] N. Subramanian, J.R. Kanwar, P. kumar Athalya, N. Janakiraman, V. Khetan, R. K. Kanwar, S. Eluchuri, S. Krishnakumar, EpCAM aptamer mediated cancer cell specific delivery of EpCAM siRNA using polymeric nanocomplex, J. Biomed. Sci. 22 (2015) 4, https://doi.org/10.1186/s12929-014-0108-9.
[218] E. Locatelli, Y. Li, I. Monaco, W. Guo, M. Maturi, L. Menichetti, P. Armanetti, R. C. Martin, M.C. Franchini, A novel theranostic gold nanorods- and Adriamycin-loaded micelle for EpCAM targeting, laser ablation, and photoacoustic imaging of cancer stem cells in hepatocellular carcinoma, Int. J. Nanomed. 14 (2019) 1877–1892, https://doi.org/10.2147/IJN.S197265.
[219] Y. Han, Y. An, G. Jia, X. Wang, C. He, Y. Ding, Q. Tang, Theranostic micelles based on upconversion nanoparticles for dual-modality imaging and photodynamic therapy in hepatocellular carcinoma, Nanoscale 10 (2018) 6511–6523, https://doi.org/10.1039/C7NR09717D.
[220] J. Chen, Q. Liu, J. Xiao, J. Du, EpCAM-antibody-labeled noncytotoxic polymer vesicles for cancer stem cells-targeted delivery of anticancer drug and siRNA, Biomacromolecules 16 (2015) 1695–1705, https://doi.org/10.1021/acs.biomac.5b00551.
[221] T. Hevonoja, M.O. Pentikäinen, M.T. Hyvönen, P.T. Kovanen, M. Ala-Korpela, Structure of low density lipoprotein (LDL) particles: basis for understanding molecular changes in modified LDL, Biochim. Biophys. Acta BBA - Mol. Cell Biol. Lipids 1488 (2000) 189–210, https://doi.org/10.1016/S1388-1981(00)00123-2.

[222] R.J. Deckelbaum, G.G. Shipley, D.M. Small, Structure and interactions of lipids in human plasma low density lipoproteins, J. Biol. Chem. 252 (1977) 744–754, https://doi.org/10.1016/S0021-9258(17)32781-3.
[223] M.S. Brown, J.L. Goldstein, A receptor-mediated pathway for cholesterol homeostasis (nobel lecture), Angew. Chem. Int. Ed. 25 (1986) 583–602, https://doi.org/10.1002/anie.198605833.
[224] D. Gal, M. Ohashi, P.C. MacDonald, H.J. Buchsbaum, E.R. Simpson, Low-density lipoprotein as a potential vehicle for chemotherapeutic agents and radionucleotides in the management of gynecologic neoplasms, Am. J. Obstet. Gynecol. 139 (1981) 877–885, https://doi.org/10.1016/0002-9378(81)90952-2.
[225] J.E. Bolden, M.J. Peart, R.W. Johnstone, Anticancer activities of histone deacetylase inhibitors, Nat. Rev. Drug Discov. 5 (2006) 769–784, https://doi.org/10.1038/nrd2133.
[226] A. Quintás-Cardama, F.P.S. Santos, G. Garcia-Manero, Histone deacetylase inhibitors for the treatment of myelodysplastic syndrome and acute myeloid leukemia, Leukemia 25 (2011) 226–235, https://doi.org/10.1038/leu.2010.276.
[227] S. Grant, C. Easley, P. Kirkpatrick, Vorinostat, Nat. Rev. Drug Discov. 6 (2007) 21–22, https://doi.org/10.1038/nrd2227.
[228] P. Chandran, K. Pavithran, N. Sidharthan, A. Sasidharan, S. Nair, M. Koyakutty, Protein nanomedicine exerts cytotoxicity toward $CD34^{+}$ $CD38^{-}$ $CD123^{+}$ leukemic stem cells, ACS Biomater. Sci. Eng. 1 (2015) 1194–1199, https://doi.org/10.1021/acsbiomaterials.5b00361.
[229] W.A. Banks, From blood–brain barrier to blood–brain interface: new opportunities for CNS drug delivery, Nat. Rev. Drug Discov. 15 (2016) 275–292, https://doi.org/10.1038/nrd.2015.21.
[230] O. van Tellingen, B. Yetkin-Arik, M.C. de Gooijer, P. Wesseling, T. Wurdinger, H. E. de Vries, Overcoming the blood–brain tumor barrier for effective glioblastoma treatment, Drug Resist. Updates 19 (2015) 1–12, https://doi.org/10.1016/j.drup.2015.02.002.
[231] D. Bocangel, S. Sengupta, S. Mitra, K.K. Bhakat, p53-Mediated down-regulation of the human DNA repair gene O6-methylguanine-DNA methyltransferase (MGMT) via interaction with Sp1 transcription factor, Anticancer Res. 29 (2009) 3741–3750.
[232] J. Ma, M. Murphy, P.J. O'Dwyer, E. Berman, K. Reed, J.M. Gallo, Biochemical changes associated with a multidrug-resistant phenotype of a human glioma cell line with temozolomide-acquired resistance, Biochem. Pharmacol. 63 (2002) 1219–1228, https://doi.org/10.1016/S0006-2952(02)00876-6.
[233] J.P. Fruehauf, H. Brem, S. Brem, A. Sloan, G. Barger, W. Huang, R. Parker, *In vitro* drug response and molecular markers associated with drug resistance in malignant gliomas, Clin. Cancer Res. 12 (2006) 4523–4532, https://doi.org/10.1158/1078-0432.CCR-05-1830.
[234] S.-S. Kim, A. Rait, E. Kim, K.F. Pirollo, M. Nishida, N. Farkas, J.A. Dagata, E. H. Chang, A nanoparticle carrying the p53 gene targets tumors including cancer stem cells, sensitizes glioblastoma to chemotherapy and improves survival, ACS Nano 8 (2014) 5494–5514, https://doi.org/10.1021/nn5014484.
[235] A. Abou-ElNaga, G. Mutawa, I.M. El-Sherbiny, H. Abd-ElGhaffar, A.A. Allam, J. Ajarem, S.A. Mousa, Novel nano-therapeutic approach actively targets human ovarian cancer stem cells after xenograft into nude mice, Int. J. Mol. Sci. 18 (2017) 813, https://doi.org/10.3390/ijms18040813.
[236] C. Liu, G. Zhao, J. Liu, N. Ma, P. Chivukula, L. Perelman, K. Okada, Z. Chen, D. Gough, L. Yu, Novel biodegradable lipid nano complex for siRNA delivery significantly improving the chemosensitivity of human colon cancer stem cells to paclitaxel, J. Controlled Release 140 (2009) 277–283, https://doi.org/10.1016/j.jconrel.2009.08.013.
[237] P.B. Gupta, T.T. Onder, G. Jiang, K. Tao, C. Kuperwasser, R.A. Weinberg, E. S. Lander, Identification of selective inhibitors of cancer stem cells by high-throughput screening, Cell 138 (2009) 645–659, https://doi.org/10.1016/j.cell.2009.06.034.
[238] D. Lu, M.Y. Choi, J. Yu, J.E. Castro, T.J. Kipps, D.A. Carson, Salinomycin inhibits Wnt signaling and selectively induces apoptosis in chronic lymphocytic leukemia cells, Proc. Natl. Acad. Sci. USA 108 (2011) 13253–13257, https://doi.org/10.1073/pnas.1110431108.
[239] J.-Y. Lee, U. Termsarasab, J.-H. Park, S.Y. Lee, S.-H. Ko, J.-S. Shim, S.-J. Chung, H.-J. Cho, D.-D. Kim, Dual CD44 and folate receptor-targeted nanoparticles for cancer diagnosis and anticancer drug delivery, J. Controlled Release 236 (2016) 38–46, https://doi.org/10.1016/j.jconrel.2016.06.021.
[240] L. Ding, Y. Jiang, J. Zhang, H.-A. Klok, Z. Zhong, pH-sensitive coiled-coil peptide-cross-linked hyaluronic acid nanogels: synthesis and targeted intracellular protein delivery to CD44 positive cancer cells, Biomacromolecules 19 (2018) 555–562, https://doi.org/10.1021/acs.biomac.7b01664.
[241] M.W. Dewhirst, Z. Vujaskovic, E. Jones, D. Thrall, Re-setting the biologic rationale for thermal therapy, Int. J. Hyperther. 21 (2005) 779–790, https://doi.org/10.1080/02656730500271668.
[242] M.R. Horsman, J. Overgaard, Hyperthermia: a potent enhancer of radiotherapy, Clin. Oncol. 19 (2007) 418–426, https://doi.org/10.1016/j.clon.2007.03.015.
[243] B.K. Eustace, T. Sakurai, J.K. Stewart, D. Yimlamai, C. Unger, C. Zehetmeier, B. Lain, C. Torella, S.W. Henning, G. Beste, B.T. Scroggins, L. Neckers, L.L. Ilag, D. G. Jay, Functional proteomic screens reveal an essential extracellular role for hsp90α in cancer cell invasiveness, Nat. Cell Biol. 6 (2004) 507–514, https://doi.org/10.1038/ncb1131.
[244] L. Whitesell, S.L. Lindquist, HSP90 and the chaperoning of cancer, Nat. Rev. Cancer 5 (2005) 761–772, https://doi.org/10.1038/nrc1716.
[245] D. Liu, Y. Hong, Y. Li, C. Hu, T.-C. Yip, W.-K. Yu, Y. Zhu, C.-C. Fong, W. Wang, S.-K. Au, S. Wang, M. Yang, Targeted destruction of cancer stem cells using multifunctional magnetic nanoparticles that enable combined hyperthermia and chemotherapy, Theranostics 10 (2020) 1181–1196, https://doi.org/10.7150/thno.38989.
[246] J. Dou, X. He, Y. Liu, Z. Huang, C. Yang, F. Shi, D. Chen, N. Gu, Targeted therapeutic effect of anti-ABCG2 antibody combined with nano silver and vincristine on mouse myeloma cancer stem cells, J. Nanoparticle Res. 15 (2013) 2127, https://doi.org/10.1007/s11051-013-2127-y.
[247] D.R. Pattabiraman, B. Bierie, K.I. Kober, P. Thiru, J.A. Krall, C. Zill, F. Reinhardt, W.L. Tam, R.A. Weinberg, Activation of PKA leads to mesenchymal-to-epithelial transition and loss of tumor-initiating ability, Science 351 (2016) aad3680, https://doi.org/10.1126/science.aad3680.
[248] J. Huang, K. Wang, Wang Liu, Chen Wu, Ni, Junshu Zhang, Hu, Novel micelle formulation of curcumin for enhancing antitumor activity and inhibiting colorectal cancer stem cells, Int. J. Nanomed. 7 (2012) 4487, https://doi.org/10.2147/IJN.S34702.
[249] J.L. Roti Roti, Cellular responses to hyperthermia (40–46°C): cell killing and molecular events, Int. J. Hyperther. 24 (2008) 3–15, https://doi.org/10.1080/02656730701769841.
[250] Y. Zheng, L. Tang, L. Mabardi, S. Kumari, D.J. Irvine, Enhancing adoptive cell therapy of cancer through targeted delivery of small-molecule immunomodulators to internalizing or noninternalizing receptors, ACS Nano 11 (2017) 3089–3100, https://doi.org/10.1021/acsnano.7b00078.
[251] D. Zou, Z. Wu, X. Yi, Y. Hui, G. Yang, Y. Liu, Tengjisi, H. Wang, A. Brooks, H. Wang, X. Liu, Z.P. Xu, M.S. Roberts, H. Gao, C.-X. Zhao, Nanoparticle elasticity regulates the formation of cell membrane-coated nanoparticles and their nano-bio interactions, Proc. Natl. Acad. Sci. USA 120 (2023) e2214757120, https://doi.org/10.1073/pnas.2214757120.
[252] N. Subramanian, V. Raghunathan, J.R. Kanwar, R.K. Kanwar, S.V. Elchuri, V. Khetan, S. Krishnakumar, Target-specific delivery of doxorubicin to retinoblastoma using epithelial cell adhesion molecule aptamer, Mol. Vis. 18 (2012) 2783–2795.
[253] N. Takebe, P.J. Harris, R.Q. Warren, S.P. Ivy, Targeting cancer stem cells by inhibiting Wnt, Notch, and Hedgehog pathways, Nat. Rev. Clin. Oncol. 8 (2011) 97–106, https://doi.org/10.1038/nrclinonc.2010.196.
[254] Y. Li, T. Zhang, H. Korkaya, S. Liu, H.-F. Lee, B. Newman, Y. Yu, S.G. Clouthier, S. J. Schwartz, M.S. Wicha, D. Sun, Sulforaphane, a dietary component of broccoli/broccoli sprouts, inhibits breast cancer stem cells, Clin. Cancer Res. 16 (2010) 2580–2590, https://doi.org/10.1158/1078-0432.CCR-09-2937.
[255] M. Kakarala, D.E. Brenner, H. Korkaya, C. Cheng, K. Tazi, C. Ginestier, S. Liu, G. Dontu, M.S. Wicha, Targeting breast stem cells with the cancer preventive compounds curcumin and piperine, Breast Cancer Res. Treat. 122 (2010) 777–785, https://doi.org/10.1007/s10549-009-0612-x.
[256] M. Mimeault, S.L. Johansson, J.-P. Henichart, P. Depreux, S.K. Batra, Cytotoxic effects induced by docetaxel, gefitinib, and cyclopamine on side population and nonside population cell fractions from human invasive prostate cancer cells, Mol. Cancer Therapeut. 9 (2010) 617–630, https://doi.org/10.1158/1535-7163.MCT-09-1013.
[257] V.P. Chauhan, R.K. Jain, Strategies for advancing cancer nanomedicine, Nat. Mater. 12 (2013) 958–962, https://doi.org/10.1038/nmat3792.
[258] N. Takebe, L. Miele, P.J. Harris, W. Jeong, H. Bando, M. Kahn, S.X. Yang, S.P. Ivy, Targeting Notch, Hedgehog, and Wnt pathways in cancer stem cells: clinical update, Nat. Rev. Clin. Oncol. 12 (2015) 445–464, https://doi.org/10.1038/nrclinonc.2015.61.
[259] R. Nusse, H. Clevers, Wnt/β-Catenin signaling, disease, and emerging therapeutic modalities, Cell 169 (2017) 985–999, https://doi.org/10.1016/j.cell.2017.05.016.
[260] T. Feng, L. Zhou, Z. Wang, C. Li, Y. Zhang, J. Lin, D. Lu, P. Huang, Dual-stimuli responsive nanotheranostics for mild hyperthermia enhanced inhibition of Wnt/β-catenin signaling, Biomaterials 232 (2020) 119709, https://doi.org/10.1016/j.biomaterials.2019.119709.
[261] M. Mani, D.E. Carrasco, Y. Zhang, K. Takada, M.E. Gatt, J. Dutta-Simmons, H. Ikeda, F. Diaz-Griffero, V. Pena-Cruz, M. Bertagnolli, L.L. Myeroff, S. D. Markowitz, K.C. Anderson, D.R. Carrasco, BCL9 promotes tumor progression by conferring enhanced proliferative, metastatic, and angiogenic properties to cancer cells, Cancer Res. 69 (2009) 7577–7586, https://doi.org/10.1158/0008-5472.CAN-09-0773.
[262] K. Takada, D. Zhu, G.H. Bird, K. Sukhdeo, J.-J. Zhao, M. Mani, M. Lemieux, D. E. Carrasco, J. Ryan, D. Horst, M. Fulciniti, N.C. Munshi, W. Xu, A.L. Kung, R. A. Shivdasani, L.D. Walensky, D.R. Carrasco, Targeted disruption of the BCL9/β-catenin complex inhibits oncogenic Wnt signaling, Sci. Transl. Med. 4 (2012), https://doi.org/10.1126/scitranslmed.3003808.
[263] J. Miller-Kleinhenz, X. Guo, W. Qian, H. Zhou, E.N. Bozeman, L. Zhu, X. Ji, Y. A. Wang, T. Styblo, R. O'Regan, H. Mao, L. Yang, Dual-targeting Wnt and uPA receptors using peptide conjugated ultra-small nanoparticle drug carriers inhibited cancer stem-cell phenotype in chemo-resistant breast cancer, Biomaterials 152 (2018) 47–62, https://doi.org/10.1016/j.biomaterials.2017.10.035.
[264] M. Jo, B.M. Eastman, D.L. Webb, K. Stoletov, R. Klemke, S.L. Gonias, Cell signaling by urokinase-type plasminogen activator receptor induces stem cell–like properties in breast cancer cells, Cancer Res. 70 (2010) 8948–8958, https://doi.org/10.1158/0008-5472.CAN-10-1936.
[265] M. Niyaz, M.S. Khan, S. Mudassar, Hedgehog signaling: an achilles' heel in cancer, transl, Oncol 12 (2019) 1334–1344, https://doi.org/10.1016/j.tranon.2019.07.004.
[266] S. Gupta, N. Takebe, P. LoRusso, Review: targeting the hedgehog pathway in cancer, Ther. Adv. Med. Oncol. 2 (2010) 237–250, https://doi.org/10.1177/1758834010366430.

[267] K.C. Corbit, P. Aanstad, V. Singla, A.R. Norman, D.Y.R. Stainier, J.F. Reiter, Vertebrate Smoothened functions at the primary cilium, Nature 437 (2005) 1018–1021, https://doi.org/10.1038/nature04117.
[268] R. Rohatgi, L. Milenkovic, M.P. Scott, Patched1 regulates hedgehog signaling at the primary cilium, Science 317 (2007) 372–376, https://doi.org/10.1126/science.1139740.
[269] R.K. Verma, W. Yu, S.P. Singh, S. Shankar, R.K. Srivastava, Anthothecol-encapsulated PLGA nanoparticles inhibit pancreatic cancer stem cell growth by modulating sonic hedgehog pathway, Nanomed. Nanotechnol. Biol. Med. 11 (2015) 2061–2070, https://doi.org/10.1016/j.nano.2015.07.001.
[270] E.R. Andersson, U. Lendahl, Therapeutic modulation of Notch signalling — are we there yet? Nat. Rev. Drug Discov. 13 (2014) 357–378, https://doi.org/10.1038/nrd4252.
[271] R. Heo, J.-S. Park, H.J. Jang, S.-H. Kim, J.M. Shin, Y.D. Suh, J.H. Jeong, D.-G. Jo, J.H. Park, Hyaluronan nanoparticles bearing γ-secretase inhibitor: in vivo therapeutic effects on rheumatoid arthritis, J. Controlled Release 192 (2014) 295–300, https://doi.org/10.1016/j.jconrel.2014.07.057.
[272] T. Sun, R. Patil, A. Galstyan, D. Klymyshyn, H. Ding, A. Chesnokova, W. K. Cavenee, F.B. Furnari, V.A. Ljubimov, E.S. Shatalova, S. Wagner, D. Li, A. N. Mamelak, S.I. Bannykh, C.G. Patil, J.D. Rudnick, J. Hu, Z.B. Grodzinski, A. Rekechenetskiy, V. Falahatian, A.V. Lyubimov, Y.L. Chen, L.S. Leoh, T. R. Daniels-Wells, M.L. Penichet, E. Holler, A.V. Ljubimov, K.L. Black, J. Y. Ljubimova, Blockade of a laminin-411–notch Axis with CRISPR/Cas9 or a nanobioconjugate inhibits glioblastoma growth through tumor-microenvironment cross-talk, Cancer Res. 79 (2019) 1239–1251, https://doi.org/10.1158/0008-5472.CAN-18-2725.
[273] J. Liu, X. Wang, A.T. Chen, X. Gao, B.T. Himes, H. Zhang, Z. Chen, J. Wang, W. C. Sheu, G. Deng, Y. Xiao, P. Zou, S. Zhang, F. Liu, Y. Zhu, R. Fan, T.R. Patel, W. M. Saltzman, J. Zhou, ZNF117 regulates glioblastoma stem cell differentiation towards oligodendroglial lineage, Nat. Commun. 13 (2022) 2196, https://doi.org/10.1038/s41467-022-29884-3.
[274] Z. Chen, F. Liu, Y. Chen, J. Liu, X. Wang, A.T. Chen, G. Deng, H. Zhang, J. Liu, Z. Hong, J. Zhou, Targeted delivery of CRISPR/Cas9-Mediated cancer gene therapy via liposome-templated hydrogel nanoparticles, Adv. Funct. Mater. 27 (2017) 1703036, https://doi.org/10.1002/adfm.201703036.
[275] Z.-Q. Zuo, K.-G. Chen, X.-Y. Yu, G. Zhao, S. Shen, Z.-T. Cao, Y.-L. Luo, Y.-C. Wang, J. Wang, Promoting tumor penetration of nanoparticles for cancer stem cell therapy by TGF-β signaling pathway inhibition, Biomaterials 82 (2016) 48–59, https://doi.org/10.1016/j.biomaterials.2015.12.014.
[276] Y. Liu, C. Chen, P. Qian, X. Lu, B. Sun, X. Zhang, L. Wang, X. Gao, H. Li, Z. Chen, J. Tang, W. Zhang, J. Dong, R. Bai, P.E. Lobie, Q. Wu, S. Liu, H. Zhang, F. Zhao, M. S. Wicha, T. Zhu, Y. Zhao, Gd-metallofullerenol nanomaterial as non-toxic breast cancer stem cell-specific inhibitor, Nat. Commun. 6 (2015) 5988, https://doi.org/10.1038/ncomms6988.
[277] Z.-Y. Wang, Z. Chen, Acute promyelocytic leukemia: from highly fatal to highly curable, Blood 111 (2008) 2505–2515, https://doi.org/10.1182/blood-2007-07-102798.
[278] P.R. Subbarayan, B. Ardalan, In the war against solid tumors arsenic trioxide need partners, J. Gastrointest. Cancer 45 (2014) 363–371, https://doi.org/10.1007/s12029-014-9617-8.
[279] Y. Huang, B. Zhou, H. Luo, J. Mao, Y. Huang, K. Zhang, C. Mei, Y. Yan, H. Jin, J. Gao, Z. Su, P. Pang, D. Li, H. Shan, ZnAs@SiO2 nanoparticles as a potential anti-tumor drug for targeting stemness and epithelial-mesenchymal transition in hepatocellular carcinoma via SHP-1/JAK2/STAT3 signaling, Theranostics 9 (2019) 4391–4408, https://doi.org/10.7150/thno.32462.
[280] V. Kannappan, Y. Liu, Z. Wang, K. Azar, S. Kurusamy, R.S. Kilari, A.L. Armesilla, M.R. Morris, M. Najlah, P. Liu, X.-W. Bian, W. Wang, PLGA–Nano-Encapsulated disulfiram inhibits hypoxia-induced NF-κB, cancer stem cells, and targets glioblastoma *in vitro* and *in vivo*, Mol. Cancer Therapeut. 21 (2022) 1273–1284, https://doi.org/10.1158/1535-7163.MCT-22-0066.
[281] D. Wang, T. Wang, Z. Xu, H. Yu, B. Feng, J. Zhang, C. Guo, Q. Yin, Z. Zhang, Y. Li, Cooperative treatment of metastatic breast cancer using host-guest nanoplatform coloaded with docetaxel and siRNA, Small 12 (2016) 488–498, https://doi.org/10.1002/smll.201502913.
[282] Z. Chen, F. Han, Y. Du, H. Shi, W. Zhou, Hypoxic microenvironment in cancer: molecular mechanisms and therapeutic interventions, Sig. Transduct. Target. Ther. 8 (2023) 1–23, https://doi.org/10.1038/s41392-023-01332-8.
[283] F. Zhang, J. Dong, K. Huang, B. Duan, C. Li, R. Yang, J. Li, F. Zhi, Z. Zhou, M. Sun, "Dominolike" barriers elimination with an intratumoral adenosine-triphosphate-supersensitive nanogel to enhance cancer chemoimmunotherapy, ACS Nano 17 (2023) 18805–18817, https://doi.org/10.1021/acsnano.3c03386.
[284] L. Huang, R. Xu, W. Li, L. Lv, C. Lin, X. Yang, Y. Yao, P.E. Saw, X. Xu, Repolarization of macrophages to improve sorafenib sensitivity for combination cancer therapy, Acta Biomater. 162 (2023) 98–109, https://doi.org/10.1016/j.actbio.2023.03.014.
[285] S. Gao, M. Liu, Y. Zhang, Z. He, Y. Li, J. Ji, L. Ye, X. Yang, G. Zhai, A precision intelligent nanomissile for inhibiting tumor metastasis, boosting energy deprivation and immunotherapy, Biomaterials 315 (2025) 122953, https://doi.org/10.1016/j.biomaterials.2024.122953.
[286] J. Wang, J.S. Lee, D. Kim, L. Zhu, Exploration of zinc oxide nanoparticles as a multitarget and multifunctional anticancer nanomedicine, ACS Appl. Mater. Interfaces 9 (2017) 39971–39984, https://doi.org/10.1021/acsami.7b11219.
[287] H. Jin, Y. He, P. Zhao, Y. Hu, J. Tao, J. Chen, Y. Huang, Targeting lipid metabolism to overcome EMT-associated drug resistance via integrin β3/FAK pathway and tumor-associated macrophage repolarization using legumain-activatable delivery, Theranostics 9 (2019) 265–278, https://doi.org/10.7150/thno.27246.
[288] X. Zhang, H. Hou, J. Wan, J. Yang, D. Tang, D. Zhao, T. Liu, K. Shang, Inhibiting COX-2/PGE2 pathway with biodegradable NIR-II fluorescent polymeric nanoparticles for enhanced photodynamic immunotherapy, Nano Today 48 (2023) 101759, https://doi.org/10.1016/j.nantod.2023.101759.
[289] J. Liu, B. Chang, Q. Li, L. Xu, X. Liu, G. Wang, Z. Wang, L. Wang, Redox-responsive dual drug delivery nanosystem suppresses cancer repopulation by abrogating doxorubicin-promoted cancer stemness, metastasis, and drug resistance, Adv. Sci. 6 (2019) 1801987, https://doi.org/10.1002/advs.201801987.
[290] K. Mehla, P.K. Singh, Metabolic regulation of macrophage polarization in cancer, Trends Cancer 5 (2019) 822–834, https://doi.org/10.1016/j.trecan.2019.10.007.
[291] W. Zeng, M. Yu, T. Chen, Y. Liu, Y. Yi, C. Huang, J. Tang, H. Li, M. Ou, T. Wang, M. Wu, L. Mei, Polypyrrole nanoenzymes as tumor microenvironment modulators to reprogram macrophage and potentiate immunotherapy, Adv. Sci. 9 (2022) 2201703, https://doi.org/10.1002/advs.202201703.
[292] V. Plaks, N. Kong, Z. Werb, The cancer stem cell niche: how essential is the niche in regulating stemness of tumor cells? Cell Stem Cell 16 (2015) 225–238, https://doi.org/10.1016/j.stem.2015.02.015.
[293] C. Wang, Q. Wang, H. Wang, Z. Li, J. Chen, Z. Zhang, H. Zeng, X. Yu, X. Yang, X. Yang, Z. Li, Hydroxyethyl starch-folic acid conjugates stabilized theranostic nanoparticles for cancer therapy, J. Controlled Release 353 (2023) 391–410, https://doi.org/10.1016/j.jconrel.2022.11.059.
[294] Z. Qin, G. Richter, T. Schüler, S. Ibe, X. Cao, T. Blankenstein, B cells inhibit induction of T cell-dependent tumor immunity, Nat. Med. 4 (1998) 627–630, https://doi.org/10.1038/nm0598-627.
[295] S. Biswas, S. Sengupta, S. Roy Chowdhury, S. Jana, G. Mandal, P.K. Mandal, N. Saha, V. Malhotra, A. Gupta, D.V. Kuprash, A. Bhattacharyya, CXCL13–CXCR5 co-expression regulates epithelial to mesenchymal transition of breast cancer cells during lymph node metastasis, Breast Cancer Res. Treat. 143 (2014) 265–276, https://doi.org/10.1007/s10549-013-2811-8.
[296] L. Shen, J. Li, Q. Liu, M. Das, W. Song, X. Zhang, K. Tiruthani, O. Dorosheva, H. Hu, S.K. Lai, R. Liu, L. Huang, Nano-trapping CXCL13 reduces regulatory B cells in tumor microenvironment and inhibits tumor growth, J. Controlled Release 343 (2022) 303–313, https://doi.org/10.1016/j.jconrel.2022.01.039.
[297] C. Zhan, X. Yang, X. Yin, J. Hou, Exosomes and other extracellular vesicles in oral and salivary gland cancers, Oral Dis. 26 (2020) 865–875, https://doi.org/10.1111/odi.13172.
[298] C.-M. Chen, T.-H. Chu, C.-C. Chou, C.-Y. Chien, J.-S. Wang, C.-C. Huang, Exosome-derived microRNAs in oral squamous cell carcinomas impact disease prognosis, Oral Oncol. 120 (2021) 105402, https://doi.org/10.1016/j.oraloncology.2021.105402.
[299] Y.-M. Zhou, Y.-L. Yao, W. Liu, X.-M. Shen, L.-J. Shi, L. Wu, MicroRNA-134 inhibits tumor stem cell migration and invasion in oral squamous cell carcinomas via downregulation of PI3K-Akt signaling pathway by inhibiting LAMC2 expression, Cancer Biomarkers 29 (2020) 51–67, https://doi.org/10.3233/CBM-191362.
[300] H. Yoon, Y.S. Chung, Y.J. Lee, S.E. Yu, S. Baek, H. Kim, S.W. Kim, J. Lee, S. Kim, H. Sung, Cancer patient tissueoid with self-homing nano-targeting of metabolic inhibitor, Adv. Sci. 8 (2021) 2102640, https://doi.org/10.1002/advs.202102640.
[301] A. Hoshino, B. Costa-Silva, T.-L. Shen, G. Rodrigues, A. Hashimoto, M. Tesic Mark, H. Molina, S. Kohsaka, A. Di Giannatale, S. Ceder, S. Singh, C. Williams, N. Soplop, K. Uryu, L. Pharmer, T. King, L. Bojmar, A.E. Davies, Y. Ararso, T. Zhang, H. Zhang, J. Hernandez, J.M. Weiss, V.D. Dumont-Cole, K. Kramer, L. H. Wexler, A. Narendran, G.K. Schwartz, J.H. Healey, P. Sandstrom, K. Jørgen Labori, E.H. Kure, P.M. Grandgenett, M.A. Hollingsworth, M. De Sousa, S. Kaur, M. Jain, K. Mallya, S.K. Batra, W.R. Jarnagin, M.S. Brady, O. Fodstad, V. Muller, K. Pantel, A.J. Minn, M.J. Bissell, B.A. Garcia, Y. Kang, V.K. Rajasekhar, C. M. Ghajar, I. Matei, H. Peinado, J. Bromberg, D. Lyden, Tumour exosome integrins determine organotropic metastasis, Nature 527 (2015) 329–335, https://doi.org/10.1038/nature15756.
[302] C. Ciardiello, A. Leone, A. Budillon, The crosstalk between cancer stem cells and microenvironment is critical for solid tumor progression: the significant contribution of extracellular vesicles, Stem Cells Int. 2018 (2018) 1–11, https://doi.org/10.1155/2018/6392198.
[303] T. Yong, X. Zhang, N. Bie, H. Zhang, X. Zhang, F. Li, A. Hakeem, J. Hu, L. Gan, H. A. Santos, X. Yang, Tumor exosome-based nanoparticles are efficient drug carriers for chemotherapy, Nat. Commun. 10 (2019) 3838, https://doi.org/10.1038/s41467-019-11718-4.
[304] L. Lu, H. Tao, A.E. Chang, Y. Hu, G. Shu, Q. Chen, M. Egenti, J. Owen, J.S. Moyer, M.E. Prince, S. Huang, M.S. Wicha, J.-C. Xia, Q. Li, Cancer stem cell vaccine inhibits metastases of primary tumors and induces humoral immune responses against cancer stem cells, OncoImmunology 4 (2015) e990767, https://doi.org/10.4161/2162402X.2014.990767.
[305] A. Dashti, M. Ebrahimi, J. Hadjati, A. Memarnejadian, S.M. Moazzeni, Dendritic cell based immunotherapy using tumor stem cells mediates potent antitumor immune responses, Cancer Lett. 374 (2016) 175–185, https://doi.org/10.1016/j.canlet.2016.01.021.
[306] M. Naseri, M. Zöller, J. Hadjati, R. Ghods, E. Ranaei Pirmardan, J. Kiani, L. Eini, M. Bozorgmehr, Z. Madjd, Dendritic cells loaded with exosomes derived from cancer stem cell-enriched spheroids as a potential immunotherapeutic option, J. Cell Mol. Med. 25 (2021) 3312–3326, https://doi.org/10.1111/jcmm.16401.
[307] Y. Li, R. Zhang, Z. Lu, G. Ma, L. Chen, Q. Tang, X. Zhang, Microenvironment-responsive three-pronged approach breaking traditional chemotherapy to target cancer stem cells for synergistic inoperable large tumor therapy, Small 12 (2016) 5516–5523, https://doi.org/10.1002/smll.201601932.

[308] H. Huang, S. Zhang, Y. Li, Z. Liu, L. Mi, Y. Cai, X. Wang, L. Chen, H. Ran, D. Xiao, F. Li, J. Wu, T. Li, Q. Han, L. Chen, X. Pan, H. Li, T. Li, K. He, A. Li, X. Zhang, T. Zhou, Q. Xia, J. Man, Suppression of mitochondrial ROS by prohibitin drives glioblastoma progression and therapeutic resistance, Nat. Commun. 12 (2021) 3720, https://doi.org/10.1038/s41467-021-24108-6.
[309] W.R. Wilson, M.P. Hay, Targeting hypoxia in cancer therapy, Nat. Rev. Cancer 11 (2011) 393–410, https://doi.org/10.1038/nrc3064.
[310] C. Ward, J. Meehan, P. Mullen, C. Supuran, J.M. Dixon, J.S. Thomas, J.-Y. Winum, P. Lambin, L. Dubois, N.-K. Pavathaneni, E.J. Jarman, L. Renshaw, I. Um, C. Kay, D.J. Harrison, I.H. Kunkler, S.P. Langdon, Evaluation of carbonic anhydrase IX as a therapeutic target for inhibition of breast cancer invasion and metastasis using a series of in vitro breast cancer models, Oncotarget 6 (2015) 24856–24870, https://doi.org/10.18632/oncotarget.4498.
[311] Z. Ma, Y. Zhang, X. Dai, W. Zhang, M.F. Foda, J. Zhang, Y. Zhao, H. Han, Selective thrombosis of tumor for enhanced hypoxia-activated prodrug therapy, Adv. Mater. 33 (2021) 2104504, https://doi.org/10.1002/adma.202104504.
[312] Y. Liu, X. Liang, X. Yin, J. Lv, K. Tang, J. Ma, T. Ji, H. Zhang, W. Dong, X. Jin, D. Chen, Y. Li, S. Zhang, H.Q. Xie, B. Zhao, T. Zhao, J. Lu, Z.-W. Hu, X. Cao, F.X.-F. Qin, B. Huang, Blockade of Ido-kynurenine-AhR metabolic circuitry abrogates IFN-γ-induced immunologic dormancy of tumor-repopulating cells, Nat. Commun. 8 (2017) 15207, https://doi.org/10.1038/ncomms15207.
[313] S.K. Rehman, J. Haynes, E. Collignon, K.R. Brown, Y. Wang, A.M.L. Nixon, J. P. Bruce, J.A. Wintersinger, A. Singh Mer, E.B.L. Lo, C. Leung, E. Lima-Fernandes, N.M. Pedley, F. Soares, S. McGibbon, H.H. He, A. Pollet, T.J. Pugh, B. Haibe-Kains, Q. Morris, M. Ramalho-Santos, S. Goyal, J. Moffat, C.A. O'Brien, Colorectal cancer cells enter a diapause-like DTP state to survive chemotherapy, Cell 184 (2021) 226–242.e21, https://doi.org/10.1016/j.cell.2020.11.018.
[314] J. Guan, Y. Wu, X. Liu, H. Wang, N. Ye, Z. Li, C. Xiao, Z. Zhang, Z. Li, X. Yang, A novel prodrug and its nanoformulation suppress cancer stem cells by inducing immunogenic cell death and inhibiting indoleamine 2, 3-dioxygenase, Biomaterials 279 (2021) 121180, https://doi.org/10.1016/j.biomaterials.2021.121180.
[315] O. Itzhaki, E. Greenberg, B. Shalmon, A. Kubi, A.J. Treves, R. Shapira-Frommer, C. Avivi, R. Ortenberg, E. Ben-Ami, J. Schachter, M.J. Besser, G. Markel, Nicotinamide inhibits vasculogenic mimicry, an alternative vascularization pathway observed in highly aggressive melanoma, PLoS One 8 (2013) e57160, https://doi.org/10.1371/journal.pone.0057160.
[316] H. Wang, W. Sun, W.-Z. Zhang, C.-Y. Ge, J.-T. Zhang, Z.-Y. Liu, Y.-Z. Fan, Inhibition of tumor vasculogenic mimicry and prolongation of host survival in highly aggressive gallbladder cancers by norcantharidin via blocking the ephrin type a receptor 2/focal adhesion kinase/paxillin signaling pathway, PLoS One 9 (2014) e96982, https://doi.org/10.1371/journal.pone.0096982.
[317] Y. Liu, L. Mei, Q. Yu, C. Xu, Y. Qiu, Y. Yang, K. Shi, Q. Zhang, H. Gao, Z. Zhang, Q. He, Multifunctional tandem peptide modified paclitaxel-loaded liposomes for the treatment of vasculogenic mimicry and cancer stem cells in malignant glioma, ACS Appl. Mater. Interfaces 7 (2015) 16792–16801, https://doi.org/10.1021/acsami.5b04596.
[318] L. Wang, Y. Lv, C. Li, G. Yang, B. Fu, Q. Peng, L. Jian, D. Hou, J. Wang, C. Zhao, P. Yang, K. Zhang, L. Wang, Z. Wang, H. Wang, W. Xu, Transformable dual-inhibition system effectively suppresses renal cancer metastasis through blocking endothelial cells and cancer stem cells, Small 16 (2020) 2004548, https://doi.org/10.1002/smll.202004548.
[319] A. Saroufim, Y. Messai, M. Hasmim, N. Rioux, R. Iacovelli, G. Verhoest, K. Bensalah, J.-J. Patard, L. Albiges, B. Azzarone, B. Escudier, S. Chouaib, Tumoral CD105 is a novel independent prognostic marker for prognosis in clear-cell renal cell carcinoma, Br. J. Cancer 110 (2014) 1778–1784, https://doi.org/10.1038/bjc.2014.71.
[320] L. Miao, J.M. Newby, C.M. Lin, L. Zhang, F. Xu, W.Y. Kim, M.G. Forest, S.K. Lai, M.I. Milowsky, S.E. Wobker, L. Huang, The binding site barrier elicited by tumor-associated fibroblasts interferes disposition of nanoparticles in stroma-vessel type tumors, ACS Nano 10 (2016) 9243–9258, https://doi.org/10.1021/acsnano.6b02776.
[321] M. Overchuk, G. Zheng, Overcoming obstacles in the tumor microenvironment: recent advancements in nanoparticle delivery for cancer theranostics, Biomaterials 156 (2018) 217–237, https://doi.org/10.1016/j.biomaterials.2017.10.024.
[322] P. Apostolova, E.L. Pearce, Lactic acid and lactate: revisiting the physiological roles in the tumor microenvironment, Trends Immunol. 43 (2022) 969–977, https://doi.org/10.1016/j.it.2022.10.005.
[323] H. Yang, W.-L. Lu, T. Huang, Q.-Y. Chen, J. Gao, Y. Zhao, An aptamer-Fe3+ modified nanoparticle for lactate oxidation and tumor photodynamic therapy, Colloids Surf. B Biointerfaces 164 (2018) 192–200, https://doi.org/10.1016/j.colsurfb.2018.01.045.
[324] Y.A. Shen, K.L. Lan, C.H. Chang, L.T. Lin, C.L. He, P.H. Chen, T.W. Lee, Y.J. Lee, C.M. Chuang, Intraperitoneal 188Re-Liposome delivery switches ovarian cancer metabolism from glycolysis to oxidative phosphorylation and effectively controls ovarian tumour growth in mice, Radiother. Oncol. 119 (2016) 282–290, https://doi.org/10.1016/j.radonc.2016.02.007.
[325] H. Ren, D. Zhang, Lactylation constrains OXPHOS under hypoxia, Cell Res. 34 (2024) 91–92, https://doi.org/10.1038/s41422-023-00872-6.
[326] F. Paredes, H.C. Williams, A. San Martin, Metabolic adaptation in hypoxia and cancer, Cancer Lett. 502 (2021) 133–142, https://doi.org/10.1016/j.canlet.2020.12.020.
[327] G.L. Semenza, Targeting HIF-1 for cancer therapy, Nat. Rev. Cancer 3 (2003) 721–732, https://doi.org/10.1038/nrc1187.
[328] P. Sridharan, G. Vinothkumar, P. Pratheesh, K.S. Babu, Biomimetic potential of cerium oxide nanoparticles in modulating the metabolic gene signature in GBM-derived cell lines, J. Mater. Sci. 55 (2020) 11622–11636, https://doi.org/10.1007/s10853-020-04872-4.
[329] F. Yang, Y. Zhao, X. Hu, Z. Liu, X. Yu, C. Li, X. Li, H. Li, Nano-realgar suppresses lung cancer stem cell growth by repressing metabolic reprogramming, Gene 788 (2021) 145666, https://doi.org/10.1016/j.gene.2021.145666.
[330] J. Yun, E. Mullarky, C. Lu, K.N. Bosch, A. Kavalier, K. Rivera, J. Roper, I.I.C. Chio, E.G. Giannopoulou, C. Rago, A. Muley, J.M. Asara, J. Paik, O. Elemento, Z. Chen, D.J. Pappin, L.E. Dow, N. Papadopoulos, S.S. Gross, L.C. Cantley, Vitamin C selectively kills KRAS and BRAF mutant colorectal cancer cells by targeting GAPDH, Science 350 (2015) 1391–1396, https://doi.org/10.1126/science.aaa5004.
[331] S.J. Dixon, K.M. Lemberg, M.R. Lamprecht, R. Skouta, E.M. Zaitsev, C.E. Gleason, D.N. Patel, A.J. Bauer, A.M. Cantley, W.S. Yang, B. Morrison, B.R. Stockwell, Ferroptosis: an iron-dependent form of nonapoptotic cell death, Cell 149 (2012) 1060–1072, https://doi.org/10.1016/j.cell.2012.03.042.
[332] K. Wang, Z. Zhang, H. Tsai, Y. Liu, J. Gao, M. Wang, L. Song, X. Cao, Z. Xu, H. Chen, A. Gong, D. Wang, F. Cheng, H. Zhu, Branched-chain amino acid aminotransferase 2 regulates ferroptotic cell death in cancer cells, Cell Death Differ. 28 (2021) 1222–1236, https://doi.org/10.1038/s41418-020-00644-4.
[333] B. Hassannia, P. Vandenabeele, T. Vanden Berghe, Targeting ferroptosis to iron out cancer, Cancer Cell 35 (2019) 830–849, https://doi.org/10.1016/j.ccell.2019.04.002.
[334] Z. Ni, X. Nie, H. Zhang, L. Wang, Z. Geng, X. Du, H. Qian, W. Liu, T. Liu, Atranorin driven by nano materials SPION lead to ferroptosis of gastric cancer stem cells by weakening the mRNA 5-hydroxymethylcytidine modification of the Xc-/GPX4 axis and its expression, Int. J. Med. Sci. 19 (2022) 1680–1694, https://doi.org/10.7150/ijms.73701.
[335] A.F. Farag, N.F. Hassabou, CD24-gold nanocomposite as promising and sensitive biomarker for cancer stem cells in salivary gland tumors, Nanomed. Nanotechnol. Biol. Med. 46 (2022) 102598, https://doi.org/10.1016/j.nano.2022.102598.
[336] S.K. Libutti, G.F. Paciotti, A.A. Byrnes, H.R. Alexander, W.E. Gannon, M. Walker, G.D. Seidel, N. Yuldasheva, L. Tamarkin, Phase I and pharmacokinetic studies of CYT-6091, a novel PEGylated colloidal gold-rhTNF nanomedicine, Clin. Cancer Res. 16 (2010) 6139–6149, https://doi.org/10.1158/1078-0432.CCR-10-0978.
[337] K. Maier-Hauff, F. Ulrich, D. Nestler, H. Niehoff, P. Wust, B. Thiesen, H. Orawa, V. Budach, A. Jordan, Efficacy and safety of intratumoral thermotherapy using magnetic iron-oxide nanoparticles combined with external beam radiotherapy on patients with recurrent glioblastoma multiforme, J. Neuro Oncol. 103 (2011) 317–324, https://doi.org/10.1007/s11060-010-0389-0.
[338] X. Liem, T. De Baère, O.I. Vivar, T.Y. Seiwert, C. Shen, Z. Pápai, V. Moreno, Z. Takácsi-Nagy, F. Helfferich, J. Thariat, Z. Gooi, S.S. Yom, P. Bossi, R.L. Ferris, T.G. Hackman, C. Le Tourneau, J. Rodriguez, C. Hoffmann, International guidelines for intratumoral and intranodal injection of NBTXR3 nanoparticles in head and neck cancers, Head Neck 46 (2024) 1253–1262, https://doi.org/10.1002/hed.27739.
[339] C. Hoffmann, V. Calugaru, E. Borcoman, V. Moreno, E. Calvo, X. Liem, S. Salas, B. Doger, T. Jouffroy, X. Mirabel, J. Rodriguez, A. Chilles, K. Bernois, M. Dimitriu, N. Fakhry, S.W. Hee Kam, C. Le Tourneau, Phase I dose-escalation study of NBTXR3 activated by intensity-modulated radiation therapy in elderly patients with locally advanced squamous cell carcinoma of the oral cavity or oropharynx, Eur. J. Cancer 146 (2021) 135–144, https://doi.org/10.1016/j.ejca.2021.01.007.
[340] S. Fulda, S. Pervaiz, Apoptosis signaling in cancer stem cells, Int. J. Biochem. Cell Biol. 42 (2010) 31–38, https://doi.org/10.1016/j.biocel.2009.06.010.
[341] N. Sasaki, Y. Itakura, F. Gomi, K. Hirano, M. Toyoda, T. Ishiwata, Comparison of functional glycans between cancer stem cells and normal stem cells, Histol. Histopathol. 34 (2019) 995–1007, https://doi.org/10.14670/HH-18-119.
[342] A.J. Chambost, N. Berabez, O. Cochet-Escartin, F. Ducray, M. Gabut, C. Isaac, S. Martel, A. Idbaih, D. Rousseau, D. Meyronet, S. Monnier, Machine learning-based detection of label-free cancer stem-like cell fate, Sci. Rep. 12 (2022) 19066, https://doi.org/10.1038/s41598-022-21822-z.
[343] Z. Zhang, H. Ishihata, R. Maruyama, T. Kasai, H. Kameda, T. Sugiyama, Deep learning of phase-contrast images of cancer stem cells using a selected dataset of high accuracy value using conditional generative adversarial networks, Int. J. Mol. Sci. 24 (2023) 5323, https://doi.org/10.3390/ijms24065323.
[344] G. Ji, J. Liu, Z. Zhao, J. Lan, Y. Yang, Z. Wang, H. Feng, K. Ji, X. Jiang, H. Xia, G. Wei, Y. Zhang, Y. Zhang, X. Du, Y. Wang, Y. Yang, Z. Liu, K. Zhang, Q. Mei, R. Sun, H. Lu, Polyamine anabolism promotes chemotherapy-induced breast cancer stem cell enrichment, Adv. Sci. 11 (2024) 2404853, https://doi.org/10.1002/advs.202404853.
[345] L. Xu, H.-W. Liang, Y. Yang, S.-H. Yu, Stability and reactivity: positive and negative aspects for nanoparticle processing, Chem. Rev. 118 (2018) 3209–3250, https://doi.org/10.1021/acs.chemrev.7b00208.
[346] B.J. Curtis, N.J. Niemuth, E. Bennett, A. Schmoldt, O. Mueller, A.A. Mohaimani, E.D. Laudadio, Y. Shen, J.C. White, R.J. Hamers, R.D. Klaper, Cross-species transcriptomic signatures identify mechanisms related to species sensitivity and common responses to nanomaterials, Nat. Nanotechnol. 17 (2022) 661–669, https://doi.org/10.1038/s41565-022-01096-2.
[347] H. Wang, X. Pan, X. Wang, W. Wang, Z. Huang, K. Gu, S. Liu, F. Zhang, H. Shen, Q. Yuan, J. Ma, W. Yuan, H. Liu, Degradable carbon–silica nanocomposite with immunoadjuvant property for dual-modality photothermal/photodynamic therapy, ACS Nano 14 (2020) 2847–2859, https://doi.org/10.1021/acsnano.9b06168.
[348] M.J. Pitkethly, Nanomaterials – the driving force, Mater. Today 7 (2004) 20–29, https://doi.org/10.1016/S1369-7021(04)00627-3.

[349] H. Tang, Y. Zhang, T. Yang, C. Wang, Y. Zhu, L. Qiu, J. Liu, Y. Song, L. Zhou, J. Zhang, Y.K. Wong, Y. Liu, C. Xu, H. Wang, J. Wang, Cholesterol modulates the physiological response to nanoparticles by changing the composition of protein corona, Nat. Nanotechnol. 18 (2023) 1067–1077, https://doi.org/10.1038/s41565-023-01455-7.
[350] Q. Xiao, M. Zoulikha, M. Qiu, C. Teng, C. Lin, X. Li, M.A. Sallam, Q. Xu, W. He, The effects of protein corona on in vivo fate of nanocarriers, Adv. Drug Deliv. Rev. 186 (2022) 114356, https://doi.org/10.1016/j.addr.2022.114356.
[351] J.S. Suk, Q. Xu, N. Kim, J. Hanes, L.M. Ensign, PEGylation as a strategy for improving nanoparticle-based drug and gene delivery, Adv. Drug Deliv. Rev. 99 (2016) 28–51, https://doi.org/10.1016/j.addr.2015.09.012.
[352] Y. Miao, L. Li, Y. Wang, J. Wang, Y. Zhou, L. Guo, Y. Zhao, D. Nie, Y. Zhang, X. Zhang, Y. Gan, Regulating protein corona on nanovesicles by glycosylated polyhydroxy polymer modification for efficient drug delivery, Nat. Commun. 15 (2024) 1159, https://doi.org/10.1038/s41467-024-45254-7.
[353] Y. Matsumura, H. Maeda, A new concept for macromolecular therapeutics in cancer chemotherapy: mechanism of tumoritropic accumulation of proteins and the antitumor agent smancs, Cancer Res. 46 (1986) 6387–6392.
[354] J. Park, J.Y. Park, Y. Jeong, J. Park, Y.H. Park, S. Kim, D. Khang, Pancreatic tumor-targeting stemsome therapeutics, Adv. Mater. 35 (2023) 2300934, https://doi.org/10.1002/adma.202300934.
[355] X. Ma, M. Yao, J. Shi, X. Li, Y. Gao, Q. Luo, R. Hou, X. Liang, F. Wang, High intensity focused ultrasound-responsive and ultrastable cerasomal perfluorocarbon nanodroplets for alleviating tumor multidrug resistance and epithelial–mesenchymal transition, ACS Nano 14 (2020) 15904–15918, https://doi.org/10.1021/acsnano.0c07287.
[356] K.-F. Xu, S.-Y. Wu, Z. Wang, Y. Guo, Y.-X. Zhu, C. Li, B.-H. Shan, X. Zhang, X. Liu, F.-G. Wu, Hyperbaric oxygen enhances tumor penetration and accumulation of engineered bacteria for synergistic photothermal immunotherapy, Nat. Commun. 15 (2024) 5147, https://doi.org/10.1038/s41467-024-49156-6.
[357] Y. Zhang, X. Wang, C. Chu, Z. Zhou, B. Chen, X. Pang, G. Lin, H. Lin, Y. Guo, E. Ren, P. Lv, Y. Shi, Q. Zheng, X. Yan, X. Chen, G. Liu, Genetically engineered magnetic nanocages for cancer magneto-catalytic theranostics, Nat. Commun. 11 (2020) 5421, https://doi.org/10.1038/s41467-020-19061-9.
[358] W. Bao, M. Liu, J. Meng, S. Liu, S. Wang, R. Jia, Y. Wang, G. Ma, W. Wei, Z. Tian, MOFs-based nanoagent enables dual mitochondrial damage in synergistic antitumor therapy via oxidative stress and calcium overload, Nat. Commun. 12 (2021) 6399, https://doi.org/10.1038/s41467-021-26655-4.
[359] Y. Yin, X. Ge, J. Ouyang, N. Na, Tumor-activated in situ synthesis of single-atom catalysts for O2-independent photodynamic therapy based on water-splitting, Nat. Commun. 15 (2024) 2954, https://doi.org/10.1038/s41467-024-46987-1.
[360] Y. Li, W. Chen, Y. Kang, X. Zhen, Z. Zhou, C. Liu, S. Chen, X. Huang, H.-J. Liu, S. Koo, N. Kong, X. Ji, T. Xie, W. Tao, Nanosensitizer-mediated augmentation of sonodynamic therapy efficacy and antitumor immunity, Nat. Commun. 14 (2023) 6973, https://doi.org/10.1038/s41467-023-42509-7.
[361] X. Bai, S. Wang, X. Yan, H. Zhou, J. Zhan, S. Liu, V.K. Sharma, G. Jiang, H. Zhu, B. Yan, Regulation of cell uptake and cytotoxicity by nanoparticle core under the controlled shape, size, and surface chemistries, ACS Nano 14 (2020) 289–302, https://doi.org/10.1021/acsnano.9b04407.
[362] W.-K. Oh, S. Kim, M. Choi, C. Kim, Y.S. Jeong, B.-R. Cho, J.-S. Hahn, J. Jang, Cellular uptake, cytotoxicity, and innate immune response of Silica−Titania hollow nanoparticles based on size and surface functionality, ACS Nano 4 (2010) 5301–5313, https://doi.org/10.1021/nn100561e.
[363] D. Van Haute, A.T. Liu, J.M. Berlin, Coating metal nanoparticle surfaces with small organic molecules can reduce nonspecific cell uptake, ACS Nano 12 (2018) 117–127, https://doi.org/10.1021/acsnano.7b03025.
[364] K. Niikura, T. Matsunaga, T. Suzuki, S. Kobayashi, H. Yamaguchi, Y. Orba, A. Kawaguchi, H. Hasegawa, K. Kajino, T. Ninomiya, K. Ijiro, H. Sawa, Gold nanoparticles as a vaccine platform: influence of size and shape on immunological responses in vitro and in vivo, ACS Nano 7 (2013) 3926–3938, https://doi.org/10.1021/nn3057005.
[365] W.A. Li, B.Y. Lu, L. Gu, Y. Choi, J. Kim, D.J. Mooney, The effect of surface modification of mesoporous silica micro-rod scaffold on immune cell activation and infiltration, Biomaterials 83 (2016) 249–256, https://doi.org/10.1016/j.biomaterials.2016.01.026.
[366] EFSA Scientific Committee, A. Hardy, D. Benford, T. Halldorsson, M.J. Jeger, H. K. Knutsen, S. More, H. Naegeli, H. Noteborn, C. Ockleford, A. Ricci, G. Rychen, J. R. Schlatter, V. Silano, R. Solecki, D. Turck, M. Younes, Q. Chaudhry, F. Cubadda, D. Gott, A. Oomen, S. Weigel, M. Karamitrou, R. Schoonjans, A. Mortensen, Guidance on risk assessment of the application of nanoscience and nanotechnologies in the food and feed chain: Part 1, human and animal health, EFSA J. 16 (2018), https://doi.org/10.2903/j.efsa.2018.5327.
[367] K. Aschberger, H. Rauscher, H. Crutzen, K. Rasmussen, F.M. Christensen, B. Sokull-Klüttgen, H. Stamm, European commission. Considerations on Information Needs for Nanomaterials in Consumer Products: Discussion of a Labelling and Reporting Scheme for Nanomaterials in Consumer Products in the EU, Publications Office, Luxembourg, 2014, https://doi.org/10.2788/3044.
[368] V. Amenta, K. Aschberger, M. Arena, H. Bouwmeester, F. Botelho Moniz, P. Brandhoff, S. Gottardo, H.J.P. Marvin, A. Mech, L. Quiros Pesudo, H. Rauscher, R. Schoonjans, M.V. Vettori, S. Weigel, R.J. Peters, Regulatory aspects of nanotechnology in the agri/feed/food sector in EU and non-EU countries, Regul. Toxicol. Pharmacol. 73 (2015) 463–476, https://doi.org/10.1016/j.yrtph.2015.06.016.
[369] S. Han, X. Bao, Y. Zou, L. Wang, Y. Li, L. Yang, A. Liao, X. Zhang, X. Jiang, D. Liang, Y. Dai, Q.-C. Zheng, Z. Yu, J. Guo, d -lactate modulates M2 tumor-associated macrophages and remodels immunosuppressive tumor microenvironment for hepatocellular carcinoma, Sci. Adv. 9 (2023) eadg2697, https://doi.org/10.1126/sciadv.adg2697.
[370] Y. Chao, Z. Liu, Biomaterials tools to modulate the tumour microenvironment in immunotherapy, Nat. Rev. Bioeng. 1 (2023) 125–138, https://doi.org/10.1038/s44222-022-00004-6.
[371] Y. Wei, J. Wu, Y. Wu, H. Liu, F. Meng, Q. Liu, A.C. Midgley, X. Zhang, T. Qi, H. Kang, R. Chen, D. Kong, J. Zhuang, X. Yan, X. Huang, Prediction and design of nanozymes using explainable machine learning, Adv. Mater. 34 (2022) 2201736, https://doi.org/10.1002/adma.202201736.
[372] H. Jiang, S. Benzaria, N. Alsadun, J. Jia, J. Czaban-Jóźwiak, V. Guillerm, A. Shkurenko, Z. Thiam, M. Bonneau, V.K. Maka, Z. Chen, Z.O. Ameur, M. O'Keeffe, M. Eddaoudi, Merged-nets enumeration for the systematic design of multicomponent reticular structures, Science 386 (2024) 659–666, https://doi.org/10.1126/science.ads7866.
[373] C. Zeni, R. Pinsler, D. Zügner, A. Fowler, M. Horton, X. Fu, Z. Wang, A. Shysheya, J. Crabbé, S. Ueda, R. Sordillo, L. Sun, J. Smith, B. Nguyen, H. Schulz, S. Lewis, C.-W. Huang, Z. Lu, Y. Zhou, H. Yang, H. Hao, J. Li, C. Yang, W. Li, R. Tomioka, T. Xie, A generative model for inorganic materials design, Nature (2025) 1–3, https://doi.org/10.1038/s41586-025-08628-5.
[374] A. Merchant, S. Batzner, S.S. Schoenholz, M. Aykol, G. Cheon, E.D. Cubuk, Scaling deep learning for materials discovery, Nature 624 (2023) 80–85, https://doi.org/10.1038/s41586-023-06735-9.
[375] Y. Tang, W. Xu, J. Cao, J. Ma, W. Gao, S. Farrell, B. Erichson, M.W. Mahoney, A. Nonaka, Z. Yao, MatterChat: a multi-modal llm for material science. https://doi.org/10.48550/arXiv.2502.13107, 2025.
[376] W. Wang, K. Chen, T. Jiang, Y. Wu, Z. Wu, H. Ying, H. Yu, J. Lu, J. Lin, D. Ouyang, Artificial intelligence-driven rational design of ionizable lipids for mRNA delivery, Nat. Commun. 15 (2024) 10804, https://doi.org/10.1038/s41467-024-55072-6.
[377] J.-N. May, J.I. Moss, F. Mueller, S.K. Golombek, I. Biancacci, L. Rizzo, A. S. Elshafei, F. Gremse, R. Pola, M. Pechar, T. Etrych, S. Becker, C. Trautwein, R. D. Bülow, P. Boor, R. Knuechel, S. Von Stillfried, G. Storm, S. Puri, S.T. Barry, V. Schulz, F. Kiessling, M.B. Ashford, T. Lammers, Histopathological biomarkers for predicting the tumour accumulation of nanomedicines, Nat. Biomed. Eng. 8 (2024) 1366–1378, https://doi.org/10.1038/s41551-024-01197-4.
[378] J. Deng, M. Gu, P. Zhang, M. Dong, T. Liu, Y. Zhang, M. Liu, Nanobody–antigen interaction prediction with ensemble deep learning and prompt-based protein language models, Nat. Mach. Intell. 6 (2024) 1594–1604, https://doi.org/10.1038/s42256-024-00940-5.
[379] D. Chen, J. Liu, G.-W. Wei, Multiscale topology-enabled structure-to-sequence transformer for protein–ligand interaction predictions, Nat. Mach. Intell. 6 (2024) 799–810, https://doi.org/10.1038/s42256-024-00855-1.